The Hong Kong Polytechnic University

Department of Health Technology and Informatics

Involvement of CD44 during Tumorigenic Transformation of Pre-cancerous Human Uroepithelial Cells

Yuen Ming, Au

A thesis submitted in partial fulfillment of the requirements for the degree of Master of Philosophy

May 2012

Certificate of Originality

I hereby declare that this thesis is my own work and that, to the best of my knowledge and belief, it reproduces no material previously published or written, nor material that has been accepted for the award of any other degree or diploma, except where due acknowledgment has been made in the text.

_____ (Signed)

___Yuen Ming, Au__ (Name of student)

Abstract of Research

Bladder cancer is a common disease in man aged over 50, making it the fourth most prevalent cancer in men. Superficial transition cell carcinoma contributes to 70% of clinical cases and is typically treated by transurethral resection (TUR) with or without Bacille Calmette-Guérin (BCG) treatment. However, effective treatment is hampered by the high cancer recurrence rate and around 30% of the patients may even progress to a high grade cancer making it the most expensive cancer to be treated.

This study proposes that the high recurrence rate may be due to the presence of sensitized cell - urothelial cells that accumulated certain degree of genetic alternations but phenotypically similar to normal cells. Therefore, they can escape from the surgery removal and stem future tumor formations, i.e. cancer recurrence. However, little is known about the existence and properties of the sensitized cell. Identification and characterization this cell type will be crucial to develop means for recurrent prediction, monitoring and prevention. Information presented by this study is not only important for understanding the cancer development process but also useful for prediction of bladder cancer recurrences.

An *in vitro* tumorigenic model involving two human uroepithelial cell lines at two different statuses, namely HUC-PC (pre-cancerous) and HUC-1 (normal) was used to study the transformation process. HUC-PC mimics the sensitized cell remained in bladder lining after TUR and tumorigenic transformation was triggered by the

exposure of bladder carcinogen, 4-aminobiphenyl (ABP). Due to the fact that HUC-PC is sensitized to ABP and will transform to cancer state while HUC-1 will not, we can then target different molecules for their involvement in cancer development by comparing the molecular changes between two statuses of cell line.

The success of transformation process was confirmed by functional assays and cancer markers. In this study, HUC-PC was treated with tobacco carcinogen ABP at concentrations 200μM for 24hr. After 6 weeks of incubation, the tumorigenicity of cells was evaluated via functional assays. The results showed that the transformed HUC-PC displayed neoplastic transformation phenotype, as marked by their induced proliferation rate and invasion ability. In addition, bladder markers, survivin and telomerase, were also found highly expressed in the transformed HUC-PC, which further confirmed the success of the transformation process.

During transformation, our target CD44 and its partner HA were quantified for evaluating their involvement in the process. Flow cytometry and RT-qPCR analyses showed that the transformed HUC-PC expressed increased levels of CD44 in the first week after exposure to 4-ABP. The elevated level of CD44 mRNA expression was great contributed by the CD44s instead of CD44v6 (exon v6 containing CD44 isoforms). In parallel, an increase in HA was found after the CD44 induction and maintained at a high level throughout the transformation process. Based on the above findings, we demonstrated that *in vitro* ABP exposure could neoplastically transform the pre-cancerous HUC-PC and suggested CD44 is involved in the initiation step of cancer development, possibly by interacting with HA.

Conference presentation

Au, G.Y.M., Yuen, J.W.M., Ng, C.F., Gohel, M.D.I. (2011). Expression of CD44 and MCP-1 during tumorigenic transformation of pre-cancerous human uroepithelial cells. Proceedings of Urological Society of Australia & New Zealand 64th Annual Scientific Meeting, New Zealand, 21-24 February 2011 (Accepted for oral presentation).

Scholarship

The Hong Kong Polytechnic University Research Studentship (2009/2011)

Acknowledgements

First thanks and praise go to God, I could never have done this without the faith I have in you, the Almighty. Also, I wish to express my gratitude to people who supported, encouraged and taught me on the study journey. I would like to start by acknowledging my supervisor **Dr. Danny Gohel** (Dept. of HTI, HK PolyU). Deeply thanks for accepting me as an MPhil student, your thoughtful guidance, critical comments, and correction of the thesis.

I would also like to express appreciation to **Dr. John Yuen** (School of nursing, HK PolyU) for his continuous support and insight that kept me focused and moving forward. Many thanks also give to **Dr. Doris Au** (Dept. Biology & Chemistry, CityU of HK), for her laboratory equipment and reagents provided.

Besides, I am especially grateful to my friends **Aimee Chiu, Blanka Lee, Tami Zhang, Isabella Cheuk, Wah Dee, Dr. Choi, Dr. Chung**, all the technical staff and postgraduate students in HTI at PolyU for their support and assistance.

Last but not least, I warmly thank and appreciate my beloved **Napo Cheung** for his professional knowledge and technical support throughout my study process.

Table of contents

Abbreviations

Numeric / characters

A/a

ABP	4-Aminobiphenyl

B/b

BCG	Bacillus Calmette-Guérin
BSA	Bovine serum albumin

C/c

CFHR	Complement factor H-related proteins
CPC	Cetylpyridinium chloride
CIS	Carcinoma in situ

D/d

DE	Differentially expressed
DMEM	Dulbecco's Modified Eagle's Medium
DMSO	Dimethyl sulfoxide
DNA	Deoxyribonucleic acid

P/p

PBS	Phosphate buffered saline

E/e

ECM	Extracellular matrix
EGR-1	Early growth response protein-1
EtOH	Ethanol

F/f

FBS	Fetal Bovine serum
FDA	Food and Drug Administration
FGFR3	Fibroblast growth factor receptor 3
FITC	Fluorescein isothiocyanate

G/g

GAGs	Glycosaminoglycans

H/h

HA	Hyaluronan
HAS	Hyaluronan synthase
HPLC	High-performance liquid chromatography
hTERT	Human telomerase reverse transcriptase
HUC	Human uroepithelial cells
HRAS	V-Ha-ras Harvey rat sarcoma viral oncogene homolog

I/i

IMP3	Insulin-like growth factor II mRNA-binding protein 3

L/l

LOH	Loss of heterozygosity

M/m

mRNA	Messager ribonucleic acid

N/n

NMP22	Nuclear Matrix Protein 22

R/r

RB	Retinoblastoma
RT-PCR	Reverse transcription polymerase chain reaction
RT-qPCR	Real-time quantitative polymerase chain reaction
RTQ-TRAP	Real-time telomeric repeat amplification protocol

S/s

SCC	Squamous cell carcinoma
SDS	Sodium dodecyl sulphate
SDS-PAGE	Sodium dodecyl sulfate polyacrylamide gel electrophoresis
shRNA	short hairpin RNA
SV40	Simian virus 40

T/t

TBP	TATA box binding protein
TCC	Transitional cell carcinoma
TUR	Transurethral resection

U/u

UPM	Urinary polyanionic macromolecules

Other

Δdi-nonS_{HA}	Unsaturated disaccharides of hyaluronan

List of Figures

List of Tables

Summary of the thesis

Chapter 1 provides an introduction and recent findings of bladder cancer. It also describes the focus of the present study which is the possible involvements of CD44 in bladder cancer development. **Chapter 2** describes the methodology of the study, detailing the experiment procedures and data analysis. **Chapter 3** presents the experimental data and the statistical analysis of the results. **Chapter 4** discusses the significant findings, limitations in this study and suggests some recommendations for further study. **Chapter 5** provides a summary of the results obtained and conclusion reached.

Chapter 1 Introduction

This chapter presents a review of literature related to the research in bladder cancer. Firstly, background information of bladder cancer, such as cancer statistics, risk factors and treatment methods, is presented. Secondly, the current obstacle in bladder cancer treatment in relation to the high recurrent rate is identified. Thirdly, existing research methods and critical findings related to bladder cancer are examined. Lastly, information about the tumor initiating marker, CD44, is investigated.

1.1 Classification of bladder cancer

1.1.1 Structure of bladder

The urinary bladder is a hollow, balloon-like organ located in the pelvis (Figure 1.1). Its function is to collect and store urine until it is ready to be discharged from the body. Urine is made in the kidneys and transported through two tube-like structures, called ureters, to the bladder for temporary storage. Pressure generated from the accumulation of urine in the urinary bladder forces the bladder wall to contract and leads to the urge of urination. The urine is then discharged from the bladder via the urethra, which is a thin tube that carries urine from the bladder to the outside of the body.

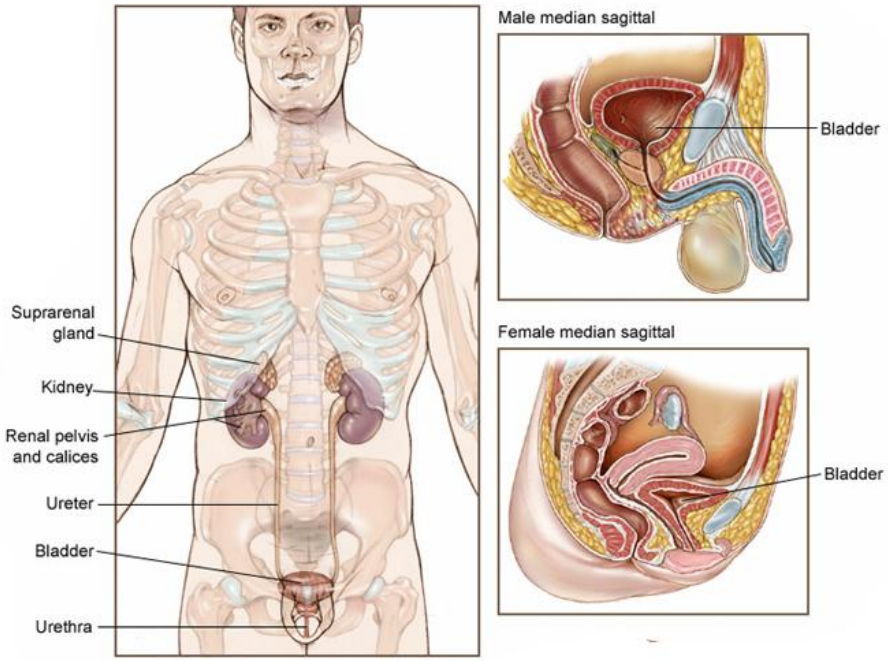

Figure 1.1 Human urinary system

(Adapted from website: http://www.cancer.net/portal/site/patient (1))

The wall of the bladder is comprised of several different layers of tissues that are important in understanding the development, progression, and treatment of bladder cancer. A cross-sectional view of the bladder wall (Figure 1.2) reveals the following layers of cells:

- Epithelium - A layer of cells that lines the interior side of the bladder wall and is also known as the urothelium or transitional epithelium. The vast majority of bladder cancers originate in this layer.

- Lamina propria - A layer of connective tissue and blood vessels located immediately beneath the transitional epithelium.

- Muscularis propria - Deep layer of muscle cells that form the wall of the bladder which is responsible for contraction during urination.

- Perivesicle soft tissue – The outermost layer of the bladder wall that consists of fat, fibrous connective tissue, and blood vessels. Bladder cancer that spreads to the perivesicle soft tissue is considered as metastasis.

As the cancer grows through the bladder wall layers, treatment becomes more challenging.

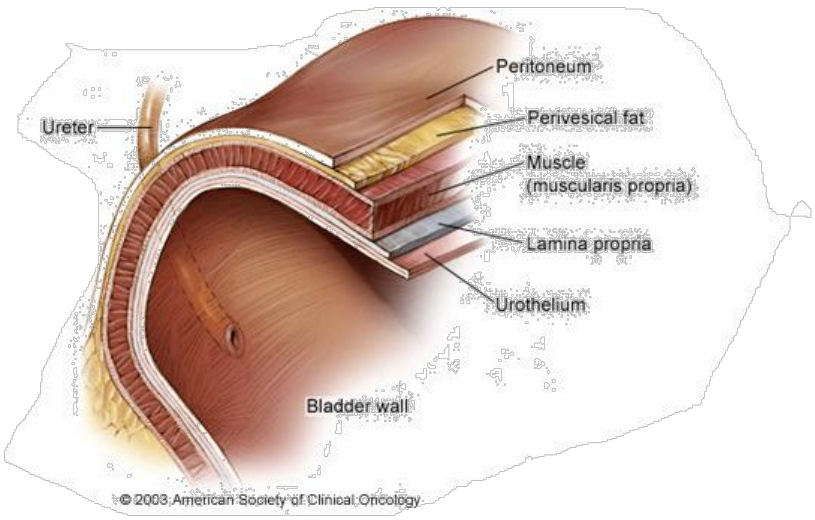

Figure 1.2 Cross section of bladder wall showing the tissue layers

(Adapted from website: http://www.cancer.net/portal/site/patient (1))

1.1.2 Types of Bladder Cancer

Bladder cancer is a heterogeneous disease that forms within the tissue layers of the urinary bladder. There are four primary types of bladder tumors that can be distinguished on the basis of the appearance (morphology) of the cells under microscope:

• **Transitional cell carcinoma (TCC)** - Also known as urothelial carcinoma, this type of bladder cancer affects the transitional epithelium that lines the wall of the bladder. In the United States, more than 90% of bladder tumors are classified as transitional cell carcinomas.

• **Squamous cell carcinoma** - This type of bladder cancer represents only about 4% of all bladder tumors. It is most commonly associated with chronic irritation of the bladder, such as long-term indwelling bladder catheters or bladder calculi (stones). Squamous cell carcinoma of the bladder has also been linked to schistosomiasis, a tropical disease spread by parasitic trematode worms, which is endemic in Africa and Middle East.

• **Adenocarcinoma** - This is an extremely rare form of bladder cancer accounting for less than 1% of all bladder tumors. It tends to occur in mostly younger patients.

• **Small cell carcinoma** - This type of bladder cancer is also very rare and represents about 1% of all bladder tumors.

1.1.3 Different stages of transitional cell carcinoma

Bladder cancer can be broadly classified into non-muscle-invasive and muscle-invasive tumors. Different stages of bladder cancer are indicated in Figure 1.3.

Non-muscle-invasive bladder cancer comprises of 70 % of all clinical cases. It spreads across the urothelial lining (Stage Ta) and lamina propria (Stage T1) of the bladder but do not penetrate deeply into the bladder wall, hence is collectively known as superficial TCC. Carcinoma in situ (CIS) is another type of non-invasive cancer that appears as red, ulcerated area in the bladder. Unlike TCC, cancer cells in CIS, if not treated effectively, can proliferate quickly and progress to invasive cancer. Approximately 70% of patients are diagnosed as having Ta, 20% as T1, and 10% with CIS lesions in the latest collaborative review of bladder cancer (2).

The muscle-invasive bladder cancer refers to the bladder tumor that is either invading the muscularis propria, which is the deeper layer of muscle cells that forms the wall of the bladder (Stage T2), or the perivesical fat located beyond the bladder muscle (Stage T3, T4). They carry higher risk of metastasis, i.e. spread beyond the bladder to other body parts. About 15 % of the non-invasive cancers eventually become invasive, yet there is no known diagnostic method that can accurately predict progression.

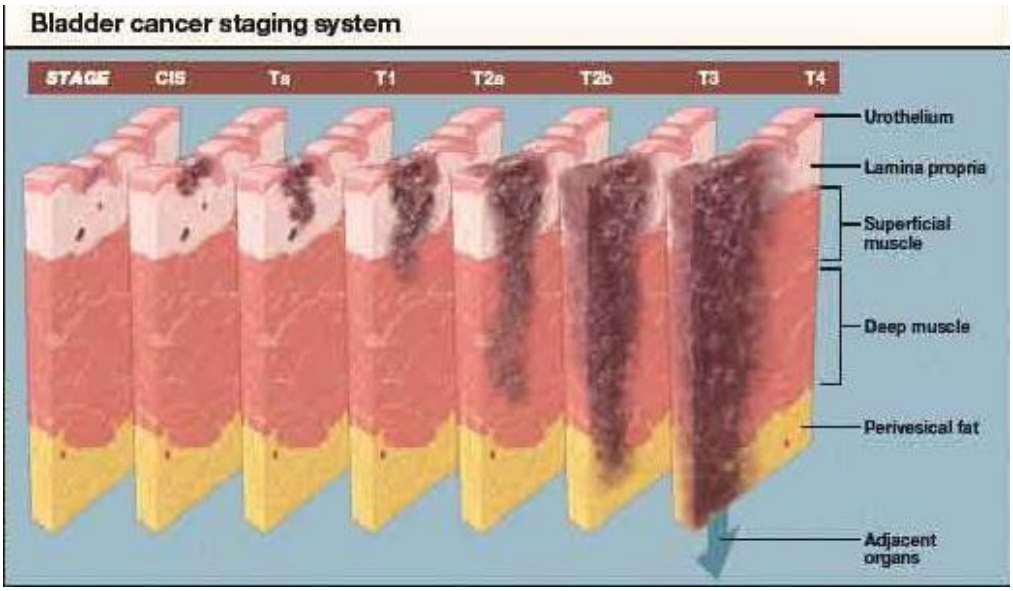

Figure 1.3 Illustration of the definitions of primary tumor (T) for primary bladder cancer, ranging from Ta to T4.

(Adapted from http://www.montereybayurology.com(3))

1.2 Epidemiology and Etiology of Bladder Cancer

1.2.1 Statistic of bladder cancer

An estimated 69,250 (52,020 males and 17,230females) new cases of bladder cancer and 14,990 deaths (males: 10,670 and females: 4,320) were reported by the United States in 2011, making it the fourth most prevalent cancer in men (4). In Hong Kong, census from the Department of Health indicated that there were 374 new cases of bladder cancer in 2008, with 283 and 91 cases for male and female respectively (Figure 1.4), and the mortality rate is 35% (5). In general, male has around 3 times higher risk of developing bladder cancer than female. Besides, bladder cancer is most frequently found in the age between 50 and 70, especially if there is a known family history of bladder cancer (6). According to the data provided by the US National Cancer Institute, bladder cancer is most prevalent in Caucasian, followed by the Blacks, then Asians (Figure 1.5).

Occupational exposures to carcinogens is one of the major causes of bladder cancer (7). In the United States, approximately 25% of the bladder cancer diagnosed among white men is due to occupational exposures (8). Chemical carcinogens, such as 2-naphthylamine, benzidine, and 4-aminobiphenyl, are tightly related to several occupations, such as painting, leather processing and hairdressing. Occupants are frequently reported to develop bladder cancers (9). On one hand, long-term exposures to these chemicals certainly increase the risk for getting bladder cancer;

On the other hand, delay of voiding, due to occupational needs, will also lengthen the time of contact between these chemicals and the urothelial cells, and thus further increases the risk of developing the cancer.

Besides, cigarette smoking is the most critical risk factors for contacting bladder cancer. It is widely known that there are more than 30 carcinogens inside a cigarette, and smoking is equivalent to chronic exposure to all these carcinogens (10). In US, about 50% of the bladder cancer attributes to cigarette smoking in both men and women (11). When compared to the nonsmokers, smokers have two- to three-fold increase in risk of developing the disease (12, 13). Moreover, the risk is thought to be dose-dependent as the people who stop cigarette smoking possess an intermediate risk between smokers and nonsmokers (14).

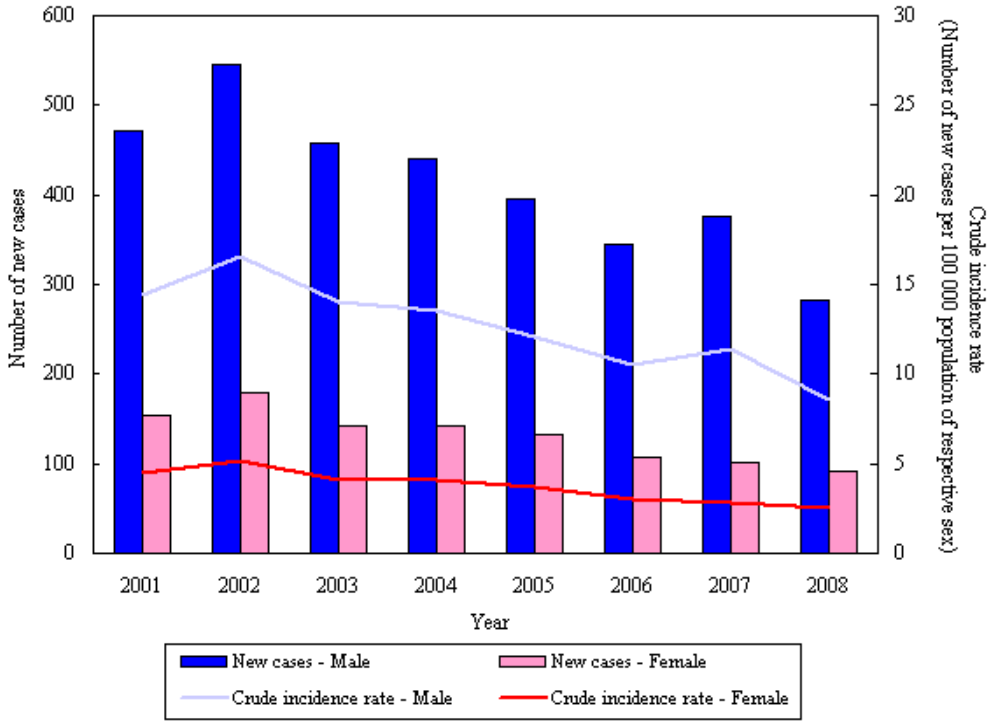

Figure 1.4 Number of new cases and crude incidence rate of malignant neoplasm of bladder by sex from 2001 to 2008. (5)

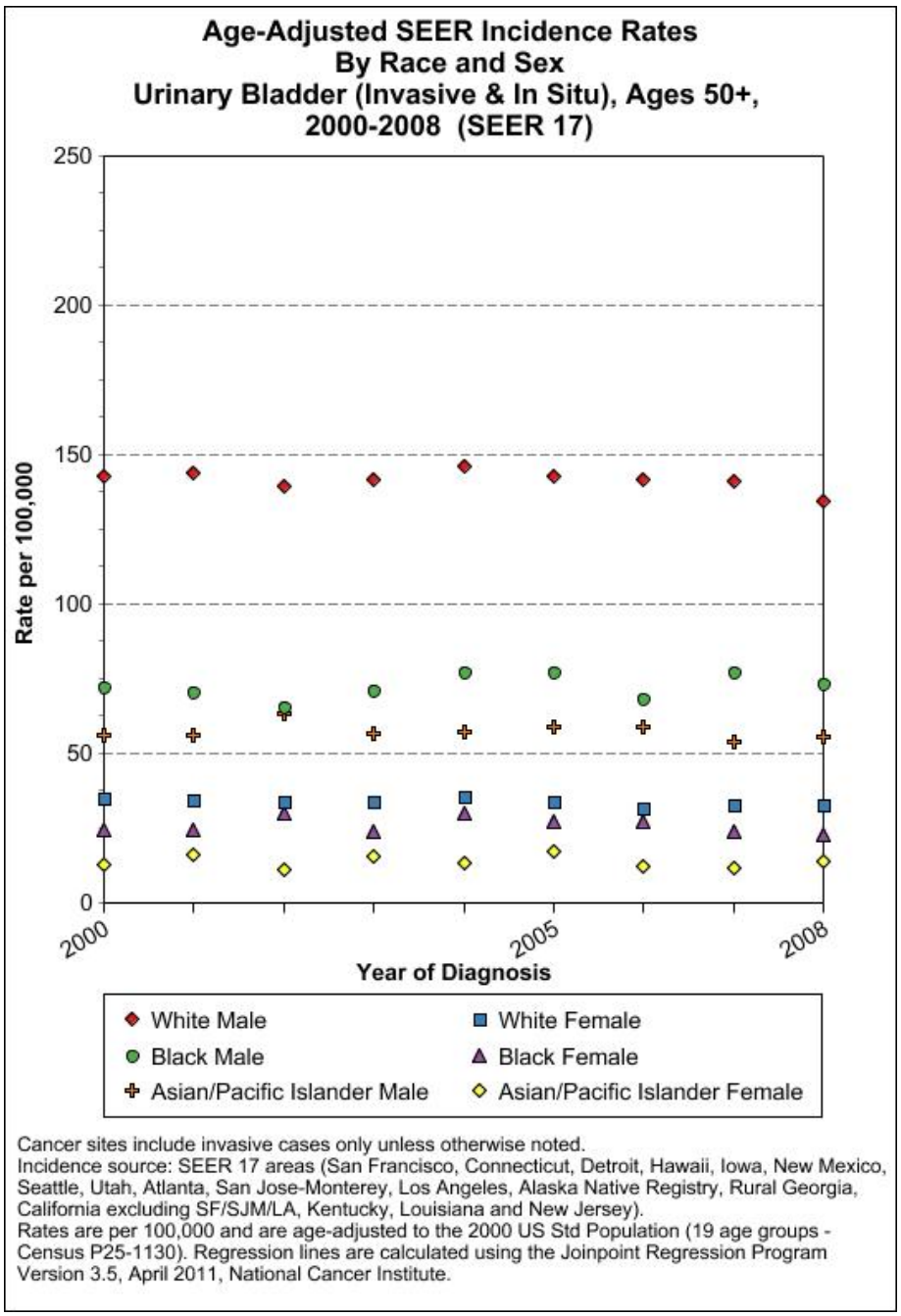

Figure 1.5 Incidence rates of bladder cancer in different races.

(Data extracted from http://seer.cancer.gov/ (15))

1.2.2 The linkage between 4-ABP and bladder cancer

Studies found that smoking is the major cause of bladder cancer due to chronic exposure to carcinogens, particularly 4-aminobiphenyl (4-ABP), in the cigarette (10, 16-18). 4-ABP is a tobacco constituent, environmental contaminant and well-known carcinogen. Its molecular structure is shown in Figure 1.6. It is often applied in biological research as surrogate model of carcinogen, mainly due to its high stability, long half-life and commercial availability. In this study, 4-ABP was chosen as the stimulant for *in vitro* transformation.

Study has suggested that 4-ABP is effectively bio-activated in biological system via various pathways, such as N-hydroxylation mediated by the hepatic cytochrome P450 enzymes (19, 20) and oxidation by prostaglandin H synthase in urothelium (21). The resultant metabolites, such as N-OH-ABP, are highly reactive and forms covalent bonds with chromosomal DNA (22) resulting as DNA adducts (16), which ultimately lead to chromosomal instability (23).

As a result of DNA damage, cell cycle checkpoints normally initiate signals to halt proliferation and activate repairing mechanisms. Apoptosis is elicited if the damage is too extensive or irreparable. It is generally believed that, in certain circumstance, the DNA is mis-repaired and the mutated cell escaped from the cell cycle checkpoints. Unregulated proliferation of the mutated cell ultimately forms the tumor. The possible pathway for causing bladder cancer by 4-ABP is shown in Figure 1.7.

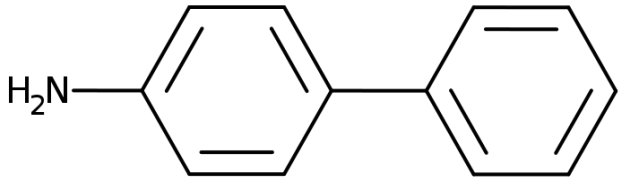

Figure 1.6 Structure of 4-Aminobiphenyl.

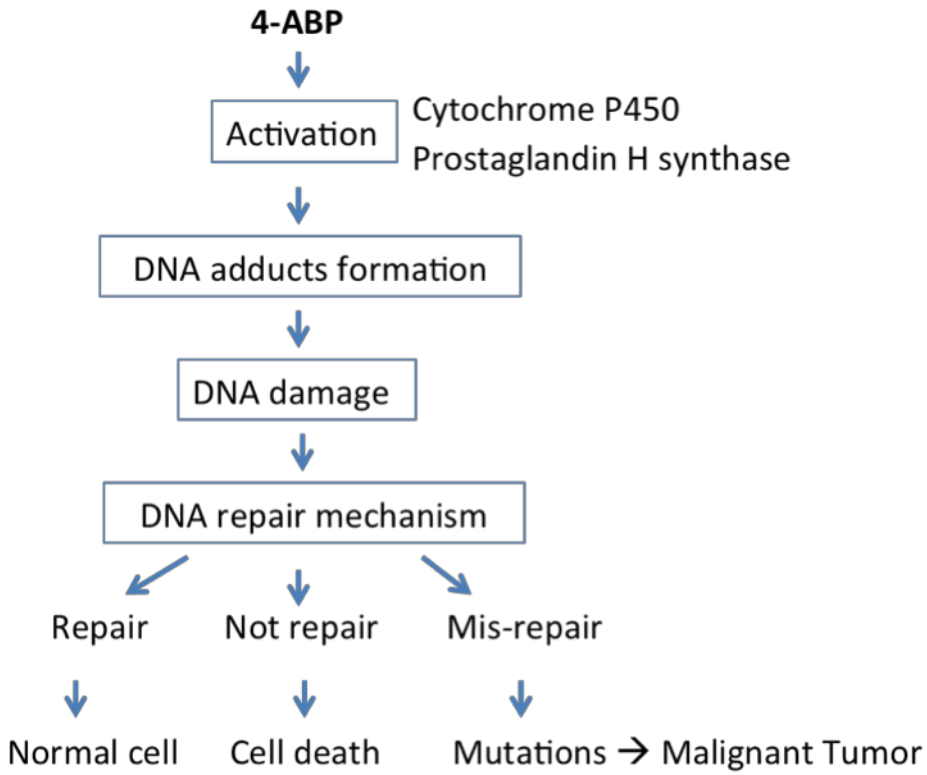

Figure 1.7 Possible pathway for causing bladder cancer by ABP.

1.3 Genetic view of bladder cancer

1.3.1 Divergent pathways of bladder cancer

In the view of genetics, deletions in- or partial loss of chromosome 9 have been commonly found in superficial TCC of all stages and grades (24). Alterations of chromosome 9 occur during early stages of the disease and seemed to be involved in the cancer development. Genetic divergence generally occurs after its alterations and gives rise to different grades/stages of bladder cancer.

Superficial TCC and invasive bladder cancer are thought to arise from different molecular pathways as illustrated by Figure 1.8. Invasive cancer is generally characterized by alterations in the p53 and retinoblastoma pathways (25), while superficial TCC commonly arise from the mutations in *HRAS* (V-Ha-ras Harvey rat sarcoma viral oncogene homolog) and *FGFR3* (fibroblast growth factor receptor 3) genes. Previous studies showed that there is a high frequency of mutations in the *FGFR3* (30-80%) and *TP53* (70%) among superficial TCC and invasive bladder cancers, respectively (26). Bakkar et al (2003) found that *FGFR3*mut/*TP53*wt was the most prevalent genotype (68%) in Ta stage, but non-existent in muscle invasive cancer (27). *FGFR3*mut/*TP53*mut genotype was found in very few tumors manifesting that the mutations in these two genes were nearly mutually exclusive. However, the *FGFR3*wt/*TP53*wt genotype accounted for a considerable proportion of tumors (29% of Ta and 50% of T1). This indicates that other pathways are also involved in bladder tumorigenesis.

Although existing study showed that expression of *FGFR3* is a characteristic of low-grade and low-stage urothelial carcinoma, as well as has a prognostic value for recurrence-free survival (28), its role as recurrence predictor is still controversial (29).

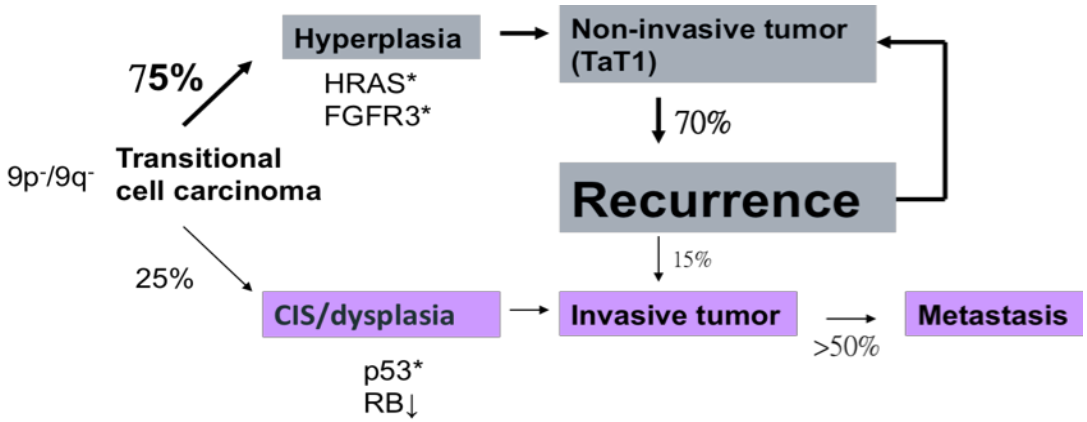

Figure 1.8 A schematic diagram showing the divergent pathways of bladder cancer progression.

1.3.2 Gene expression study for bladder cancer

The cDNA microarray, originally developed by Schena et al in 1995 (30), is now a widely used tool for high-throughput and multiplex gene expression profiling. This technology provides a cost-effective, holistic overview of the genomic/transcriptomic changes during cancer development and facilitates the identification of specific genes and pathways involved. Microarray-based transcriptomics have been applied in many clinical studies to predict the clinical outcome of patient (31-35). From a cDNA microarray analysis, Dyrskjot et al (2003) identified a panel of 26 genes to predict the recurrence of bladder cancer patient (32), but the result is not reproducible (36, 37). Recently, Kim et al (2011) identified a four-gene signature (*IL1B*, *S100A8*, *S100A9* and *EGFR*) as prognostic indicator for cancer progression in muscle invasive bladder cancer (38), but the result is not consistent with the findings from previous study (35). It is generally recognized that microarray analysis can be very helpful in identifying the gene expression pattern of the disease, but any proposed signature of prognostic value must be validated using a large number of samples prior to clinical application. The next generation of the bladder cancer management will embrace the use of multimarker panels for prognostic prediction and shift to targeted therapy that aims at bladder cancer-specific biomolecules.

1.4 Major obstacle in bladder cancer treatment

1.4.1 Management of transition cell carcinoma

Transurethral resection (TUR) is the most typical treatment for early-stage bladder cancers, the superficial TCC. Common treatments and management of primary non-muscle-invasive bladder cancer are indicated in Figure 1.9. A Population-based study conducted in 1992 showed that from 535 patients with superficial TCC, more than 90% of patients were treated with TUR alone (39). In essence, TUR is simply having a cystoscope inserted into the bladder via urethra and the bladder tumor was scraped off from the bladder wall using a small wire loop or fulgurated by the use of laser or electrocautery.

Adjuvant intravesical chemotherapy is commonly applied, following TUR surgery, to the patients. This therapy is almost always mediated by the administration of Bacille Calmette-Guérin (BCG), an attenuated strain of the bovine tuberculosis bacteria, into the urinary bladder via a urinary catheter. While BCG is widely used as a vaccine against tuberculosis, its treatment effect on bladder cancer is puzzling, nonetheless proven effective. There are two proposed pharmaceutical mechanisms of BCG on bladder cancer: the immune response generated by BCG stimulation in the bladder also activates the immune system against the cancer cells (40-43); or, the inflammation caused by a BCG infection is toxic to the cancer cells (44). However, not all patients are suitable for BCG treatment due to its side effects, such as bacterial cystitis and dysuria, hematuria, and low-grade pyrexia. Others

immunotherapy agents such as Interferon or chemotherapy medicines like valrubicin (Valstar), mitomycin C, epirubicin (Ellence), or doxorubicin (Adriamycin) can also been used.

Yet, regardless of the combinations of treatment received, there is an inevitable high risk of recurrence in bladder cancer patients, which will be discussed as follows.

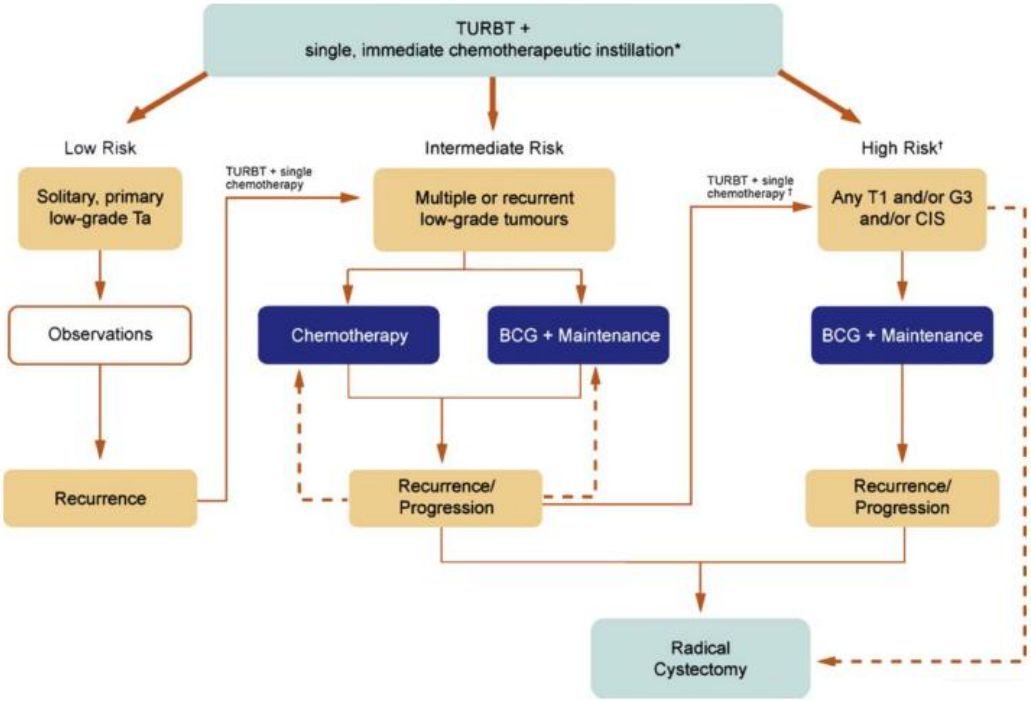

Figure 1.9 Algorithm for the treatment and management of primary non–muscle-invasive bladder cancer proposed by the International Bladder Cancer Group. (Adapted from Lamm et al, 2008(45))

Superficial TCC is primary treated with TUR. Risk of recurrence or progression is depending on the tumor grade and previous history. Chemotherapy is applied for the patient with high risk of recurrence. Surgical removal of the urinary bladder is the last resort for patient with high recurrence rate.

1.4.2 Recurrence in superficial transitional cell carcinoma

Nowadays, one of the biggest challenges in bladder cancer treatment is the high frequency of recurrence in superficial TCC. After TUR surgery, the recurrence rate is as high as 60% within one year (46). Despite adjuvant treatment is commonly applied to suppress recurrence, 15.7% and 45.8% of patients with single and multiple tumors, respectively, experienced tumor recurrence within three months (47). Furthermore, 10-30% of the recurrent tumors may progress to a higher grade and/or stages. Recurrent tumor usually appears at the original tumor site or, sometimes, other parts of the body. Such phenomena are generally described as intraepithelial migration and intraluminal seeding from primary carcinoma, respectively (48). Therefore, a lifelong follow-up by regular cystoscopy is necessary for these patients, making bladder cancer the fifth most expensive cancer in terms of total medical care expenditures (49). The management of bladder cancer, particularly surveillance for recurrence and treatment of eventual recurrences, results in major clinical and economic burdens (50). Therefore, reducing recurrence may significantly lower the cost of health care. The distribution of the medical cost for each bladder cancer patient at M.D Anderson is illustrated in Figure 1.10.

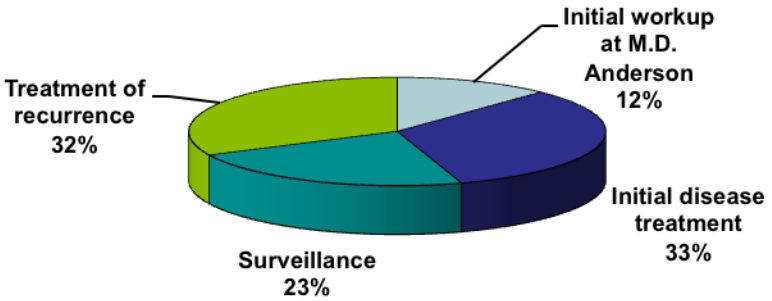

Figure 1.10 Medial care expenditures for each patient with superficial transition cell carcinoma at M.D Anderson.

1.4.3 Possible reasons for the high recurrence rate

Many researchers devoted to pursuit the cause of recurrence in bladder cancer and four mechanisms of the recurrence are proposed (51):

1. Incomplete resection of the primary tumor;
2. Tumor cell re-implantation;
3. Growth of microscopic tumors present at the time of resection; And
4. New tumor formation.

Among these proposed mechanisms, incomplete resection (#1) is the most probable cause of early cancer recurrence (52). Grimm *et al*. found that residual tumor was frequently located at the site of initial TUR (81%). Also, as reviewed by Hoglund, majority of the recurrence are proven to be monoclonal (53), i.e. originated from the same parental cell mass. Both findings suggested that residual cells from incomplete initial surgery might stem the future recurrent tumor (54, 55). These residuals cells may have substantial genetic mutations, but not yet tumorigenic, and present the same morphology as the normal urothelium (48, 56). As a result, they were not identified and removed during surgery.

The existence of phenotypically normal but genetically aberrant cells that fuelled subsequent tumor formation has long been recognized. Slaughter et al. hypothesized the whole field of tissue has increased risk of cancer development after exposure to carcinogen and thus coined the term "field cancerization" (57). Hoglund further expanded this theory by a normal-chronic-acute phase model (48). In this model (Figure 1.11), a field of premalignant cells is formed through the exposure to carcinogen. The cells within this field continuously accumulate genetic changes during cell division or exposure to carcinogens. Because of the randomness of mutations, some of the cells will acquire additional aberrations at different chromosomal location at different rate. It is rationalized that the heterogeneous levels/positions of mutations among the cells in the field leads to asynchronous advent of criticality and, hence, appearance of tumors, with those that formed before surgery were routinely called 'primary' and those that emerged after surgery were classified as 'recurrent' (58, 59). This model is supported by a study in attempt to

classify the biopsy specimens from 30 bladder cancer patients to the categories of "tumors", "bladder epithelium adjacent to the tumor" and "random distant bladder epithelium" using cancer markers (60). It was found that biochemical alterations in bladder tissue are often detectable before the appearance of any pathological sign, and the tumor markers were expressed in the morphologically normal tissue samples that were distant from the tumors.

Understanding these phenotypically normal but genetically aberrant cells will, with no doubt, helps to explain not only frequent recurrence, but also the tumorigenesis of bladder cancer. To facilitate the following discussion, these cells are termed "sensitized cells", i.e. cells that can easily become malignant in response to additional minor mutations ('sensitive') and fuel new tumor formation. However, the exact trigger(s) for these cells to become cancerous has not yet been identified.

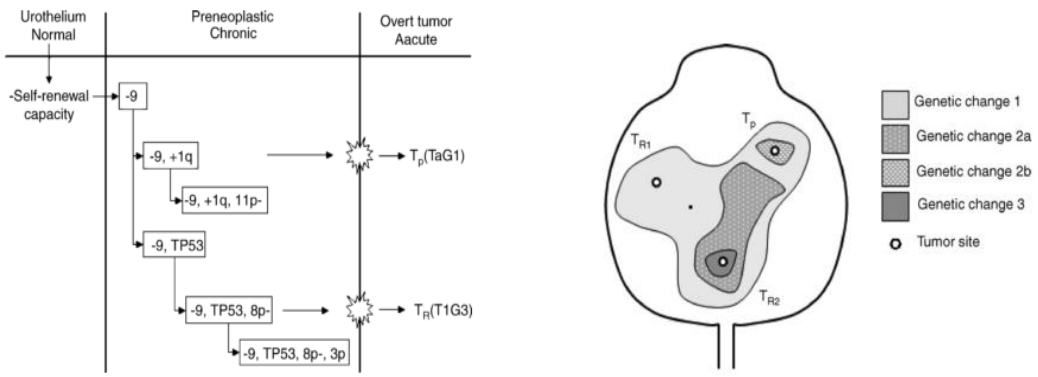

Figure 1.11 A schematic representation of normal-chronic–acute phase model. (Adapted from reference (48))

1.5 Molecular markers of bladder cancer detection

As a result of the high recurrence rate in bladder cancer, a lifelong surveillance by scheduled cytoscopic evaluation is needed for the patients who suffer from superficial TCC. Markers for bladder tumor were then raised to provide a convenient and non-invasive method so as to reduce the cost and discomfort of regular detection. Currently available bladder cancer markers are listed in Table 1.1. Six tumor marker tests, including BTA-Stat, BTA Trak, Nuclear Matrix Protein 22, bladder chek, ImmunoCyt test and UroVysion test, have been approved by the United States Food and Drug Administration (FDA) for routine patient monitoring. Although this, the above tests are not commonly used clinically because of the high false-positive rate or even low sensitivity and thus their diagnostic performances are still evaluating. For these reasons, there is a need for new markers for diagnosis and follow-up of bladder cancer. There are many potential markers such as survivin and telomerase that are being investigated.

Table 1.1 Currently available urine markers for bladder cancer

(Adapted and modified from (61))

Cancer Marker	Proposed Uses	FDA approved
BTA Stat	Early Detection/ Monitoring for recurrence	Yes
BTA Trak		
NMP22		
Bladder Chek		
Immunocyt		
UroVysion		
Hyaluronic acid	Clinical Research	No
Telomerase		
Survivin		
BLCA-4		
Microsarellite markers		
Cytokeratin 8, 18, 19		
DD23monoclonal antibody		
Fibronectin		
HCG – protein and mRNA		
DNA promotor regions of hypermethylated tumor suppressor and apoptosis genes		
Proteomic profiles (Mass spectrometry)		

1.5.1 Bladder tumor antigen

Complement factor H-related proteins (CFHR) are usually found in the urine of bladder cancer patient. CFHR interrupts the complement cascade and protects cells from lysis by complement proteins *in vitro*. Production of CFHR may confer a selective growth advantage to cancer cells *in vivo* by allowing the cells to evade the host immune system. CFHR is one of the most widely applied bladder tumor marker and sometime aliased as 'bladder tumor antigen' (BTA). Qualitative point-of-care assay in the form of test trip and quantitative test in standard enzyme immunoassay format for this marker are commercially available as BTA stat® and BTA TRAK® from Polymedco Inc. Despite these assays are seemingly promising in bladder cancer diagnosis, sensitivity for superficial (Tis, Ta, T1) and invasive (T2-T4) tumors are report to be 50-60% only, and the specificity is as low as 72%. False-positive test results are also reported in patients with infection in the urinary system (62), and thus they are not recommended for cancer screening or diagnosis (61).

1.5.2 Nuclear Matrix Protein 22

Nuclear Matrix Protein 22 (NMP-22) is a nuclear mitotic apparatus protein involved in proper distribution of chromatin to daughter cells during cellular replication. It may be released from the nucleus of tumor cells during apoptosis. NMP-22 BladderChek test (Matritech) is a flow immunochromatographic assay that detects the amount of nuclear mitotic apparatus protein with cutoff 10U/ml. Although NMP22 test is approved for clinical application by FDA, a large prospective

validation study which included 1609 subjects monitoring from 2003 to 2010 showed that its specificity was only 28.57% (63). The study concluded that NMP22 results are affected by haematuria, infection and concentrated urine, thus it is not recommended for BC screening.

1.5.3 ImmunoCyt test

ImmunoCyt test from Diagno-Cure Inc. detects bladder cancer markers (carcinoembryonic antigen and mucin) on exfoliated cells using a panel of three fluorescent monoclonal antibodies (64). 19A211 labeled with Texas red identifies a high molecular weight form of carcinoembryonic antigen, while M344 and LDQ10 labeled with fluorescein are directed against mucins (65). These antigens were expressed preferentially on low-grade superficial bladder (66) and claimed to have a high sensitivity in certain studies (64, 67). However, the promising results could not be confirmed in other studies (65, 68). In addition to controversial results on its sensitivity, this test is quite labor intensive and a high amount of urine is needed (65).

1.5.4 UroVysion test

UroVysion test (Abbott Diagnostics) is a multi-target fluorescence *in situ* hybridization assay for detecting aneupoloidy for chromosomes 3 (red), 7 (green), 17 (aqua) and loss of the 9p21 (gold) locus which are associated with bladder cancer (69). It works by detecting the above chromosomal abnormalities in urinary cells. Studies showed that UroVysion is more sensitive than urine cytology for bladder cancer detection (70, 71). However, this test is more expensive than

traditional cytology testing. Besides, it is a labor-intensive and complex test which requires highly trained personnel and sophisticated equipment (72) making it difficult to adopt in routine practice.

1.5.5 Telomerase activity (TA)

In human, telomere is a repetitive sequence of TTAGGG located at the ends of chromosome. It stabilizes and protects the chromosome from end-replication problem (73). It is generally recognized that telomere length is one of the key factors that limit cell proliferation. Telomere shortens by 50-200bp during each cell division, and the cell will be forced to enter senescence when telomeric length decreases to a certain threshold (74). This mechanism imposed a limit on the number of rounds of cell divisions, which is now known as Hayflick limit (75).

Telomerase is an RNA-dependent DNA polymerase that stabilizes and maintains the telomere. When recruited to the chromosomal ends, telomerase adds TTAGGG repeats to the telomere via reverse transcription using its intrinsic RNA template (76). While the proliferation of normal cell is limited (77), tumor cells express a higher level of telomerase to maintain a constant telomeric length which allows them to divide indefinitely (78). Telomerase activity (TA) is proposed to be a marker of bladder cancer (79-84). A study showed that telomerase activity was detected in 39 out of 40 bladder tumors but no activity was found in the normal tissues (82). Also, tumors with high telomerase activity showed a higher grade and invasiveness. Similar study was done on the exfoliated cells in 109 urine samples, in which the sensitivity and specificity for TA in bladder cancer detection were 62% and 96%,

respectively (80). A comparative study of NMP-22, BTA and telomerase in bladder cancer detection indicated that telomerase activity demonstrates the highest specificity among the bladder cancer markers (85).

1.5.6 Survivin

Survivin is a member of the inhibitor of apoptosis protein (IAP) family, which has been implicated in inhibition of apoptosis and control of mitotic progression by interfering caspase activities (86, 87). Since its expression is high in cancer cell but usually undetectable in normal tissue, it is a candidate marker for superficial bladder cancer (88). Result from a multicenter study also suggested that survivin could be a prognostic marker for bladder cancer (89). Another study even showed that survivin outperformed the NMP22 test for bladder cancer detection (90). A recent systematic review of urine-based survivin test using simple real-time PCR was reported to be 80% sensitive and 93% specific for bladder cancer detection (91).

1.5.7 Hyaluronic acid (HA)

Hyaluronic acid (HA) is a nonsulfated liner glcosaminoglycans that widely distributed throughout the neural, connective and epithelial tissues. HA is synthesized by hyaluronan synthase (HAS) which consists of three isoforms: HAS1, HAS2 and HAS3 (92). They lengthen HA by adding glucuronic acid and N-acetylglucosamine to the nascent polysaccharide repeatedly, through the cell membrane into the extracellular space. The molecular structure of HA was showed in Figure 1.12. As a main component of extracellular matrix, HA involves in

different process of cancer development included cell proliferation, migration and progression. The major cell surface receptor for HA is CD44 (93). Their binding was proved to be involved in cancer development (94).

On the other hand, the role of HAS in cancer development have been widely investigated. HAS1 overexpression has been shown to promote tumor growth and invasion in bladder cancer cell line by modulating HA synthesis (95). HAS2 was reported to function in controlling the cell growth and migration in breast cancer cell lines (96, 97). Overexpression of HAS3 was shown to enhance tumor cell growth, extracellular matrix deposition, and angiogenesis of prostate cancer cell line (98). It is believed that the HAS control the malignant phenotype of cells by modulating the synthesis of HA (95, 96).

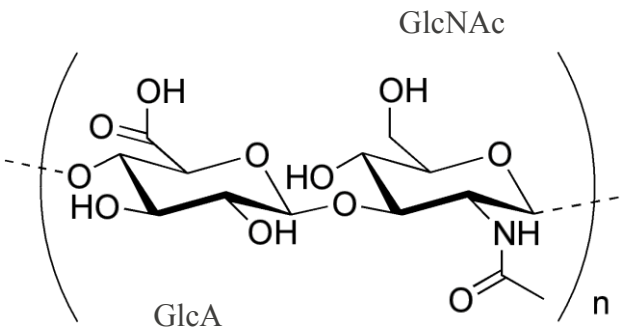

Figure 1.12 Molecular structure of hyaluronic acid.

It composes of repeating polymeric disaccharides D-glucuronic acid (GlcA) and N-acetyl-D-glucosamine (GlcNAc) linked by a glucuronidic (1–3) bond.

1.6 Tumor initiating cell marker- CD44

1.6.1 Tumor initiating cell

There are accumulating evidences supporting that primary and recurrent tumors are derived from a minor population of cells, which is called tumor initiating cell or cancer stem cell, through clonal expansion. Similar to normal stem cell, this kind of cells is highly proliferative and capable of self-renewal. The cancer stem cells can recreate heterogeneity of the parental tumor, and seemed to be more resistant to anticancer drugs than other cancer cells. The origin of these cells has yet to be known. It is theorized that they are generated from mutated stem cells that cannot regulate its proliferation, or from progenitor cells that acquire self-renewal ability through differentiation.

Isolation of such cells can be achieved by studying the differential expression of a panel of stem cell markers which included CD44, CD133, CD49f/integrinα6, CD166, CD105 and markers that define epithelial differentiation such as CD24 (99). Recent studies have shown that CD44 can also be used as a marker for isolating the tumor initiating cell from a wide range of cancers, including breast (100), colon (101, 102), gastric (103), prostate (104, 105) and bladder cancer (99). The cell surface markers can be used together for the selection of tumor initiating cells e.g. $CD44^{+}CD24^{-}$ for breast cancer cell (100), $CD133^{+}/CD44^{+}$ for colon cancer cells (101), and $CD44^{+}$/alpha2beta1hi/$CD133^{+}$ for prostate cancer cells (104). All these studies

reported that $CD44^+$ cancer cells are more tumorigenic, clonogenic and metastatic than $CD44^-$ cells.

1.6.2 Introduction of CD44

CD, which stands for "cluster differentiation", is a class of glycoproteins on the cell surface that act as identifying markers and define the function of the cells. CD44 molecule belongs to a family of polymorphic transmembrane glycoproteins and presents on a wide range of normal and malignant cells in epithelial, mesothelial and hemopoiesis tissues. CD44 is encoded by a single gene located on chromosome 11p13. Its structure composed of an amino-terminal domain, hyaluronan binding domain, a stem region, a transmembrane domain and a cytolasmic domain. The protein structure of CD44 is illustrated in Figure 1.13. The stem region is the primary site for alternative splicing. The most abundant (standard) form of CD44 (CD44s; 85-95 kDa) is formed by splicing out all 9 variable exons but the first and last 5 exons remains. Alternative splicing of the central 9 variable exons, as well as posttranslational modification generate multiple variants (CD44v). Examples of alternative spliced CD44 such as exon v3 containing CD44 isoforms (CD44v3) are shown in Figure 1.14.

CD44 is a well-known receptor for hyaluronic acid, collagen, laminin, and fibronectin. It binds with its ligands via the binding sites in amino-terminal domain and interacts with actin-binding proteins (ankyrin, ERM proteins, merlin), non-receptor kinase (Src) and signal transducers (PI3K/ Akt, MAPK) with its cytoplasmic domain (106). It controls cellular activities such as cell-cell interactions,

cell adhesion and migration, lymphocyte activation, recirculation and homing, and hematopoiesis via associations of cytosolic proteins and growth factors.

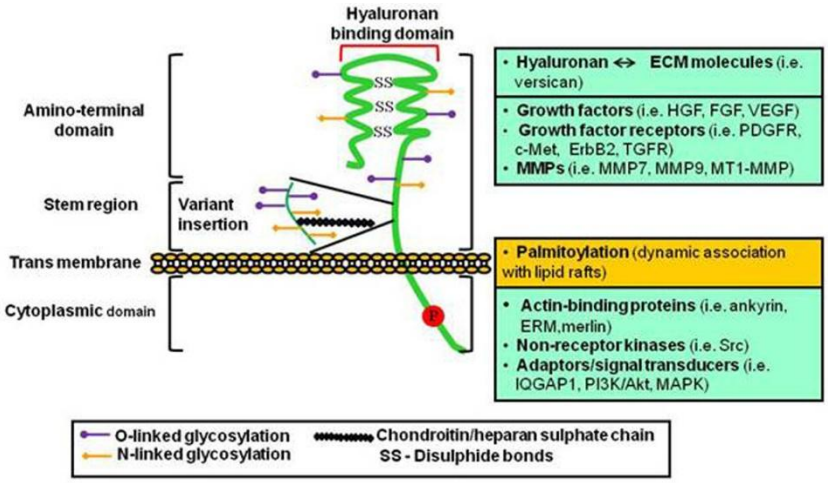

Figure 1.13 The protein structure of CD44. (Adapted from (106))

The function of CD44 is depended on its structural modification which included: A) alternative splicing in extracellular proximal domain (red) that generate different variants; B) *N*-glycosylation (orange) and *O*-glycosylation (purple).

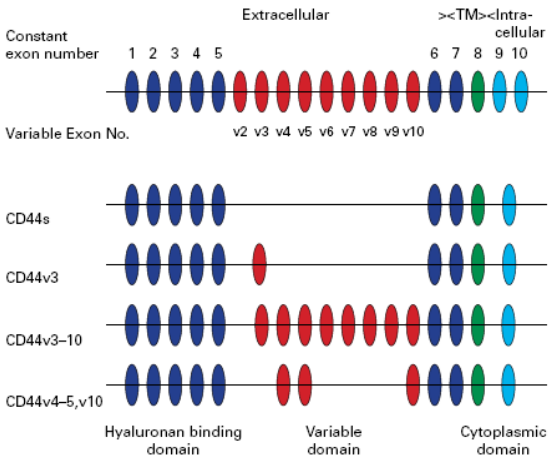

Figure 1.14 The gene structure of CD44 and it variants.

Different variants are generated by alternative splicing of exon in the extracellular membrane (Adapted from Sneath and Mangham, 1998 (107)).

1.6.3 CD44 in cancer development

In addition to its functions in normal cells, CD44 plays a vital role in cancer development, which is summarized in Figure 1.15. As a multifunctional cell surface receptor, CD44 can detect the change of extracellular matrix components and co-ordinate signaling events that enable the cell to response. The signaling output of CD44-involved pathways, including induction of inflammation, promoting cell proliferation and migration and inhibition of apoptosis, are strongly related to cancer development (discuss detail in review (108)).

Indeed, it has been suggested that it is the CD44-Ligand complex, instead CD44 alone, mediates the tumor-like phenotypes. Cell adhesion formed between CD44 and HA plays an important role in cell migration, tumor growth and progression (106, 109-111). A cluster of four amino acids (Arg-41, Tyr-42, Arg-78 and Tyr-79) within extracellular distal domain is essential for HA binding (112). Many studies indicated that CD44-HA binding causes cytoskeletal reorganization that leads to cell proliferation, invasion and migration (113-116). Bourguignon *et al*, showed that CD44 – HA signaling can activate c-Src-mediated twist signaling through induction of specific intermediates which included RhoA/RhoC leading to rearrangement of actin cytoskeleton (115). Their interaction can also activate EGFR-mediated signaling pathway to promote cell migration and chemotherapy resistance (116). Besides, HA fragments were shown to activate NF-κB in a diversity of cell lines that expressed CD44 (117). The triggered chronic inflammation may induce proliferation ability of tumor cell (118).

Moreover, CD44 can also bind with other ligands such as osteopontin to activate phosphoinositide 3-kinase (PI3K) and Akt, initiating the expression of the anti-apoptotic genes, hence suppressing apoptosis (119). Furthermore, binding between CD44 and receptor tyrosine kinases, such as ERBB1 and c-Met receptor, is found to be playing a vital role in tumor progression (120).

The relationship between CD44 is well illustrated by its high abundance in most bladder carcinoma cell line (121) and the characteristic expression pattern in the urothelium at different tumor stages. Immunohistochemical analysis of CD44 in normal bladder urothelium revealed that CD44 is expressed primarily in basal layers (Figure 1.16). This layer consists of cells possessing undifferentiated phenotype and displaying characteristics of adult tissue progenitor and transit amplifying cells. For the neoplasmic bladder, both basal and superficial cells are CD44-positive but the expression decreases along with tumor dedifferentiation and advancing pathologic stages (99, 122-124) (Figure 1.17).

Besides, CD44 variants are postulated to have different roles in bladder cancer development. For example, a study examined 55 tissue samples of TCC found that the expression of CD44v10 was positively related to tumor recurrence and the expression of CD44v5 showed the opposite (125). Another study even suggested that CD44v6 was a bladder cancer initiating cell marker (126). Specificity and sensitivity of CD44 as cancer marker were extensively investigated and summarized in Table 1.2 (123, 127-131). Recently several papers reported that the expression of CD44s and CD44v6 was correlated with the grade and stage of bladder cancer (122, 132).

The expression profiles of them are of great interest to be study in bladder cancer development.

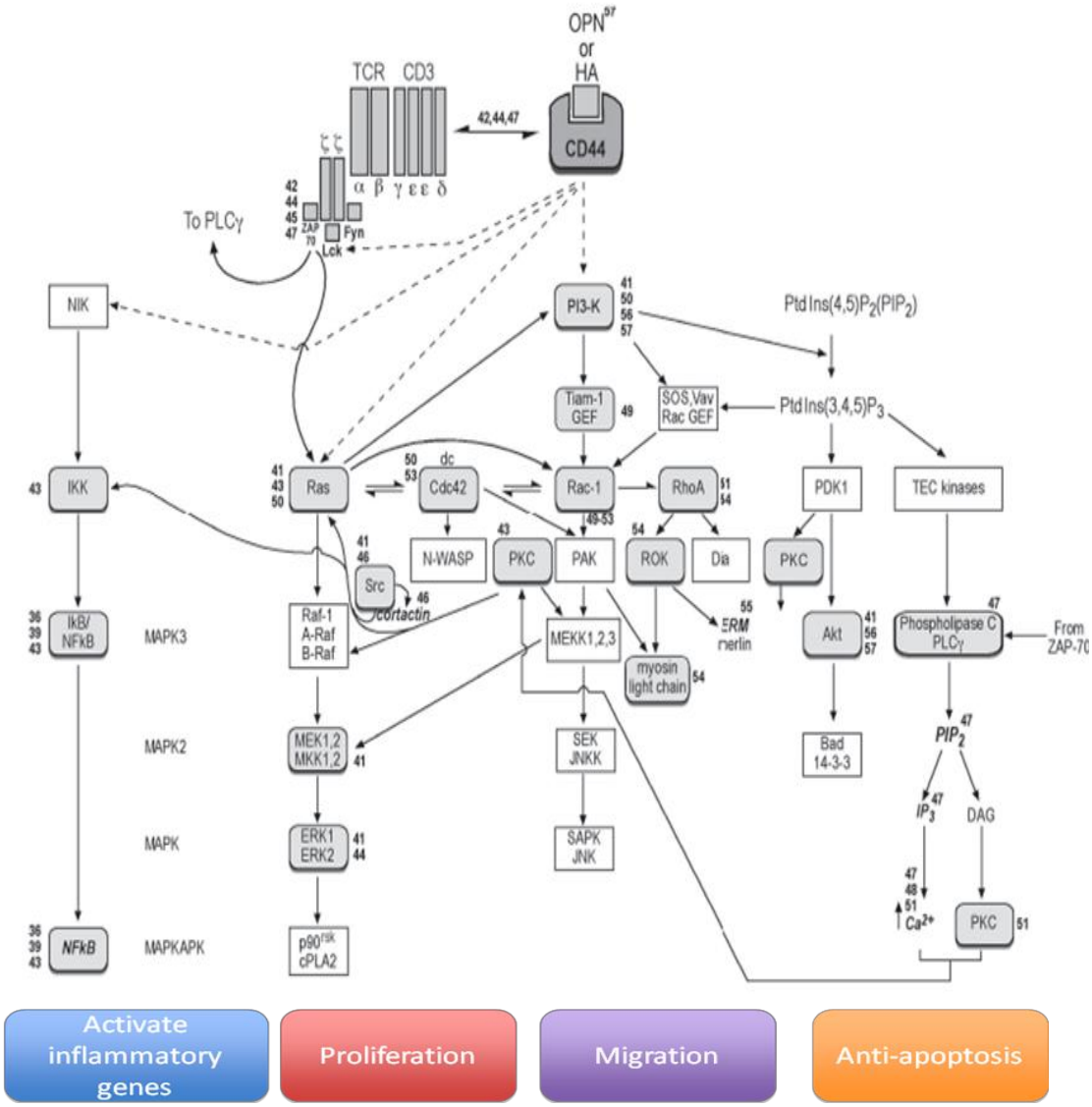

Figure 1.15 A schematic diagram showing some of the signaling pathway triggered by CD44 during cancer development.

(Adapted and modified from review (108))

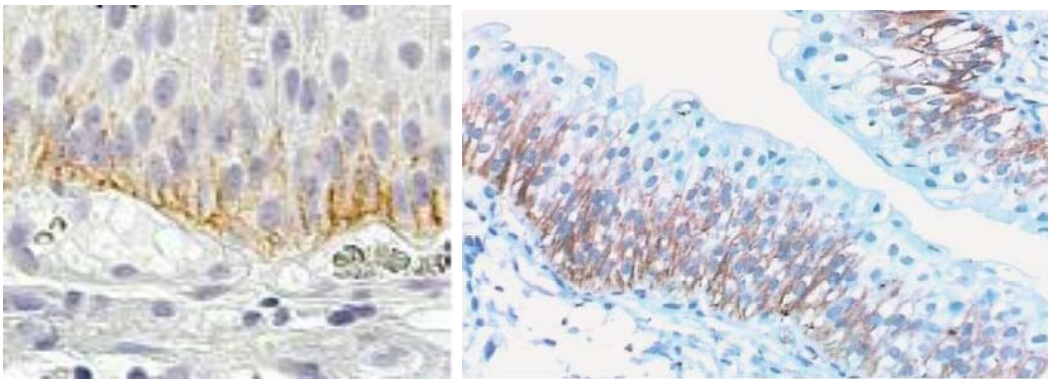

Figure 1.16 CD44 expression in normal bladder urothelium.

Maximum CD44 expression was found in the basal cell layers and the intensity decrease in a step-wise manner towards the superficial cell layer. This picture was Adapted from Left: (99), Right: (122) .

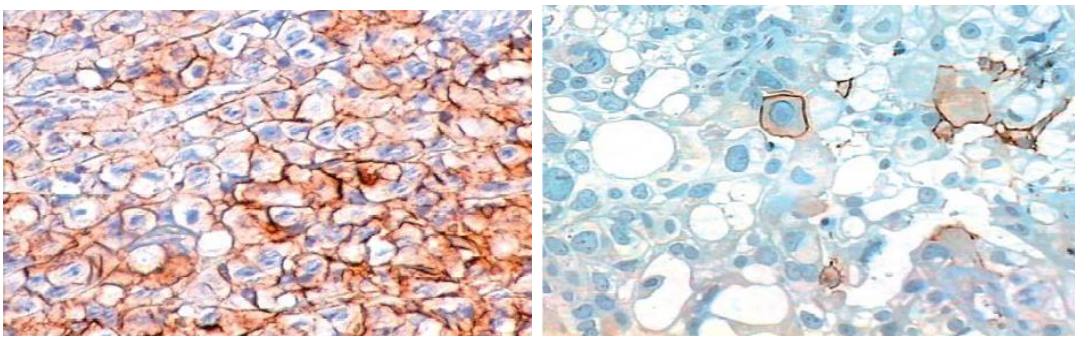

Figure 1.17 CD44 expression in neoplastic bladder.

Left: Irregular immunostaining for CD44s in Grade 3 TCC; Right: Reduction of CD44 expression in Grade 3–4 TCC. Pictures were Adapted from (122).

Table 1.2 Detection of bladder cancer using CD44 as markers

Detection target	Detection Method	Sample no.	Sample Type	Sensitivity %	Specificity %	Reference
CD44v6	PCR	44 patients, 46 controls	Exfoliated cells	91	83	(127)
CD44 isoforms > 160 kDa	Western blot	47 patients, 43 controls	Exfoliated cells	75	100	(123)
CD44 splice variants	RT-PCR	25 patients, 11 controls	Tissues	92	89	(128)
CD44 v8-10	RT-PCR	71 patients, 50 controls	Exfoliated cells	77	100	(129)
CD44 isoforms >1500 base pairs	RT-PCR	22 patients, 11 controls	Tissues	82	74	(130)
CD44 isoforms	RT-PCR	20 patients, 20 controls	Exfoliated cells	90	100	(131)

1.7 Research gap

Nowadays, one of the biggest challenges in the treatment of bladder cancer is its high frequency of recurrence in superficial transitional cell carcinoma (Ta/T1). There is no single causal gene or pathway has been identified to explain the high recurrence rate. In this study, we proposed that the high recurrence rate of superficial TCC is due to the presence of pre-cancerous, i.e. sensitized, cell in the urothelium after TUR.

CD44 is one of the foci of this study since it is expressed by a wide range of malignant tumors and plays a critical role in cancer development, including cell proliferation, migration and progression. Also, a recent study showed that it is a tumor initiating marker of bladder cancer. However, little is known about its contribution in tumorigenic transformation or the pathway involved during the process.

1.8 Hypothesis and objectives of the present study

In this study, we hypothesize that pre-cancer (sensitized) cell is a major source of bladder cancer recurrence; and CD44, a tumor initiation marker, may involved in the transformation process. To evaluate this hypothesis, specific objectives are set as follow:

1) To verify the presence of sensitized cell

2) To identify the characteristic of sensitized cell

3) To investigate the involvement of CD44 during transformation process

The information obtained would be useful to address part of cancer prevention and prediction as well as target therapies.

Chapter 2 Methodology

This chapter describes the general cell culture techniques, molecular biology methods and data analysis used in this thesis. The methodology can be divided into 4 parts to achieve the aims of this study. **Part 1** is related to the analysis methods of the published microarray data; **Part 2** describes the used of malignant transformation model for studying the ABP-induced transformation process; **Part 3** mainly focuses on the methods used to measure CD44 during tumorigenic transformation while **Part 4** describes the measurement of HAS and HA. The materials and reagents are listed in the Appendix I.

2.1 Microarray analysis

A published, open-access microarray data was used to demonstrate any difference in gene expression profile between normal bladder epithelium and the tissue that is near to the tumor ("tumor-surrounding"). Pre-processed data (accession number: GSE13507) was retrieved from NCBI Gene Expression Omnibus in the form of Series Matrix Files and imported into R/Bioconductor 2.9 for subsequent analysis. This dataset includes individual Illumina Human-6 v2 Expression BeadChips for each of the 10 normal urothelium (Control) and 58 urothelial samples that were near to primary tumor (Surrounding).

Differentially expressed (DE) genes were detected using the limma package (version 3.10.3). *p*-values of the empirical Bayes moderated statistics were adjusted for false discovery control by use of Benjiamini and Hochberg procedure. Expression levels of the DE genes were visualized using as heatmap. Hierarchical clustering of the DE genes and samples were performed based on correlation metric (1 – |Kendall's tau|) and weighted average linkage (McQuitty's Similarity Analysis).

2.2 ABP- induced transformation model

2.2.1 Carcinogen- ABP

Tumorigenic transformation is a process that the cells acquire abnormal characteristics such as self-sufficiency in growth signals, insensitivity to anti-growth signals, evading apoptosis, limitless replicative potential, sustained angiogenesis and tissue invasion & metastasis (77). This process may occur primarily in normal tissue, or secondarily in benign tumor. The causes of tumorigenic transformation vary but the underlying principle is genetic mutation either by inheritance (germinal mutation) or, more commonly, by accumulating mutations in life-time (somatic mutation). These mutations can be induced by exposure to carcinogens.

Tobacco smoke contains over 4000 chemical compounds, many of which are carcinogenic and one of these is 4-aminobiphenyl (4-ABP). This study focuses on the cause for cancer recurrence and the early stage after exposure to carcinogen is of utmost important. Tumor initiating cell markers can be used as the indicators in this

model during the period of tumorigenesis. The change of expression of these markers may be useful for tracing the pathway for tumor formation.

2.2.2 Malignant transformation model

In order to investigate the transformation process, a special derivative (PC stock) of SV40-HUC cell line (University of California, Los Angeles) and HUC-1 (ATCC, USA) were used as models in this study. The HUC family is a well-established *in vitro* tumorigenic model (133). HUC-1 is an SV40 immortalized human uroepithelial cell line. It was proven non-tumorigenic when inoculated into athymic nude mice even after 56th passage (134). HUC-PC is derived from the immortalized HUC by cryopreservation at passage 10, thawed, expanded and then cryopreserved again at passage 21. It carries higher level of chromosomal instability and has been widely used as malignant transformation model in cancer transformation process (133, 135-138). HUC-PC has been applied to study the effect of carcinogen 4-aminobiphenyl (ABP) on bladder cancer transformation (139). 24-hr exposure to 200μM ABP followed by 6 weeks of passage resulted in tumor after being injected into nude mice, while none of the controls (without ABP treatment) were tumorigenic. Similar result was also observed in another study using the occupational carcinogen N-hydroxy-4,4'-methylene bis(2-chloroaniline) (N-OH-MOCA) (138).

HUC-PC resembles the sensitized cells, the postulated cause of high recurrence rate in bladder cancer patient, that it is phenotypically normal (similar to HUC-1) but carries extensive genetic defects and is prone to become tumorigenic if additional mutations occur. This tumorigenic model can be used to mimic the sensitized cells in

the epithelium of bladder cancer patient after TUR. The transient ABP treatment imitates stimulations that lead to additional mutations (e.g. rapid cell proliferation in wound recovery after the surgery, contact with carcinogens due to occupational need or active/passive smoking, etc) which slowly drives (6 weeks of replication) the cell to become cancerous.

2.2.3 Cell Culture

1 x 10^6 viable cells was seeded on 100 mm dish, in Dulbecco's Modified Eagle's Medium/Nutrient Mixture F-12 Ham (DMEM; Sigma-Aldrich Corporation) with 10% Fetal Bovine Serum (FBS; Invitrogen), maintained in humidified incubators at 37^oC in 5% CO_2 and 95% air.

2.2.4 Transformation study after exposure to carcinogen

The two cell lines were incubated with 200µM ABP (Sigma) dissolved in 50µl DMSO (Sigma) or, as control, with DMSO alone, for 24 hrs. Treated cells were passaged weekly for 6 weeks and characterized for proliferation and invasion abilities. CD44 expression was monitored throughout the passages.

2.3 Assessment of the tumorigenicity of ABP exposure

To confirm the treated cells are transformed, bladder cancer markers and functional assay were applied to assess the tumorigenicity.

2.3.1 Telomerase Activity Assay

Since telomerase activity shows a high specificity among bladder cancer markers (detail in Chapter 1), it was used to access the tumorigenicity of the ABP exposed pre-cancerous HUC-PC after 6-week incubation. Functional telomerase activity was assessed using real-time telomeric repeat amplification protocol (RTQ- TRAP) (140, 141). It is based on the use of an engineered telomerase substrate (TS) primer, which mimics telomeres and is elongated by telomerase. The length of elongated TS primer is proportional to the telomerase activity and is quantified by routine real-time PCR (qPCR) procedure.

2.3.1.1 Protein extraction

$3x10^6$ cells were centrifuged at 1000 g for 15 mins briefly rinsed in DMEM. Cell pellet was lysed in 80 µl 1X CHAPS lysis buffer by rapid pipetting up-and-down for 30 sec and incubated on ice for 20 minutes. The lysate was then centrifuged at 14000rpm for 30minutes at 4 ℃ and the supernatant was collected and stored at -80℃.

2.3.1.2 Protein concentration determination

Protein concentrations of the lysates were determined by use of Bradford assay. 5µl of protein lysate was diluted with 145µl of 1x CHAPS buffer and incubated with Protein Assay Reagent (Bio-Rad, USA). A standard curve (serial dilution of bovine serum albumin stock solution at 25, 50, 100, 200, 400µg/ml) was run along with the samples. Reaction mixture was incubated at room temperature for 15mins. Colorimetric signals were measured at A595 using microplate reader. Absolute protein amount was interpolated from the standard curve.

2.3.1.3 RTQ – TRAP assay

0.1µg of protein extract was incubated with 2.25µl of 10X TRAP buffer, 0.25µl dNTPs (10mM), 1µl TS primer (0.1µg/µl; 5'-AATCCGTCGAGCAGAGTTAG-3'; HPLC purified), 1µl ACX primer (0.08µg; 5'-GCGCGG(CTTACC)$_4$-3'; HPLC purified), 0.25µl SYBR Green I dye (1/250; Applied Biosystems, USA), 0.25µl ROX reference dye (1/5000; Invitrogen, USA), 0.25µl Hot-star Taq polymerase (Promega, USA) in a total volume of 25 µl at 25°C for 30 mins. Telomerase reaction was then terminated by heating at 95°C for 15 mins. Subsequent PCR profile included 40 cycles of heat denaturation at 95°C for 30 s, annealing at 60°C for 30 s and extension at 72°C for 1 min in Applied Biosystems 7500 Fast Real-Time PCR System. The relative telomerase activity in each sample was represented by the fold difference calculated using $2^{-\Delta Ct}$ method.

2.3.2 Measurement of survivin mRNA expression

2.3.2.1 RNA isolation and cDNA synthesis

After 6 weeks of transformation, the cell samples were collected and the total RNA was extracted using RNeasy mini kit (QIAGEN) according to the manufacturer's instruction. Genomic DNA contamination was prevented by DNase (Promega) treatment. 1μg total RNA was converted to cDNA by reverse transcription with BluePrint RT reagent kit (TaKaRa) and the final product was stored at -20°C. The reason we choose QPCR is that it is a cheaper and time-saving method with higher sensitivity. It is a common method for measuring survivin clinically (142-144).

2.3.2.2 Real-time PCR

Gene-specific primers were designed using NCBI Primer-Blast with default settings (specificity check: Human RefSeq database). Gene-specific primer sequences were listed in Table 2.1. PCR efficiency was guaranteed to be 90-110% using the routine standard curve method and the results are shown in Appendix II. Primer specificity was validated by the use of melt curve analysis.

1 μl of 10-fold diluted cDNA was mixed with 1 μl forward primer (10 μM), 1 μl reverse primer (10 μM), 10 μl SYBR® Premix Ex Taq™ ll (TaKaRa) and 7 μl DNase-/RNase- free distilled water (Gibco). Hot-start Taq polymerase was activated at 95°C (10 mins). Samples were cycled through a thermal profile of denaturation at 95°C, annealing at 60°C and extension at 72°C (each for 30 s) in Applied Biosystems 7500 Fast Real-Time PCR System. Each sample was assayed in

triplicate wells. Threshold cycle numbers (Ct) of each target gene in each sample was automatically determined by the ABI SDS Software (v1.4) and normalized to the Ct of endogenous control. In our study, TATA-box binding protein (TBP) mRNA was chosen as the endogenous control because it was shown to be the most stable housekeeping gene in bladder cancer and recommended as reference gene for relative gene quantification (145). Relative expression was expressed by the routine $2^{-\Delta\Delta Ct}$ method.

Table 2.1 Primer sequence for Real-time PCR of survivin

Gene	Forward primer sequence	Reverse primer sequence	Amplicon length (bp)
Survivin	**GGAGAATATCACAGTGGTT**	**GCCAATTACTAAGCAACAG**	**135**
TBP	**CGGAATCCCTATCTTTAG**	**GACTATTGGTGTTCTGAA**	**77**

2.3.3 Proliferation assay

CellTiter® 96 AQueous One Solution Cell Proliferation Assay (Promega) was used to evaluate the proliferation rate of the treated human urothelial cell. It is a colorimetric method utilized the capability of viable/proliferative cells to reduce MTS tetrazolium compound to colored formazan product. The quantity of formazan product can be quantified by measuring the absorbance at 490nm, and is directly proportional to the number of living cells in culture.

Cells were seeded at a density of 5 x 10^3 in 96-well plates with 100µl of culture medium. After 48 hours, 20µl of CellTiter® 96 AQueous One Solution was dispensed to each well, and the plate was incubated for 1-4 hour at a humidified, 5% CO_2 atmosphere. Absorbance was measured at 490 nm using microplate reader.

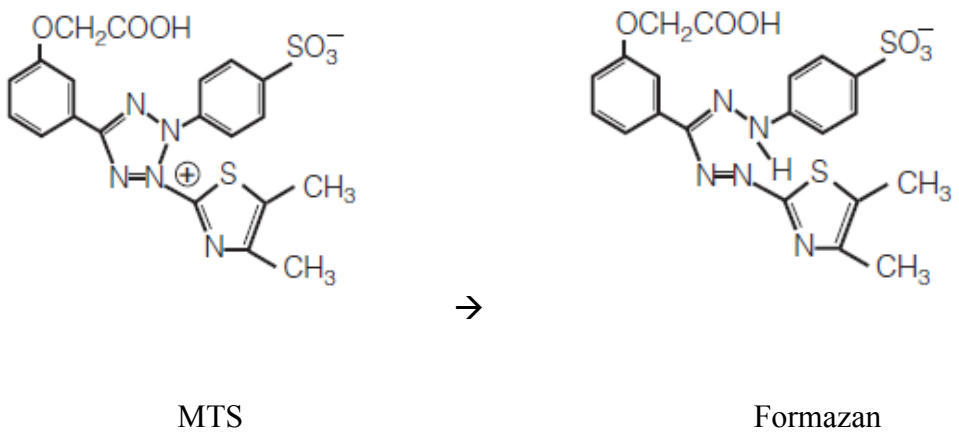

Figure 2.1 Mechanism of CellTiter® 96 AQueous One Solution Cell Proliferation. A MTS assay: the tetrazolium salts (MTS) is bio-reduced by the dehydrogenases and reductases. The rate of reduction is proportional to the number of viable cells.

2.3.4 Invasion assay

After 24 hr incubation with 200 μM ABP, HUC-PC was passaged for 6 weeks. Invasion assay was applied to test the invasiveness of cancerous transformed cells and the DMSO control. Cells were seeded into a chamber with two medium-filled compartments separated by a microporous membrane coated with a layer of Matrigel.

Transwell inserts with 8 μm pores were coated with Matrigel in 1:5 dilution. 7.5 x 10^4 cells suspended in serum-free medium were seeded to the insert (Upper chamber) in duplicate, whereas medium containing 10% FBS was added to each well (Lower chamber) as a chemoattractant (Figure 2.2). Following incubation for 48 hours at 37°C, invaded cells that passed through the membrane to the lower surface were fixed in neutral buffered formalin and stained using 0.5% (w/v) toluidine blue in 2% (w/v) sodium carbonate (Na_2CO_3) solution. Non-invaded cells on the upper surface of the membrane were then wiped out with a cotton wool swab. The invaded cells were captured under a light microscope at 100x magnification.

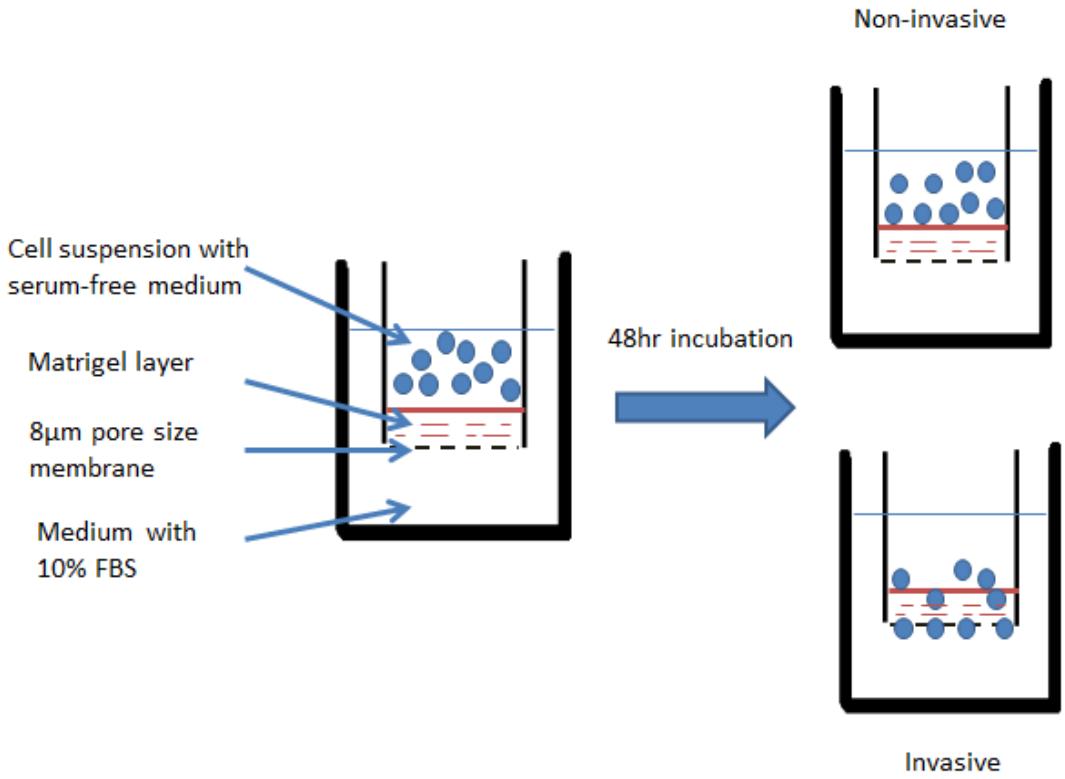

Figure 2.2 A schematic diagram showing the setup of *in vitro* invasion assay. It was applied to test the invasiveness of cells. This set up contains with two medium-filled compartments which is separated by a microporous membrane coated by a layer of Matrigel. Cells suspended in serum-free medium were seeded to the Upper chamber, whereas medium containing 10% FBS was added to the Lower chamber as a chemoattractant.

2.4 Measurement of CD44

In our study, we focused on precise evaluation and analysis of the CD44 standard molecule expression during transformation of HUC-PC. Simultaneously, we also measured the CD44 isoforms mRNA expression.

2.4.1 Dose response of on ABP toward CD44 induction

Different concentrations of carcinogen 4-ABP (0, 50, 100, 200 mM) were used to induce transformation of pre-cancerous HUC-PC. DMSO was used as a solvent for dilution and 50µl of the diluted carcinogen was added to each plate. After 24hr exposure, the medium with carcinogen were removed and replaced with fresh medium. The change of CD44 expression after 1 week of incubation was measured by flow cytometer.

2.4.2 Measurement of cell surface CD44 expression

Anti-CD44 (FITC) antibodies (clone J.173; Beckman Coulter), with excitation and emission spectrum wavelengths 468-509 nm and 504-541nm, respectively, were used to label the CD44 transmembrane proteins on the cell surface. Flow cytometer (FC500 Beckman Coulter) was applied to measure the CD44 expression level. Gating parameters were set by side and forward scatter to eliminate dead and aggregated cells.

2.4.3 Measurement of CD44 mRNA expression

After 6 weeks of transformation, CD44s and CD44v6 expression were assessed using qPCR. Procedure was identical to those described in Ch 2.3.2.1 (Page 46).

2.4.3.1 Real-time PCR

Real-time quantitative polymerase chain reaction (RT-qPCR) was performed. The primer sequence for the target genes are shown in Table 2.2. Detail procedures are described in Ch 2.3.2.2 on P.46.

Table 2.2 Primer sequences for Real-time PCR of CD44 isoforms

Gene	Forward primer sequence	Reverse primer sequence	Amplicon length (bp)
CD44 v6	CCTAGTAGTACAACGGAAGAA	TTTGGGTGTTTGGCGATA	87 (v1, v2)
CD44 standard	CCTGCTACCAGAGACCAAGA	ATGTGAGTGTCCATCTGATTCA	84 (v4, v8)
CD44 total	ACTTCAGGAGGTTACATCT	GATTCTGTCTGTGCTGTC	93 (v1,2,3,4,6,7,8)
TBP	CGGAATCCCTATCTTTAG	GACTATTGGTGTTCTGAA	77

2.5 CD44 knockdown

A stable HUC-PC clone of CD44-knockdown was generated to demonstrate whether the CD44 induced after ABP stimulation was essential for transformation. If CD44 suppression can reduce the carcinogenic effect of ABP in HUC-PC, it will be used therapeutically to reduce the recurrence. CD44-specific short hairpin RNA (shRNA) constructs that target all the CD44 isoforms, along with a scrambled (Scr) construct plasmid cassette in pGFP-V-RS vectors, were acquired from Origene. The scrambled non-effective plasmid was served as a negative control to exclude any potential interferon response. The sequences of the CD44 shRNA are listed in Table 2.3, and the schematic diagram of pGFP-V-RS vectors is shown in Figure 2.3.

2.5.1 Plasmid amplification

1μl of diluted plasmid (1ng/μl) was used to transform the competent E. coli strain DH5α. The transformants were plate on the LB-kanamycin (25μg/ml) plates and incubated overnight at 37°C. Single bacterial colonies were inoculated into 7ml LB-kanamycin broth and cultured overnight. Plasmid was recovered and purified by the use of PureYield ™ Plasmid minprep system (Promega). The concentration of the purified plasmid DNA was determined using NanoDrop® ND-1000 spectrophotometer (Thermo Fisher Scientific) and stored at -20°C.

2.5.2 Plasmid transfection

$7x10^5$ cells of HUC-PC were seeded to 6-well plate with 2ml complete medium in each well and incubated for 24hrs to reach 80% confluent. Transfection complexes consisting of 2 µg plasmid DNA, 6µl FuGENE HD Transfection Reagent (Promega) and 200 µl Opti-MEM I (Invitrogen) were incubated for 20 min at room temperature then added to each of the wells and incubated with the cells for 48 hrs. The transfected cells were passaged into a fresh vessel containing growth medium.

2.5.3 Stable clone selection

Stable clone (plasmid was integrated into the genome) was selected for 2 weeks in presence of puromycin (0.5-1µg/ml). Knockdown was confirmed by immunoblotting for CD44. A frozen stock of the stable clone was stored under liquid nitrogen in DMEM with 5% DMSO and 10% FBS for further experiments.

Table 2.3 CD44-specific short hairpin RNA (shRNA) constructs.

Sequences of 4 unique 29mer shRNA constructs in retroviral GFP vector are specific to human CD44 gene.

Tube ID	Sequences
GI356313	GGTGGAGCAAACACAACCTCTGGTCCTAT
GI356314	GCTGACCTCTGCAAGGCTTTCAATAGCAC
GI356315	GACAGAAAGCCAAGTGGACTCAACGGAGA
GI356316	GGACTCCAGTCATAGTATAACGCTTCAGC

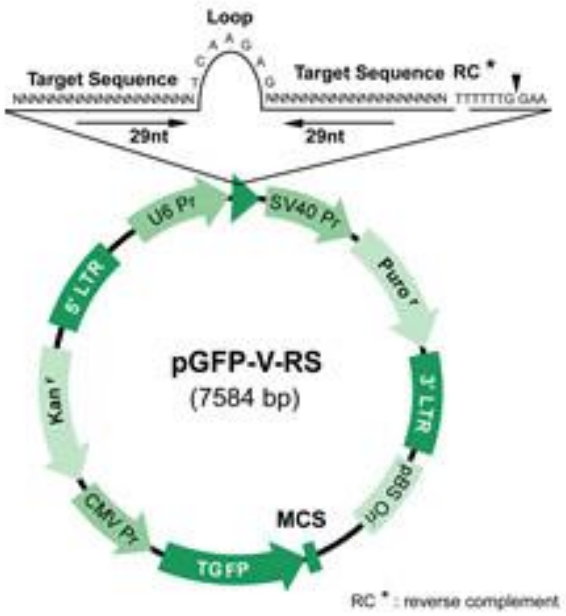

Figure 2.3 The schematic diagram of pGFP-V-RS vectors for cloning shRNA expression cassettes.

This vector is designed for long term gene silencing studies. It contains the pCMV to drive the expression of tGFP gene for monitoring the transfection efficiency. Besides, its puromycin resistance property is designed for stable clone selection.

2.6 Measurement of HAS

The way that CD44 involves in the early stage for tumorigenesis is unknown. Its interactions with hyaluronic acid and other ligands e.g. osteopontin (a chemotactic phosphoprotein) are required to investigate so as to find out the pathways for cancer development. In this study, we measured the quantity of HAS mRNA by using real-time PCR as well as HA by HPLC.

2.6.1 RNA isolation and cDNA synthesis

After 6 weeks of transformation, the cell samples were collected and total RNA was isolated. Detail procedures were described in Chapter 2.3.2.1 on P.46.

2.6.2 Real-time PCR

Real-time quantitative polymerase chain reaction (RT-qPCR) was performed. The primer sequence for the target genes are shown in **Table** 2.4. Detail procedures are described in Ch 2.3.2.2 on P.46.

Table 2.4 Primer sequences for Real-time PCR of HAS isoforms

Gene	Forward primer sequence	Reverse primer sequence	Amplicon length (bp)
HAS1	CAGGGAGGGTATTTATTG	ATAAGAACGAGGAGAAAG	77
HAS2	ATGGTGCTTGATGTATGA	TATCTGATGCCACAATACT	97
HAS3	AGCAACTTCCATGAGGCAGG	GCACCACATCCCGCACAC	79
TBP	CGGAATCCCTATCTTTAG	GACTATTGGTGTTCTGAA	77

2.7 Measurement of HA by HPLC

High-performance liquid chromatography (HPLC) is a chromatographic technique to separate a mixture of compounds with the purpose of identifying and quantifying the individual components of the mixture. The method for quantifying HA in cell culture medium is described as below.

2.7.1 Recovery of crude extracts of urinary polyanionic macromolecules

8ml cell culture medium samples were collected and diluted with 24ml of 0.025M sodium acetate buffer at pH 5.8. 800µl cetylpyridinium chloride (CPC) in acetate buffer was added into the diluted medium and allowed to stand overnight at 4°C. The precipitate was washed twice with ice-cold distilled water and re-dissolved in 100µl propan-1-ol. 400µl of sodium acetate-saturated ethanol was added to the propanolic solution to re-precipitate the urinary polyanionic macromolecules (UPM) as sodium salts by standing the mixture overnight at 4°C. The precipitate was washed twice with ice-cold cooled ethanol (EtOH) and then dried in Speed Vac.

2.7.2 Recovery of urinary GAG from crude extracts

The dried UPM was dissolved in water to 20mg/ml. An equal volume of papain buffer (2X) and 0.1ml of papain suspension were added to the solution and incubated at 65°C overnight. The digestion mixture was then centrifuged. The supernatant

containing GAG was collected. The residue was washed 3 times with 65°C distilled water before it was discarded. The supernatant and the extractions were pooled followed by the sequential CPC-EtOH precipitation procedure for GAGs recovery.

2.7.3 Selective digestion of Hyaluronan

GAG extract was dissolved in 30 µl 0.02M acetate buffer at pH6.0 together with 30 µl Streptomyces hyalurinidase and incubated at 37°C for 16 hrs. Resistant macromolecules in the digestion mixture were precipitated by 4 volumes of EtOH at 4°C for 16 hr. The digested products in the supernatant were recovered after vaporization of EtOH and incubate with 50 µl Chondroitinase-ABC buffer and 10 µl Chondroitinase-ABC at 37°C for 16 hrs. Resistant macromolecules in the digestion mixture were, again, precipitated with EtOH at 4°C for 16 hr. The disaccharide products in the supernatant were recovered after vaporization of EtOH and then reconstituted in 50µl mobile phase.

2.7.4 HPLC analysis

Chromatography was performed at room temperature on a Partisil SAX 5u (250 x 4.6-mm inner diameter) column (Alltech) with a Waters 2695 HPLC system. The column elute was monitor at 232nm. Unsaturated disaccharides (Δdi-nonS_{HA}) were eluted with 5mM sodium dihydrogen orthophpsphate/orthophosphoric acid (pH 2.55). Nonsulfated tetrasaccharides and hexasaccharides as well as di-monoS_{CS} were eluted with 50mM sodium dihydrogen orthophosphate/ orthophosphoric acid (pH

2.5). A standard curve of serial HA concentrations (0, 1.56, 6.25 and 12.5μg) was generated.

2.8 Statistical analysis

The ABP treatment effects on telomerase activity, proliferation and expressions of aforementioned target genes (CD44, HAS, survivin) were tested by the use of Student's t-test or Mann-Whitney rank sum test, whenever normality assumption was violated as indicated by Shaprio-Wilk's test. Levene's test was employed to ensure the validity of the homoscedascity assumption of both tests. Interactions between effects of ABP-exposure (treatment effect) and time-post-exposure (temporal changes) on CD44 expressions were tested by the use two-way analysis of variance (ANOVA). If statistical significant interaction was found, the main effects of ABP-exposure and time-post-exposure were illustrated, respectively, by: (1) Student's t-test (or Mann-Whitney rank sum test, as above) by each week-post-exposure. False discovery rate in multiple testing was controlled by the Benjiamini and Hochberg procedure; (2) one-way ANOVA for each treatment group, followed by Tukey's post-hoc test (Tukey–Kramer method). Normality and homoscedascity of residuals in the ANOVA were validated as above. All statistical tests were carried out in R (version 2.14) at the significance level of 0.05. All charts were graphed as mean ± SEM.

The methodology of this research study was all mentioned in this chapter including the experimental design and general setting. The results of this thesis are provided in Chapter 3.

Chapter 3 **Results**

3.1 Evidences to support the presence of sensitized cell

There were 444 transcripts differentially expressed between the normal urothelium ('normal') and the urothelial cells that were near to the tumor sites ('neighboring'). The gene list is shown in Appendix III and the biological functions of these DE transcripts were summarized in Appendix IV.

The 'neighboring' samples were segregated into two distinct groups, indicating that these samples are in fact a collection of biopsies with two major genotypes. As revealed by cluster analysis, one subset of the 'neighboring' samples was clustered with, hence similar to, 'normal' (Figure 3.1: Group 1). Nonetheless, majority of the 'neighboring' samples agglomerated into a distinct cluster (Figure 3.1: Group 2), suggesting they were very different from normal.

As is shown by the Venn diagram (Figure 3.2), all, except one, of these DE transcripts were also differentially expressed between the normal urothelium and primary tumor. These results highlighted that the 'neighboring' tissue possessed an essential portion of genetic changes that were exhibited by the primary tumors.

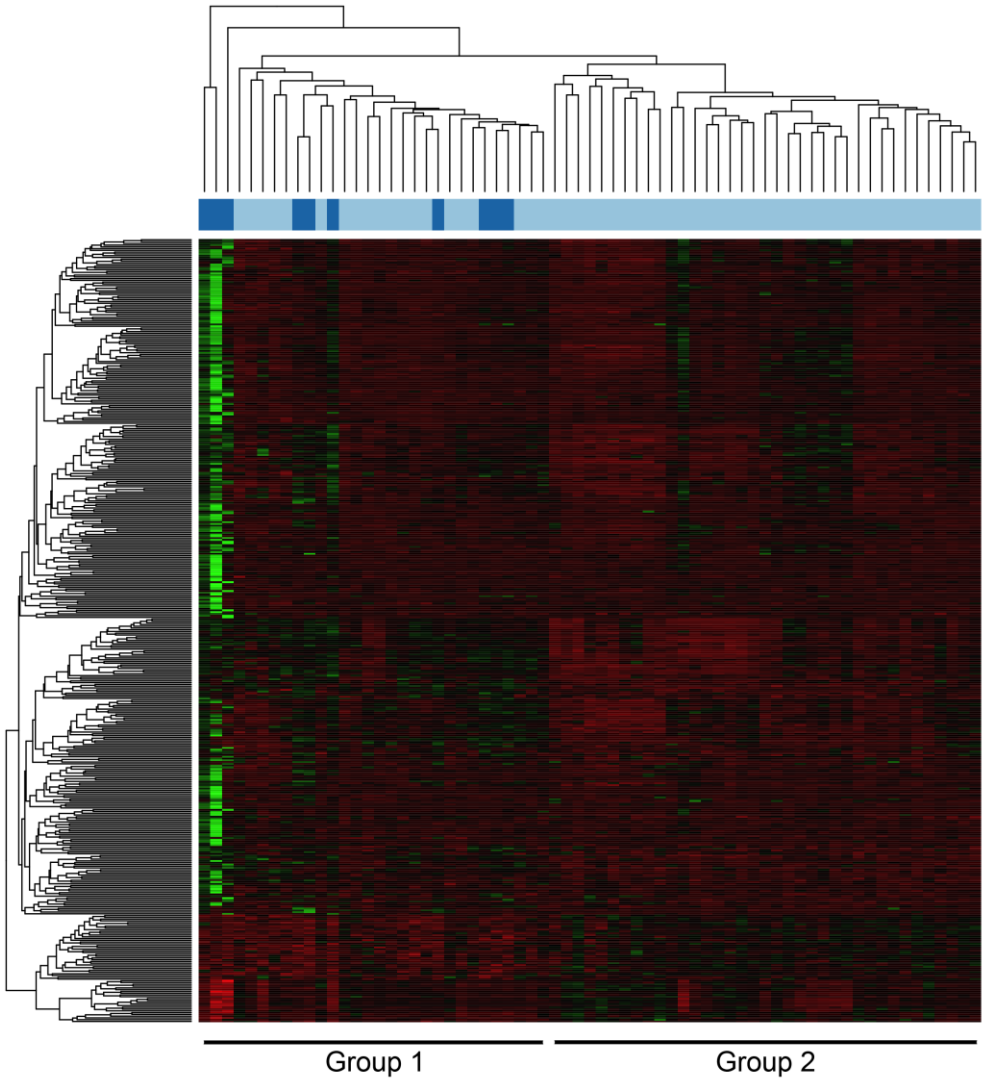

Figure 3.1 Heatmap representation of the differentially expressed genes.

444 genes were differentially expressed (FDR-adjusted $p < 0.05$) between normal urothelium ('normal') and the urothelial cells ('neighboring') that were near to the tumor site. Sample classes were marked by the bar beneath the top dendrogram: dark blue = 'normal', light blue = 'neighboring'.

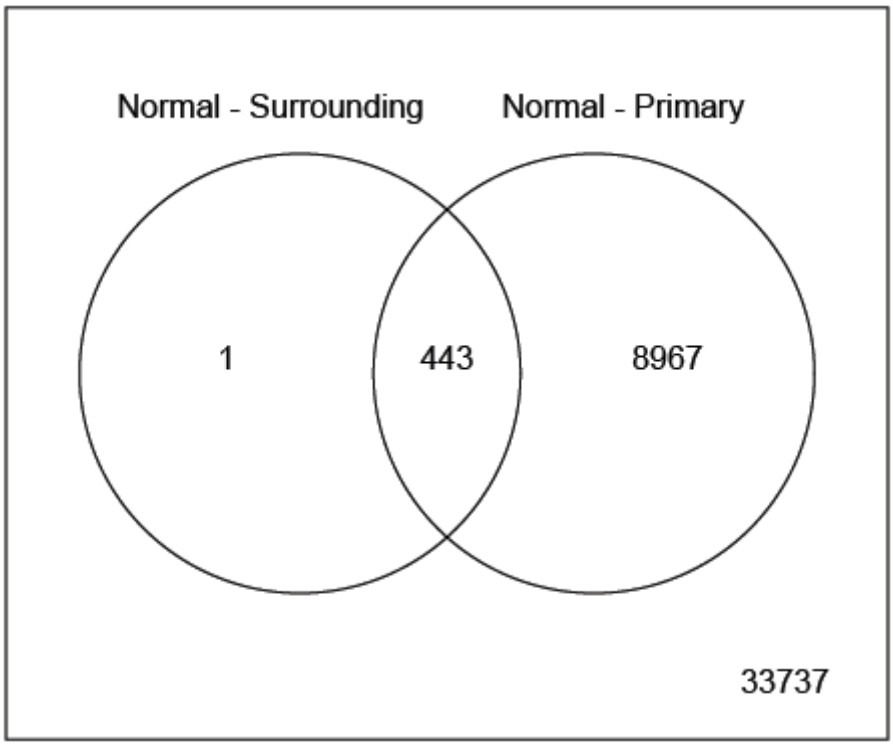

Figure 3.2 Venn diagram showing the relationship of two DE transcript lists. 'Normal - Surrounding' = Contrast between normal urothelium and the urothelial tissue that was near to the tumor site (444 DE transcripts); 'Normal - Primary' = Contrast between normal urothelium and the primary tumor (9410 DE transcripts). Note that 443 out of 444 DE genes from the former contrast were also differentially expressed in the later. 33373 transcripts were not differentially expressed either contrasts.

3.2 High basal CD44 level in pre-cancer cell

Prior to investigation on the involvement of CD44 during tumorigenesis, we compared its basal expression level in the pre-cancer state (HUC-PC) and, the normal mother cell line, HUC-1. The flow cytometry results showed that both the normal and pre-cancer cell expressed CD44 (Figure 3.3). However, HUC-PC has a much higher CD44 level than that of HUC-1 (Figure 3.4). This implied that pre-cancerous HUC-PC express more CD44 antigen on its cell surface and that might prepare the cell ready for transformation.

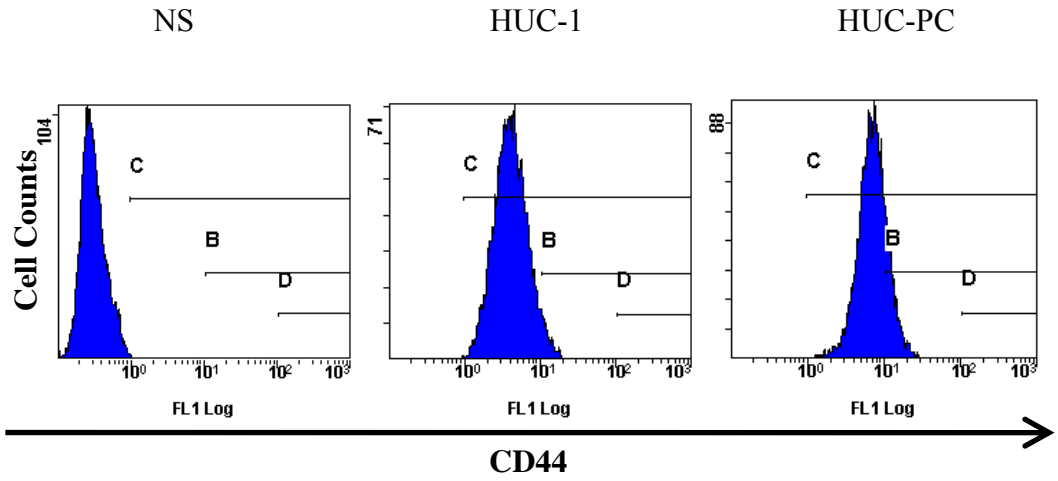

Figure 3.3 Basal CD44 expression level measured by flow cytometry.

A total of 10,000 cells were analyzed. The cell distribution is shown in the blue area in which X-axis represents the fluorescent intensity while Y-axis represents the cell number. Left: non-stain control; Middle: fluorescent labeled HUC-1; Right: fluorescent labeled HUC-PC.

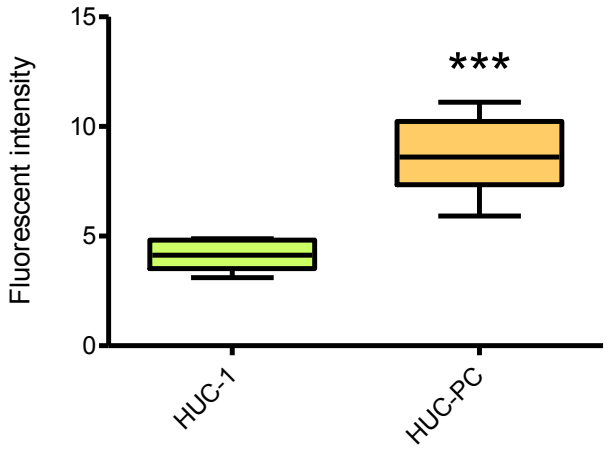

Figure 3.4 Basal level of CD44 expression in normal (HUC-1) and pre-cancerous (HUC-PC) stages of uroepithelial cell surface.

The expression level of CD44 was markedly higher in HUC-PC than HUC-1. N = 3, t_{16}=7.647, $p < 0.001$ (asterisks).

3.3 Expression of CD44 during tumorigenic transformation

To investigate the roles of the CD44 in tumorigenic transformation, we examined the expression of pan-CD44 (all CD44 isoforms) during the process. 4-aminobiphenyl (4-ABP) is a well known carcinogen that causes bladder cancer and was used in this experiment to induce the tumorigenic transformation. CD44 expression levels of the two cell lines were measured weekly during the 6 weeks of passage after 24 hrs ABP treatment. The flow cytometry data of HUC-1 and HUC-PC is shown in Figure 3.5 and Figure 3.6 respectively.

Our results showed that the two cell lines had different responses after exposure to ABP. For HUC-1, CD44 expression was constantly maintained at low level throughout 6 weeks of monitoring, and ABP treatment has no significant effect on the expression (Figure 3.7). This indicated that HUC-1 is not sensitive to the carcinogen ABP. The response of the pre-cancer HUC-PC was entirely different. There was a significant increase of CD44 expression at 1 week after ABP exposure (Figure 3.8). Then, it dropped back to the control level throughout the tumorigenic transformation process. These signified a transient induction of CD44 during the initiation state of cancer transformation. This induction may trigger sequential responses to promote cancer development. As mentioned on P.42 of the thesis, both HUC-PC and HUC-1 are immortalized cell lines.

HUC-1 DMSO ABP

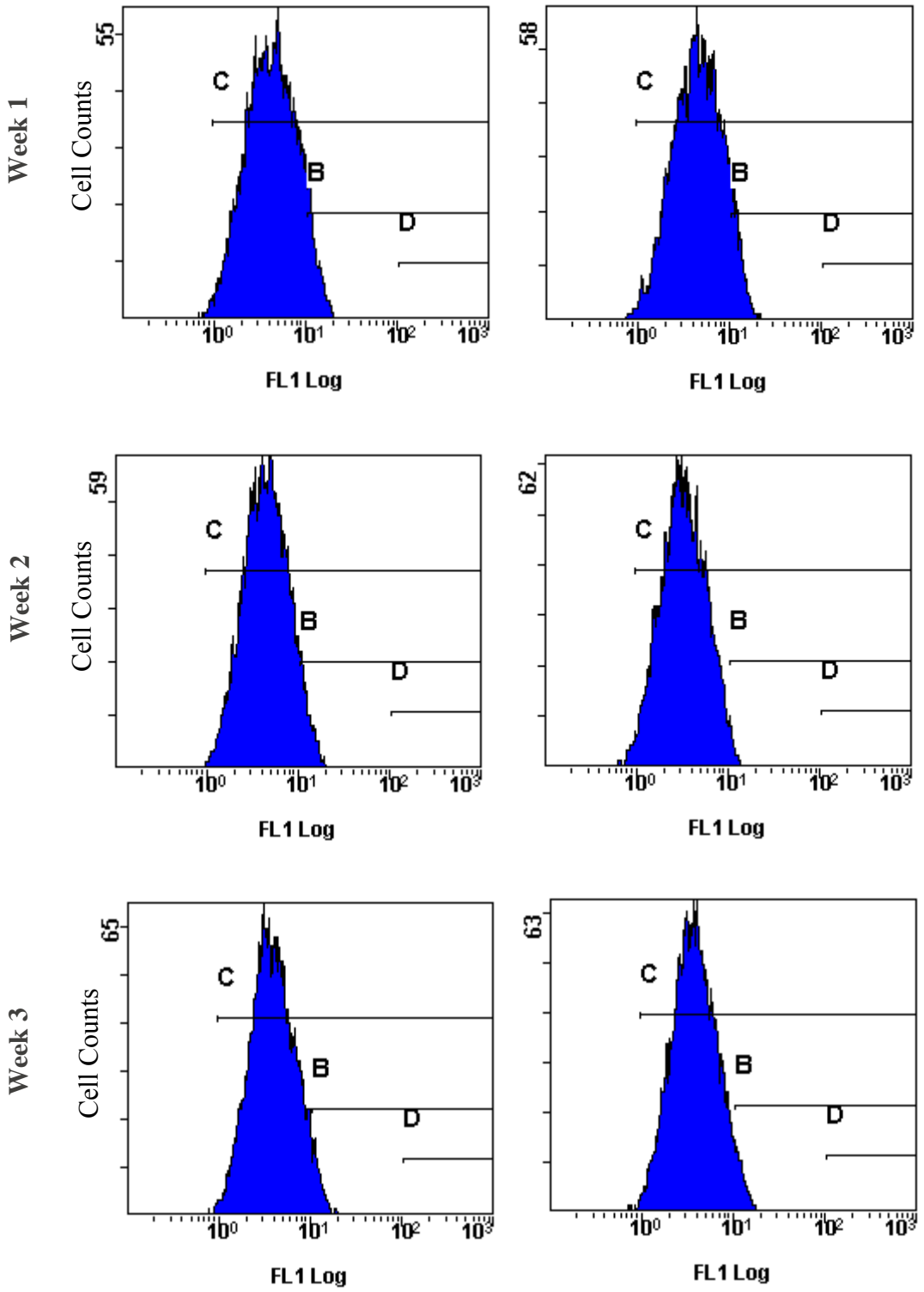

HUC-1 DMSO ABP

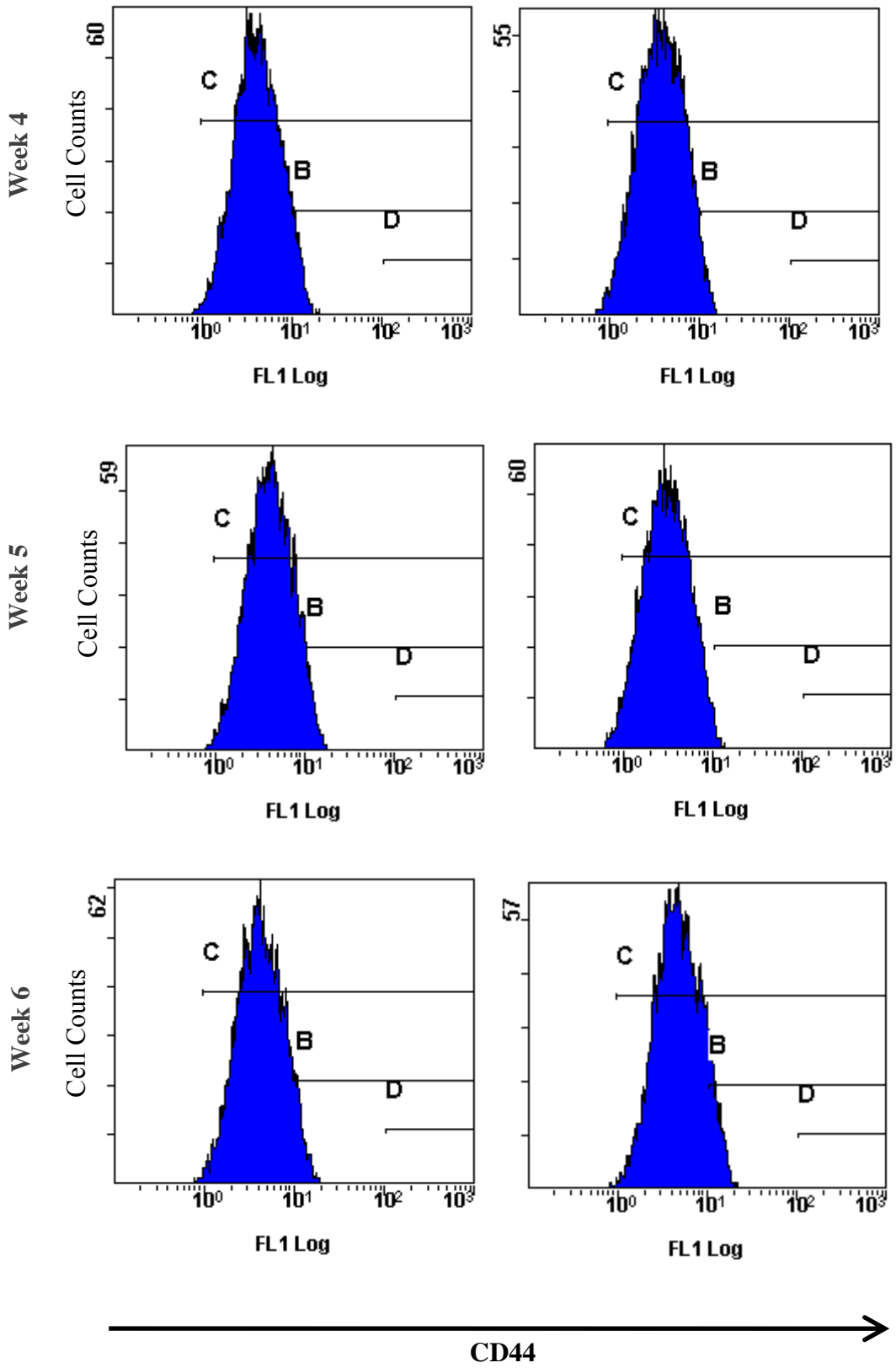

Figure 3.5 Flow cytometry results of HUC-1 across 6-week after ABP treatment.

HUC-1 cells were labeled with anti-CD44 antibodies. A total of 10,000 cells were analyzed. The cell distribution is shown as the blue histogram, in which the X-axis represents the fluorescent intensity; while the Y-axis represents cell counts. Left column: solvent control; Right column: pre-exposed to ABP for 24 hrs. The size, pattern and location of histograms were highly similar between ABP treated- and control cells.

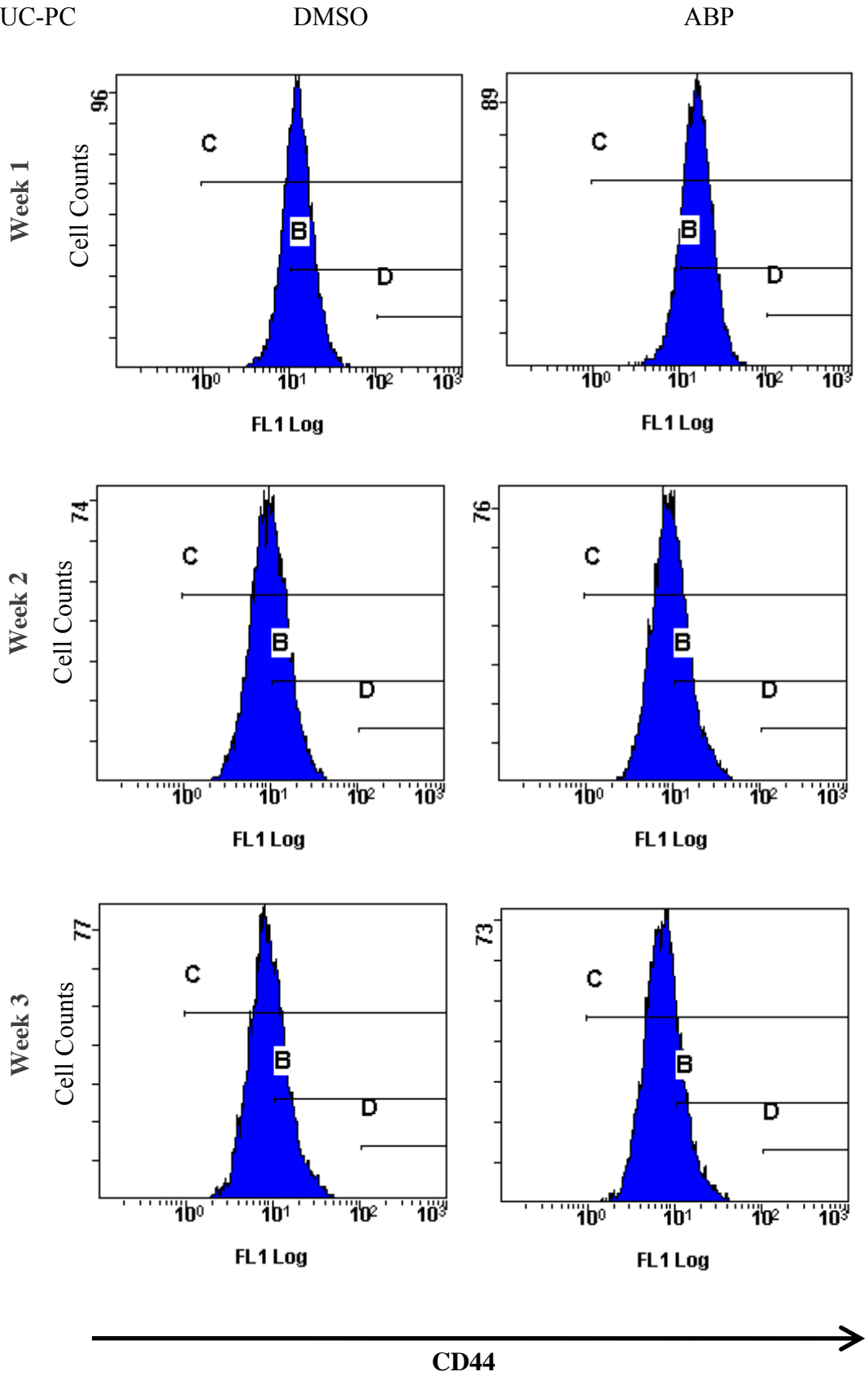
HUC-PC
DMSO
ABP
Week 1
Week 2
Week 3
Cell Counts
96
89
74
76
77
73
C
B
D
FL1 Log
CD44

HUC-PC DMSO ABP

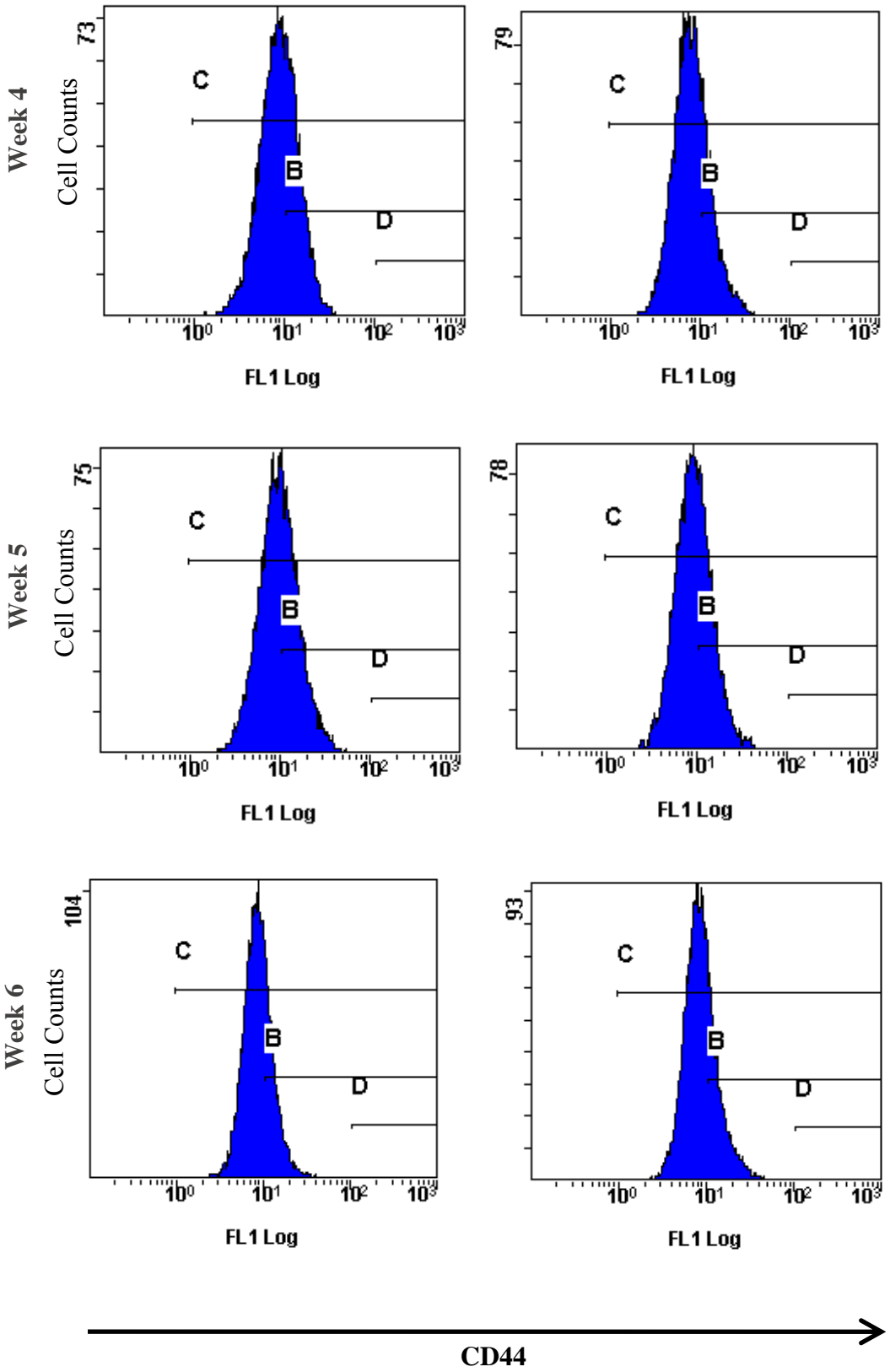

Figure 3.6 Flow cytometry results of HUC-PC across 6-week after ABP treatment.

HUC-PC cells were labeled with anti-CD44 antibodies. A total of 10,000 cells were analyzed. The cell distribution is shown as the blue histogram, in which the X-axis represents the fluorescent intensity; while the Y-axis represents cell counts. Left column: solvent control; Right column: pre-exposed to ABP for 24 hrs. The fluorescent signal was much stronger, i.e. increased CD44 expression on cell surface, in cell populations at one week post- ABP exposure.

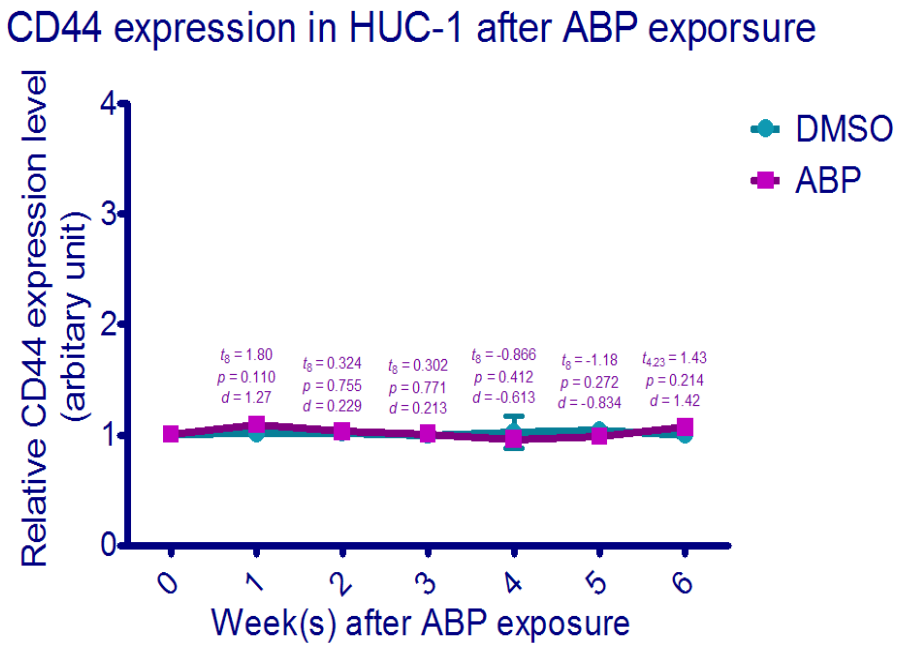

Figure 3.7 CD44 expression remained constant in HUC-1 throughout the 6-week of passage after ABP exposure.

The figure is expressed as the mean relative expression levels (±SEM) when compared to the DMSO control at 0 day after exposure (N = 5 for each treatment condition at each time point). No significant interaction between time and effect of ABP treatment was observed (two-way ANOVA: $F_{5,48}$ = 1.457, p = 0.222). The CD44 expression was not dependent on time ($F_{5,48}$ = 0.757, p = 0.585) or ABP treatment ($F_{1,48}$ = 0.201, p = 0.656) throughout the 6 weeks incubation. Individual *t*-test, followed by FDR adjustment, was performed for each week to test the null hypothesis / reassure that ABP treatment did not affect the CD44 expression level.

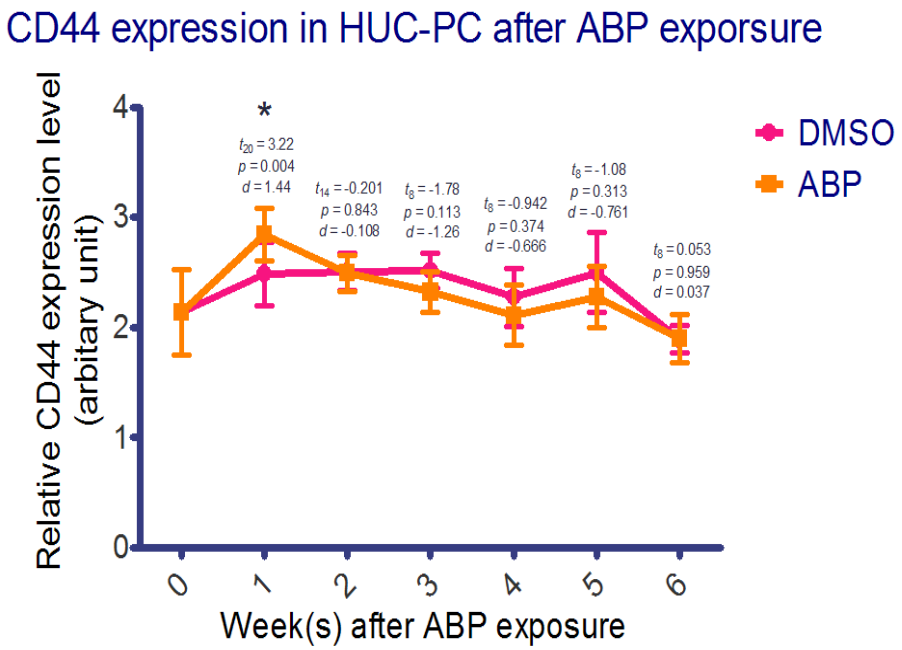

Figure 3.8 The change of CD44 expression in HUC-1 throughout the 6-week of passage after ABP exposure.

The figure is expressed as the mean relative expression levels (±SEM) when compared to the DMSO control of HUC-1 at 0 day after exposure (N = 5 for each treatment condition at each time point). Significant interaction was found between the variables, time and ABP treatment (two-way ANOVA: $F_{5,66} = 3.525$, $p = 0.007$), i.e. the effect of ABP treatment varied across time. Individual *t*-test, followed by FDR adjustment, was performed for each week to test the significance of ABP treatment on CD44 expression. Asterisks: $p < 0.05$.

3.4 Dose response of ABP in HUC-PC

Different concentrations of ABP were used to analyze its inductive effect on CD44 expression. The previous results showed there was an induction of CD44 expression in HUC-PC, but not HUC-1, at 7 days after 24 hr incubation of 200μM ABP. Base on this finding, further experiment was conducted to examine possible dose effect of ABP on CD44 expression using HUC-PC as model. Different concentrations (0, 50, 100, 200 μM) of ABP were used to induce CD44 expression. The flow cytometry data is shown in Figure 3.9. Although no significant difference was found between 0, 50 and 100μM of ABP, there was a seemingly increasing trend of CD44 expression with the ABP concentrations. CD44 expression increased with ABP dosage in a partial dose-dependent manner. A threshold that resulted in prominent increase in CD44 was found to be ~200μM of ABP (Figure 3.10). This result further confirmed the relationship between carcinogen ABP and CD44 expression in HUC-PC.

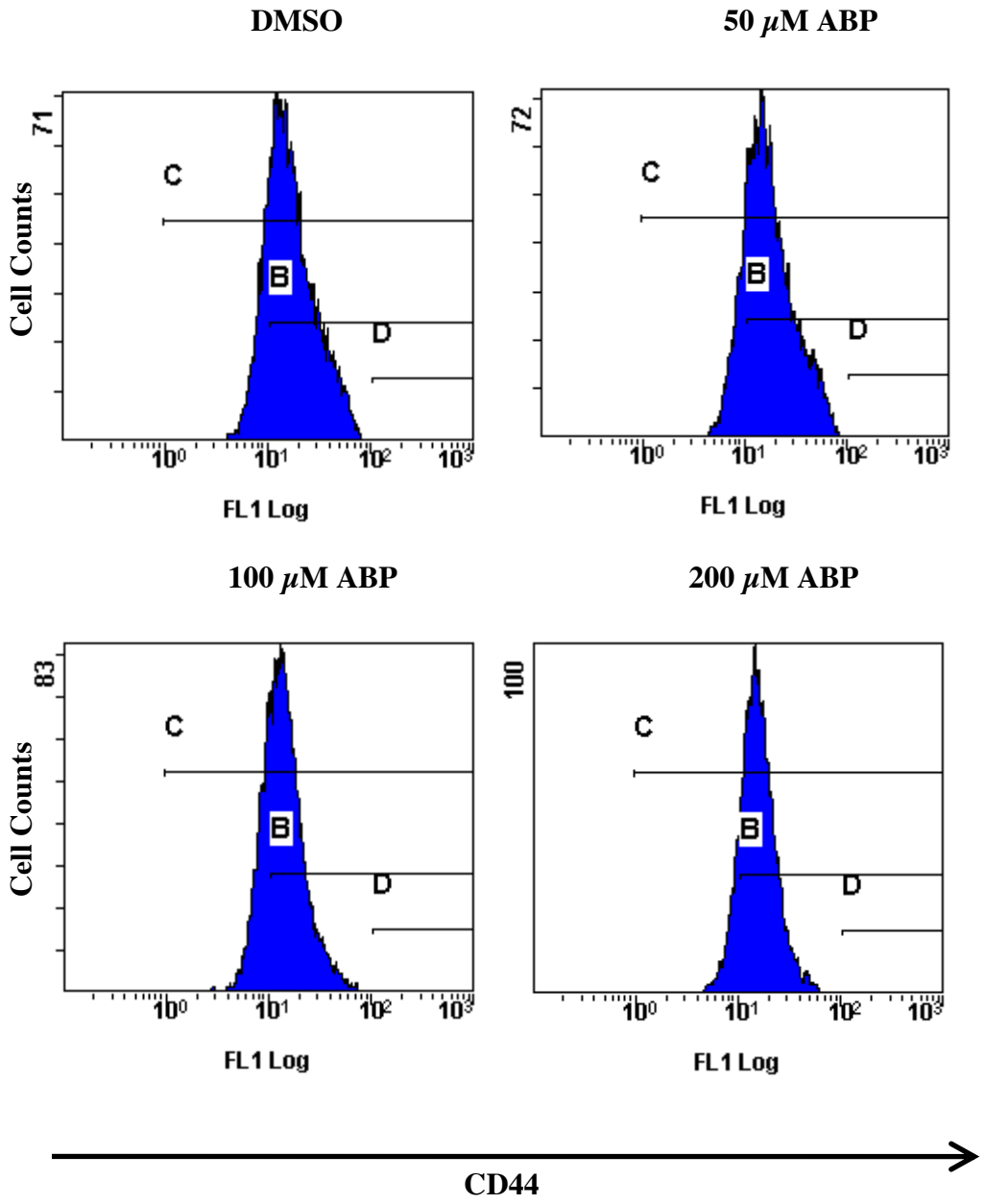

Figure 3.9 Flow cytometry result showed the dose response of ABP on CD44 expression in HUC-PC at one week after ABP treatment.

HUC-PC cells were labeled with anti-CD44 antibodies. A total of 10,000 cells were analyzed. The cell distribution is shown as the blue histogram, in which the X-axis represents the fluorescent intensity; while the Y-axis represents cell counts. Several concentrations of ABP (0, 50, 100 and 200 μM) were used to stimulate the cell surface CD44 expression.

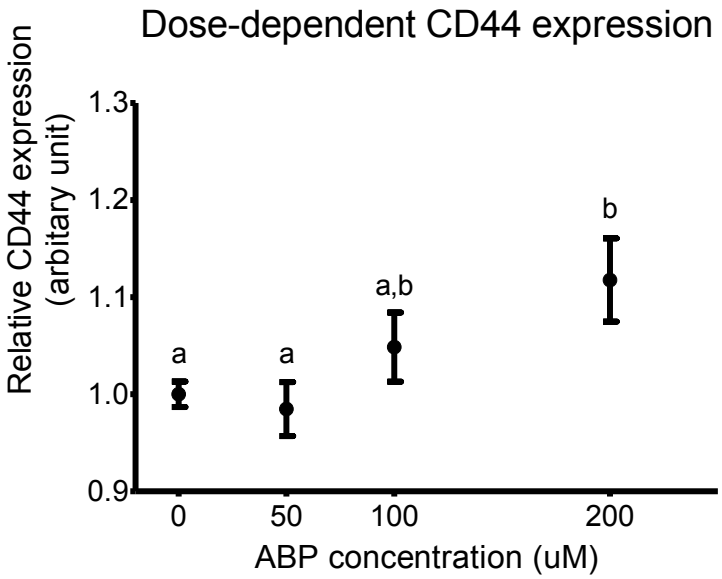

Figure 3.10 Dose-dependent effects of ABP CD44 expression measured at week 1.

Expressions were expressed as the fluorescent intensity relative to the median fluorescent intensity of DMSO control (0 μM ABP). N = 4 for each treatment concentration. Treatment groups annotated with the same alphabets were not statistically different in Tukey's Honestly Significant Difference (HSD) test, $p > 0.05$. A trend of CD44 induction was observed as ABP concentration increased. Significant induction of CD44 was only found in 200μM ABP, which is consistent with our previous result.

3.5 Molecular markers of bladder cancer

After transformation, two molecular markers - telomerase and survivin, were used to access the tumorigenicity of the cell line after exposed to the carcinogen 4-ABP and 6-weeks incubation process.

3.5.1 Induced Telomerase activity

After comparing the basal level of telomerase activity, it was found that pre-cancer cells (HUC-PC) have similar telomerase activity compared with that of the normal stage (HUC-1) (data not shown). While after ABP induced transformation, there was a significant induction of telomerase activity in the HUC-PC cell line but no such change was found in the HUC-1 cells (Figure 3.11). The data suggested that transformed HUC-PC acquire a higher telomerase activity after ABP exposure which governs the cell with unlimited cell dividing ability.

3.5.2 Assessment of survivin mRNA expression

While previous findings suggested that anti-apoptotic ability conferred by survivin (86) can be one of the features of neoplasia, our data supported this hypothesis to only some extend. On one hand, it was found that survivin expression in pre-cancerous HUC-PC was generally higher than that of the HUC-1. On the other hand, the survivin expressions were similar between ABP-induced, transformed HUC-PC and it DMSO control (Figure 3.12). It seemed that the ABP-induced transformation did not invoke apoptosis inhibition via survivin.

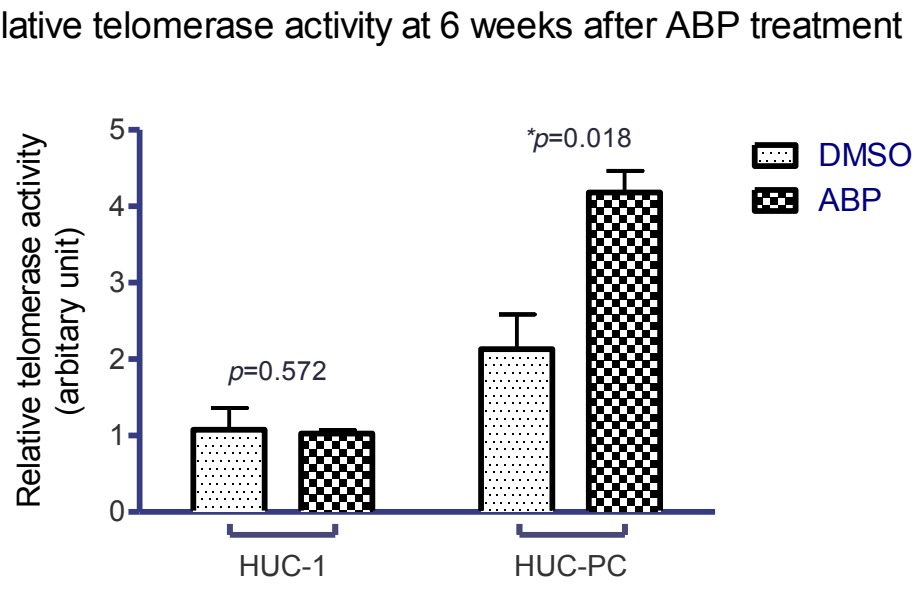

Figure 3.11 The relative telomerase activity of HUC-1 and HUC-PC after the tumorigenic transformation.

Both cell lines were exposed to 200μM ABP for 24hr, followed by 6-week incubation. Cells grew in medium containing 0.1% DMSO (solvent) were used as control. Two-way ANOVA indicated that interaction effect was significant between cell lines and treatments ($F_{1,4}$ = 13.1, p = 0.007). Separate Student's t-test (one for each cell line), followed by FDR adjustment, to evaluate differential treatment effect in the two cell lines. Significant induction of telomerase activity was only demonstrated by the ABP-treated HUC-PC, when compared to the solvent control. N = 3 for each treatment group in each cell line; Error bar: SEM; *: $p < 0.05$.

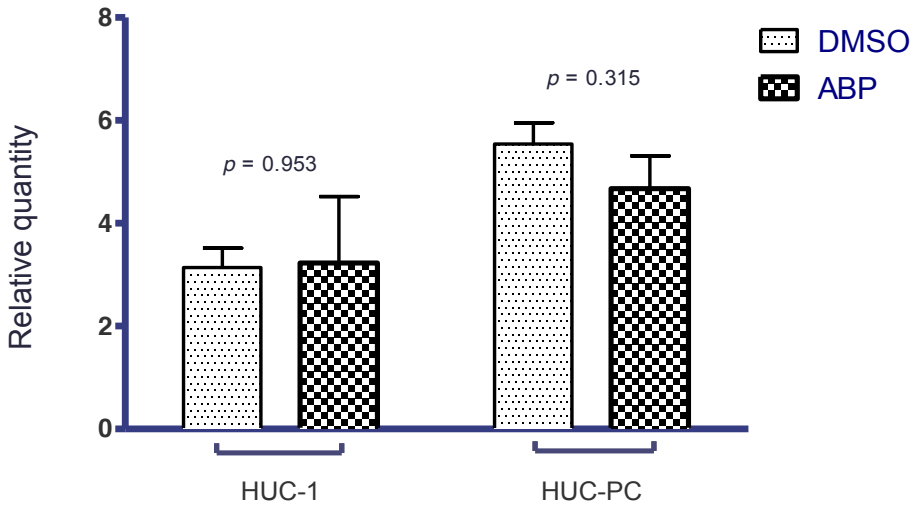

Figure 3.12 The relative survivin mRNA expression of HUC-1 and HUC-PC after the tumorigenic transformation.

Both cell lines were exposed to 200μM ABP for 24hr, followed by 6 weeks of incubation. Cells grew in medium containing 0.1% DMSO were used as the solvent control. No statistical significant change of survivin expression was observed after transformation. N = 3 for each treatment group in each cell line; Error bar: SEM, *: $p < 0.05$.

3.6 Phenotypic properties of the transformed cell

After 24 hr exposure to ABP and 6-week transformation, phenotypic properties in terms of proliferation and invasion of the transformed HUC-PC were assessed.

3.6.1 Induced proliferation of transformed HUC-PC

Results from proliferation assay indicated that HUC-PC and HUC-1 had similar basal rate of proliferation (Figure 3.13). However, they have different response towards the carcinogen ABP. After ABP exposure, HUC-PC had an induced proliferation rate compared to the DMSO solvent control; while that of HUC-1 remained the same. The induction of proliferation of HUC-PC may favor the accumulation of mutation and finally led to cancer development.

3.6.2 Induced invasion of transformed HUC-PC

Invasive behavior was detected in the ABP-transformed HUC-PC but not in the DMSO control. As is shown in Figure 3.14, there were a significantly larger number of transformed cells that passed through the membrane; while the control cells were blocked. The invasiveness of the transformed cells was realized by their effectiveness in digesting and migrating through the ECM-mimic (Matrigel). This data showed that the invasive ability of HUC-PC was induced after the ABP exposure.

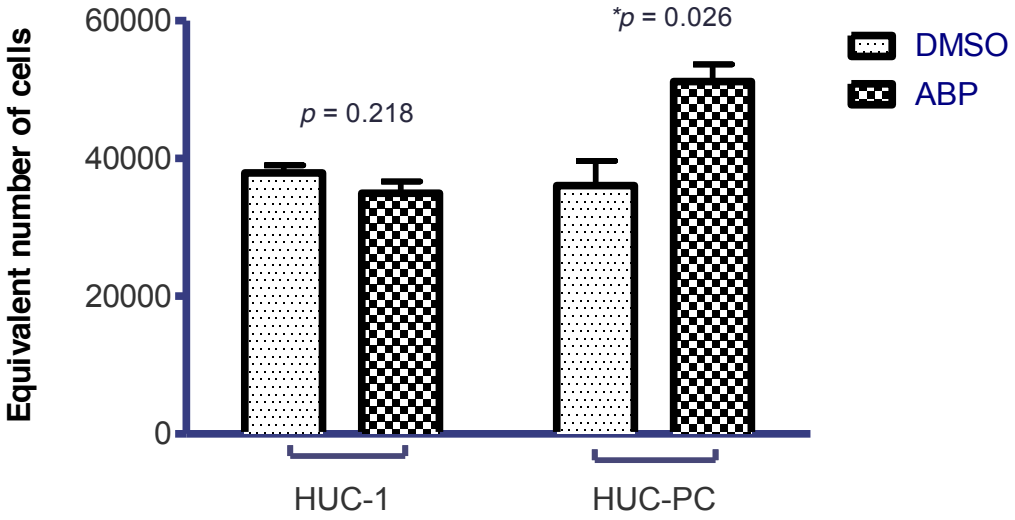

Figure 3.13 The proliferation rate of HUC-1 and HUC-PC in term of cell number after the tumorigenic transformation.

Both cell lines were exposed to 200μM ABP for 24hr, followed by 6 weeks of incubation. Cells grew in medium containing 0.1% DMSO were used as solvent control. Two-way ANOVA indicated that the statistical significant interaction (p = .006) signified the two cell lines may respond differently towards ABP treatment. We performed two separate Two-sample t-test (one for each cell line) to evaluate the treatment effect. Growth induction was observed in ABP-exposed HUC-PC, when compared with its solvent control. N = 3 for each treatment group in each cell line; Error bar: SEM, *: $p < 0.05$.

DMSO Control

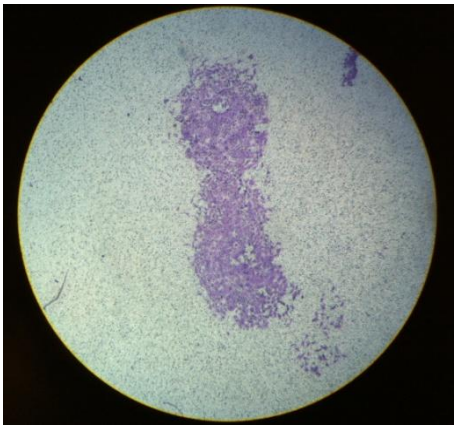

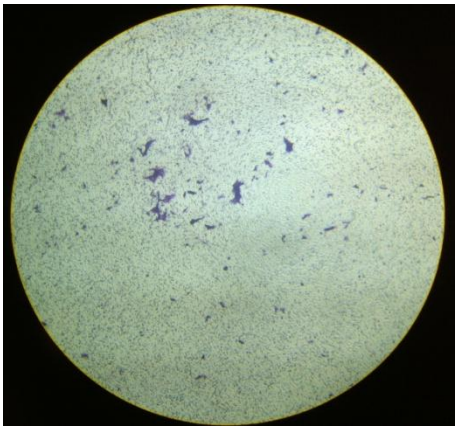

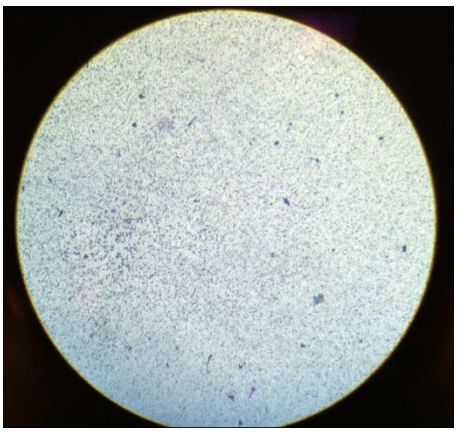

ABP treated HUC-PC

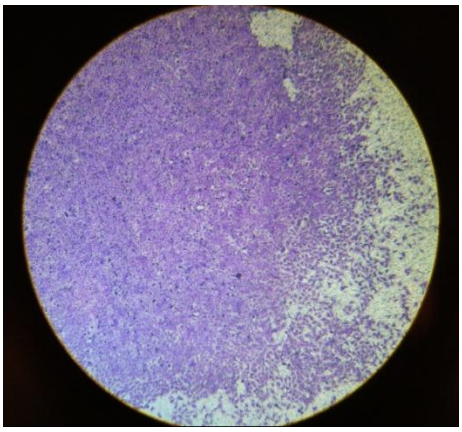

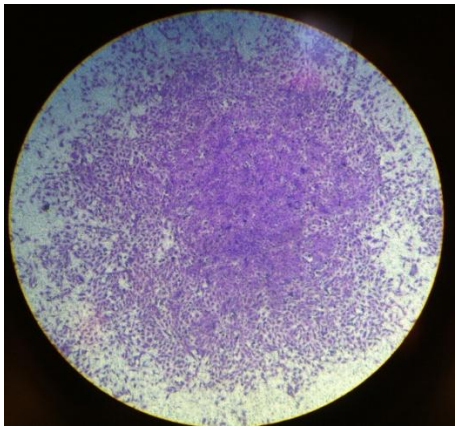

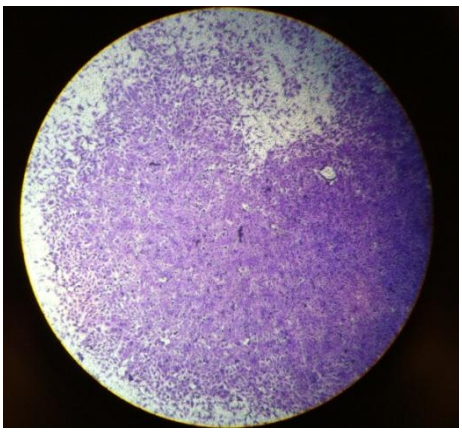

Figure 3.14 Representative photos of invasion assays captured under 100X magnification.

Invaded cells were stained purple. The number of cells invading through the membrane was significantly higher in the ABP-treated HUC-PC cells (right) than that of the solvent control (left). N=3.

3.7 Expression profile of CD44 Isoforms mRNA in transformed HUC-PC

Consistent with our result in flow cytometry, total CD44 mRNA expression level in ABP exposed HUC-PC was higher than that of the control in Week 1 (Figure 3.15). Around half of the total CD44 mRNA was expressed in form of CD44s; while CD44v6 only occupied a negligible portion. Additionally, the CD44 qPCR results demonstrated that the mRNA expression of CD44s was induced after ABP exposure, while no significant change was observed for CD44v6. Therefore, the induction of total CD44 was mostly contributed by the induced CD44s mRNA expression.

At the end of the transformation (Week 6), a similar pattern of the CD44s and CD44v6 expression profile was found (Figure 3.16). However, the mRNA expression of total CD44, as well as that of the CD44s, in the transformed HUC-PC returned to a level similar to the control.

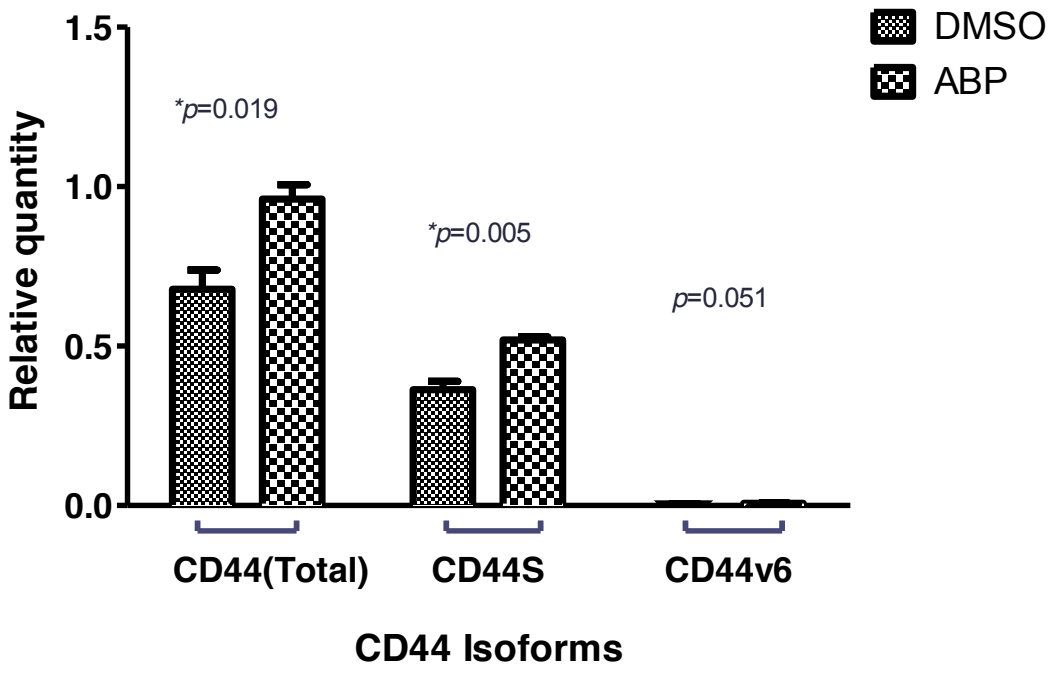

Figure 3.15 Expression CD44 variants at Week 1 after ABP treatment.

The initial change of CD44 mRNA expression after ABP exposure was compared by using RT-qPCR. Total CD44 expressions in ABP-treated HUC-PC increased significantly. The increase of CD44 was mainly contributed by the standard form instead of the v6 isoform. N = 3 for each isoform in each treatment group; Error bar: SEM, *: $p < 0.05$.

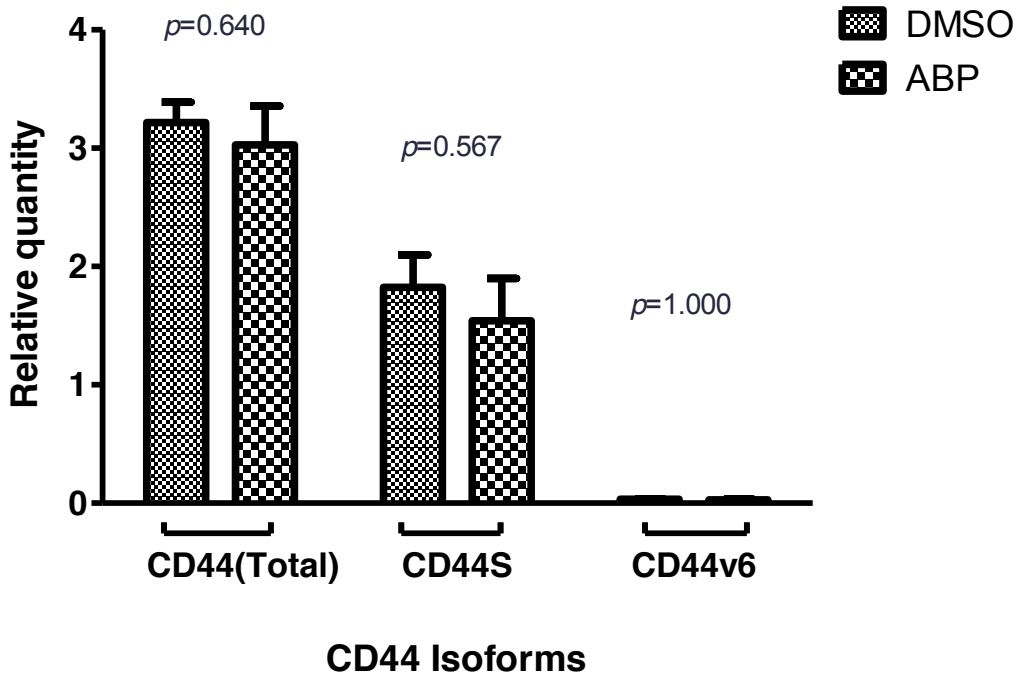

Figure 3.16 Expressions CD44 variants at Week 6 after ABP treatment.

The change of CD44 mRNA expression at the end of transformation was compared by using RT-qPCR. It found that the CD44 expression level of ABP-treated HUC-PC returned to the control level. N = 3 for each isoform in each treatment group; Error bar: SEM, *: $p < 0.05$.

3.8 Expression profile of hyaluronan synthase isoform mRNA

qPCR was used to measure the transcript levels of HAS family members in HUC-PC at Week 1 (initiation) and Week 6 (transformed). It has been found that HAS1 and HAS2 mRNA level were significantly lower in ABP exposed samples, when compared with the DMSO control, while their expression levels of HAS3 were similar to that in the initial state (Figure 3.17).

After transformation, no significant difference was found in the transcript levels of all HAS isoforms (Figure 3.18). Although HAS2 expression was increased, a similar response was also found in the control. Therefore, the change of HAS2 expression was likely to be a temporal fluctuation during the 6 weeks of passages, instead of the ABP treatment effect.

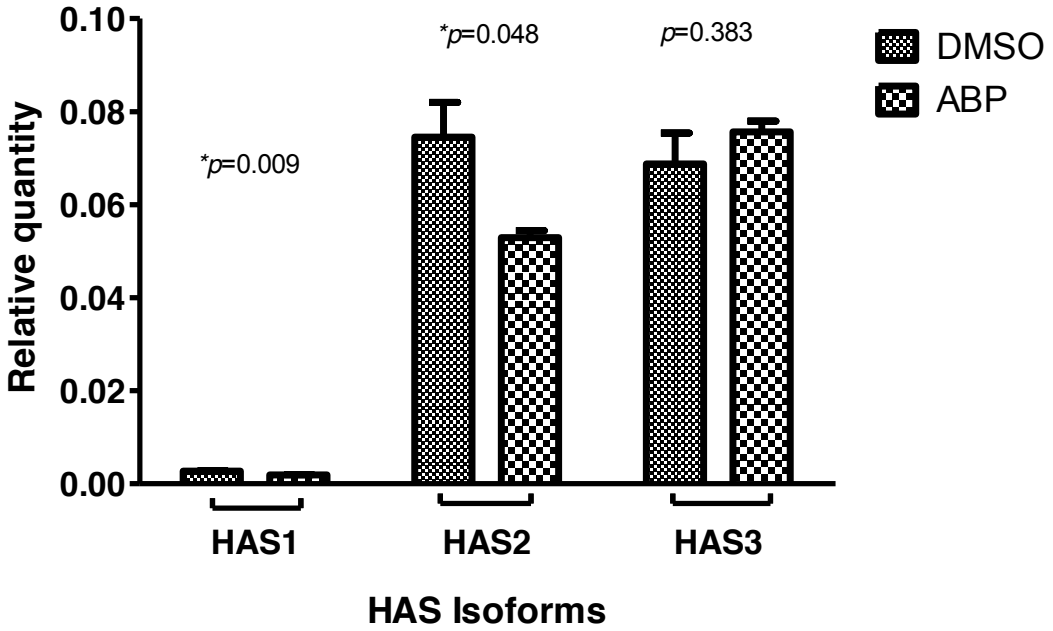

Figure 3.17 Expression of HAS isoforms at Week 1 after ABP treatment.

Compared the initial change of mRNA expression of three HAS isoforms after ABP exposure by using RT-qPCR. ABP-treated cells exhibited significantly lower levels of HAS1 and HAS2. Note that the expression level of HAS1 was much lower than the other two isoforms, regardless of treatment. N = 3 for each isoform in each treatment group; Error bar: SEM, *: $p < 0.05$.

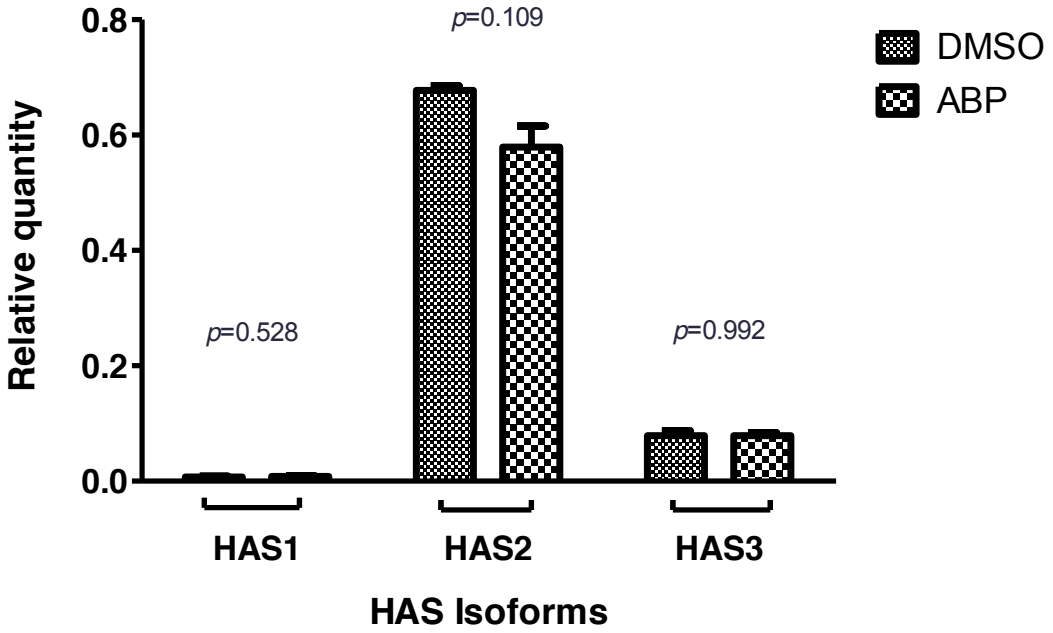

Figure 3.18 Expressions of HAS isoforms at Week 6 after ABP treatment

Compared the change of mRNA expression of three HAS isoforms after transformation using RT-qPCR. No significant change in the expression of all three isoforms was detected between DMSO control and ABP-treated cells. N = 3 for each isoform in each treatment group; Error bar: SEM, *: $p < 0.05$.

3.9 HA measurement by HPLC

The quantity of HA in cell culture medium was measured using analytical HPLC system. It was a preliminary study to find out how CD44 involved in the transformation process. Since HA is a major ligand that bind with CD44 to trigger the transformation properties, we tried to measure the HA concentration during the process.

The retention time of HA was around 7min as is shown by the spiked-in HA standards in Figure 3.19. The concentration of HA was calculated by using the standard curve in Figure 3.20 and the results were presented in Figure 3.21.

Overall, the amount of HA in medium incubated with ABP-treated cell was higher than that of control cells throughout transformation, except at Week 1 As is shown, HA secretion was reduced at one week after exposure to carcinogen but there was a drastic increase of HA content at Week 3 until the end of transformation.

As is shown in Figure 3.22, the amount of HA was significantly increased only if the cells were pre-stimulated with ABP. On average, there was a 3-folds increase of HA in the culture medium of the transformed cells compared with that of the controls cells.

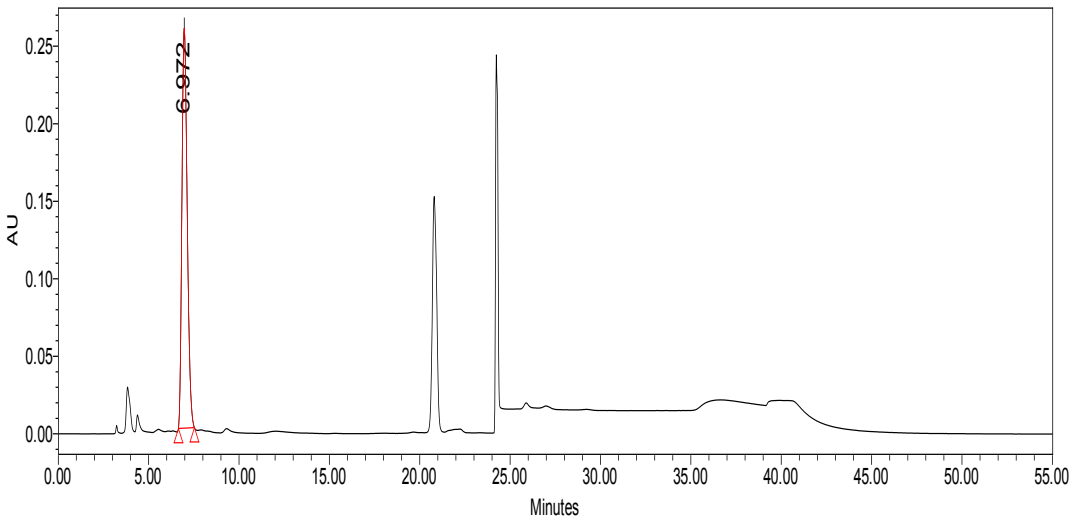

Figure 3.19 Chromatogram of digested HA in HPLC

20µl of the purified HA standards with several concentrations were injected and measured at 232nm. Reproducible peak eluted at around 7min was identified as the study target (HA).

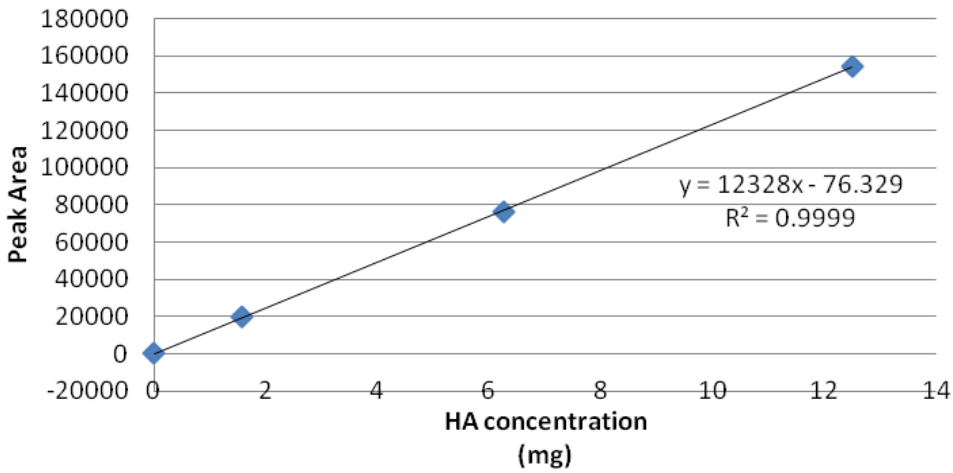

Figure 3.20 Standard curve for the determination of Δdi-nonS_{HA}

The respective area under the identified peak in chromatograms were integrated and plotted against the amounts of serially diluted reference standards.

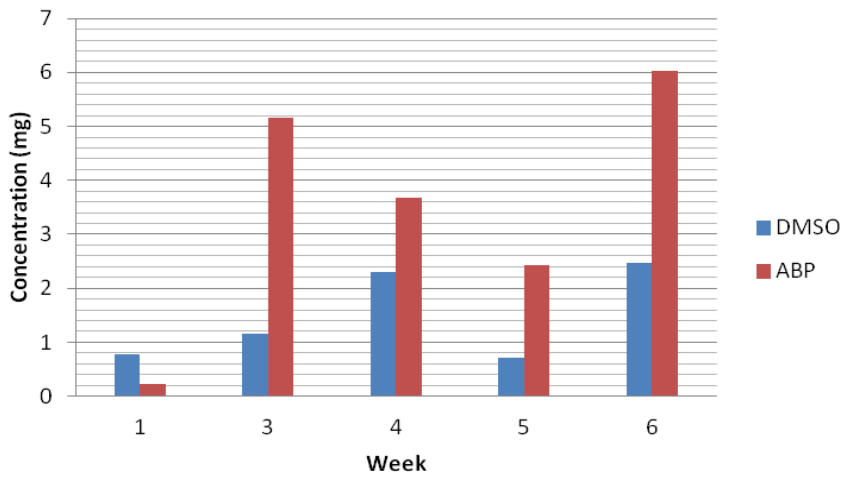

Figure 3.21 Concentration of HA in cell culture medium incubated with HUC-PC

The amount of HA recovered in cell culture medium was quantify using HPLC. The amount of HA recovered in cell culture media was consistently higher among ABP-treated HUC-PC, than the DMSO control, from 3-weeks post-treatment onwards. (N=1)

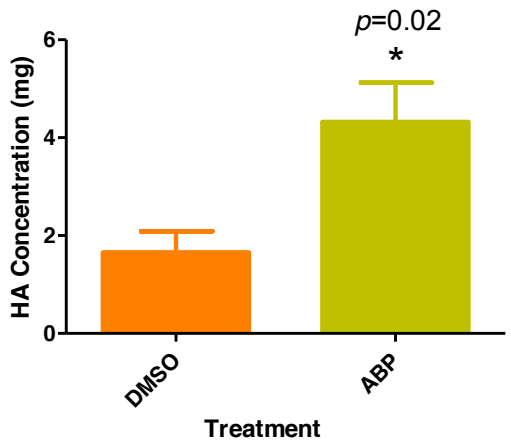

Figure 3.22 Average weekly secretion of HA throughout of transformation

ABP-treated HUC-PC produced statistically larger quantity of HA than the DMSO control counterpart. *: Student's *t* test, $p < 0.05$. N = 4 for each treatment group.

3.10 Stable clone generation

In order to illustrate the function of CD44, we attempted to generate a stable clone with CD44 suppression. Transfected cells expressed GFP protein and gave green fluorescence when illuminated. The transfection efficiency was around 60% (Figure 3.23).

However, once CD44 was suppressed, the proliferation of the transfected cells was also inhibited (N=4). Due to this reason, there was inadequate number of cells for the previously described functional assays.

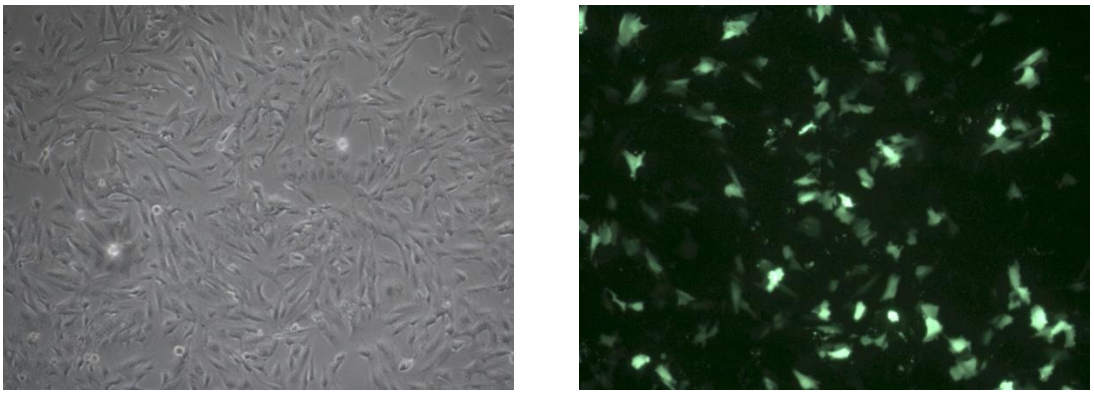

Figure 3.23 Transfection of CD44 shRNA

HUC-PC was cultured in 6-well plate and transfected with CD44 shRNA plasmid using transfection reagent. Transfected cells expressed GFP protein and illuminated under excitation. Left: phase contrast view; Right: fluorescence view.

3.11 A summary of major findings

In summary, the gene expression data from microarray study confirmed the presence of sensitized cell which displayed a large number of differentially expressed transcripts, when compared to that of the normal urothelial cells. The current study focused on the cell surface marker - CD44 which was strongly expressed in the pre-cancer cell at protein level. Upon stimulated by the carcinogen ABP, HUC-PC showed a transient induction in the early state (initiation) of the transformation process. This induction was found to be dose-dependent. By the use of real-time PCR, it was found that the up-regulation of CD44 was mainly due to the contribution of its standard isoform, CD44s. Molecular markers and different assays were applied to gauge the cancerous properties of the transformed HUC-PC. A multitude of evidences, including induction of proliferation and invasion, signified the success of transformation. Molecular markers, including telomerase and survivin, also confirmed the cancerous properties of HUC-PC.

For the pathway analysis, HA was identified as our prime target since CD44 is its major receptor. It is synthesized by HAS and thus expressions of the three HAS isoforms were also analyzed using real-time PCR. Interestingly, reduction of HAS was found in the initiation state of transformation. Consistent with this result, the amount of HA released in the culture medium was reduced at 1 week after ABP treatment. The amount of HA was increased dramatically 3-weeks after exposure, and there was 3 times increase in the HA content at the end of transformation. However, the induction of HA cannot be explained by the change in HAS expression.

Chapter 4 **Discussion**

4.1 Study highlights

Despite frequent recurrence is the major obstacle in bladder cancer therapy, there is virtually no documented research in attempt to resolve the source and the process of recurrence. In this study, we hypotheses that the tumor neighboring cells (sensitized cells) may be the source of recurrences. However, it is unethical and aberrant to delve into uncharacterized, presumably complex biological process by taking those cells in patients. Therefore, an alternative model, the pre-cancerous HUC-PC cell line, is proposed for studying the properties of sensitized cells and the involvement of the tumor initiating marker, CD44, during the transformation process. We envision this study serves pivotal insights to the mechanism of- and fuels further research studies in understanding the bladder cancer recurrence.

4.2 Different proposed mechanisms of bladder cancer recurrences

Different mechanisms have been proposed for the high recurrence rate of bladder cancer: (1) new tumor formation, (2) tumor cell re-implantation, and (3) incomplete resection of primary tumor.

As described in Chapter 1.4.3, recurrences due to new tumor formation are unlikely since bladder cancer almost always recurs within a few months. Tumorigenesis usually stems from accumulating mutations, which ultimately reprograms a cell to undergo uncontrolled cell division. It is unrealistic to develop a new tumor from ground-up that rapidly in patients who are undergoing intensive medical care and well isolated from mutagens. On the other hand, tumors usually recur at the same position where it was originally located. It is preposterous that tumor cells re-implantation, which is a random process, can seed tumor cells with such a high precision.

On the contrary, we believe that incomplete initial surgery may be the prime reason for significant number of bladder cancer recurrences. The latest review of bladder cancer management also criticized that "the procedure for oncological clearance TUR is undoubtedly imperfect" (146). In fact, bladder cancer development is a process of accumulation of genetic changes, thus, different regions of the urothelium may have different degrees of mutation - the so called "field defect theory". Based on this theory, we hypothesize that the cells that are adjacent to the primary tumor are actually 'sensitized", i.e. they accumulated certain level of mutations that is just below the threshold (criticality) of conferring malignance. These mutated cells may morphologically resemble normal cells and thus are not removed during TUR.

Recently, DNA microarray technique has been applied for studying cancer recurrences. A prostate cancer study compared gene-expression profile of 98 prostate tumors to 52 benign adjacent prostate tissue samples and found that 28 transcripts significantly associated with recurrences after radical prostatectomy (147). Similar

approach was applied in this study, in which we compared the gene-expression profiles of 10 normal urothelium with that of 58 urothelial tissues near to the tumor site ('tumor neighboring') that were morphologically normal. Surprisingly, tumor neighboring tissues were very different from normal urothelium, i.e. 'abnormal', showing over 400 DE transcripts. In addition, all these DE transcripts were constitutional part of the primary tumor's transcriptome. These manifested the urothelial tissues adjacent to tumor site were not only mutated but also bore resemblance of the tumor. This finding provides direct evidence to support the field defect theory and the existence of sensitized cells, i.e. the tumors were originated from cells having the same genotype (mutations) of the neighboring tissue (sensitized cells) but collected additional genetic changes that triggered malignancy. Under our hypothesis, these neighboring tissues (sensitized cells) might also receive additional mutations (just as the primary tumors did) and fueled future tumor formations – the recurrence. The proposed pathway of bladder cancer recurrence is shown below.

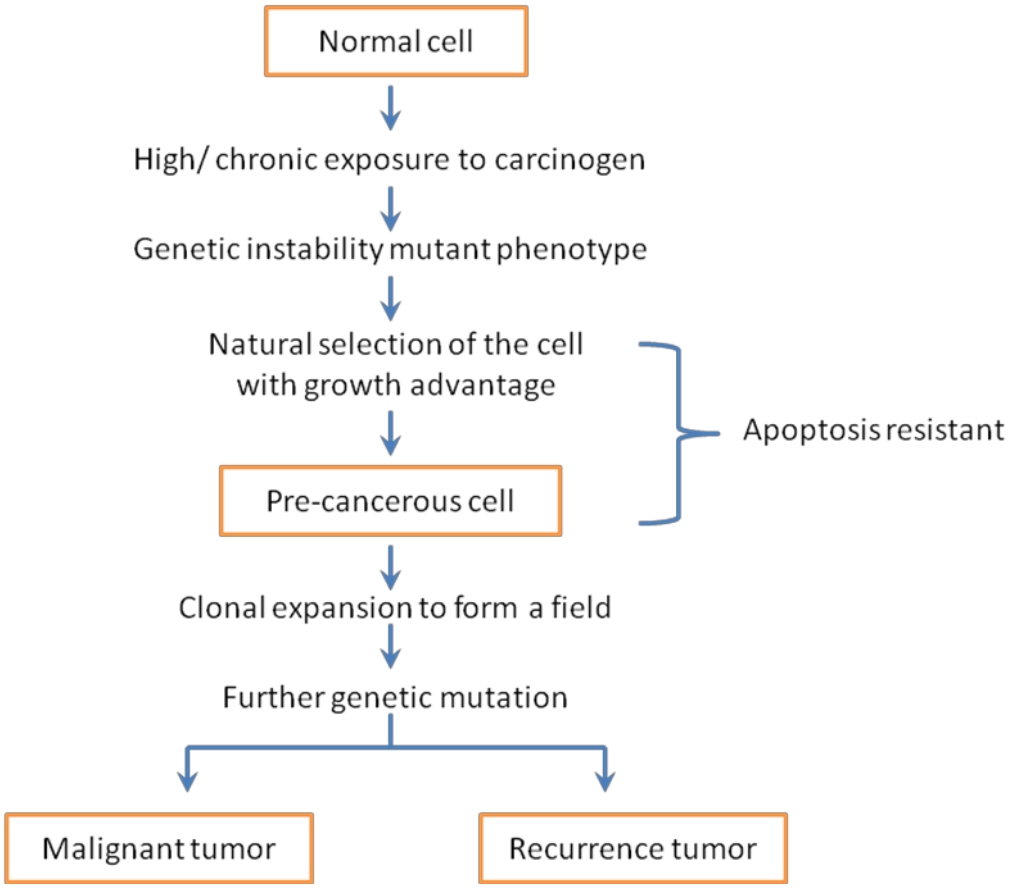

Figure 4.1 Proposed pathway for malignant and recurrence tumor formation

4.3 Studying bladder cancer recurrence: the challenge and our solution

The process that a normal urothelial cell transforms into a malignant cell is complex and likely to involve interaction of a spectrum of genes, proteins and other bio-molecules. Unraveling this process will, with no doubt, advance our understanding of tumorigenesis and facilitate the development of effective means to cure bladder cancer and prevent recurrence.

As a routine, cancer research usually starts with data obtained from clinical observations. The observations often lead to hypotheses about the abstract tumorigenic process (e.g. aberrant cellular signaling, chromosomal abnormalities, etc). Yet, testing these hypotheses in human subjects are often hindered by the limited sample size and, more importantly, undeniably unethical. Hence, the most popular, and arguably the most suitable, model deployed in this research aspect is cancer cell lines. Only with solid data collected from cell lines and supplemented with validations using mammalian models, clinical trials on human subjects can then be arranged for confirmation.

With the gene expression profiles of clinical samples examined, we hypothesized the transformation of sensitized cell to malignant cell is the major source of bladder cancer recurrence. Our next logical move is to investigate the details of this transformation process. A simple *in vitro* transformation model, HUC-PC, was applied in this study. HUC-PC is a well establish model for studying tumorigenic

transformation. In 1992, Bookland et al. first demonstrated reproducible transformation of this model by a chemical carcinogen, 4-aminobiphenyl. For detailed information of this model, please refer to Chapter 2.2.2 on Page 42. The only difference between them is that HUC-PC received more passages and expanded procedure that induced higher level of chromosomal instability. It makes HUC-PC more sensitive to the carcinogen. In other words, HUC-PC seems to have lower ability to restore the normal functions of cell such as the regulation of CD44 expression in our case.

HUC-PC can be a relevant model to represent the sensitized cell in the bladder lining as they share a certain degree of similarity. First of all, they are both morphologically normal but genetically unstable. Also, once stimulated (minor additional mutations), they have a high tendency to transform in a short period of time. Therefore, this cell line may provide a valuable tool for studying the molecular events during transformation process from pre-cancerous to tumorigenic state. However, it has to be emphasized that HUC-PC, as an immortalized cell line, does not truly represent the sensitized cells in human bladder. Nonetheless, it is the best alternative available at this moment for studying mechanism of tumor transformation and cancer recurrence.

4.4 Contrast between the properties of HUC-PC before and after ABP exposure

4.4.1 Characteristic of pre-cancerous HUC-PC

The pre-cancerous HUC-PC seemingly acquired certain characteristics that allowed the cell to transform. Previous study has already shown that HUC-PC is sensitive to the carcinogen ABP and, once stimulated, will slowly transform to cancer cells; while its mother cell line HUC-1 is not sensitive at all (139). In this study, we investigated the different between HUC-1 and HUC-PC at the molecular level.

A higher survivin mRNA level was found in HUC-PC compared with HUC-1, which implicates that the pre-cancer cell acquired anti-apoptosis ability. This property may allow the cell to accumulate mutations without triggering programmed cell death. A colon cancer study indicated that 50% of the survivin-positive tumors with normal appearing mucosa also expressed this gene (148). It was suggested that survivin expression may represent a pre-cancerous stage and allow for identifying risk of neoplastic transformation. Another study conducted using urine exfoliated cells of bladder cancer patients followed up for 15 months after operation (144) found that bladder cancer patients had a higher survivin mRNA level than that of healthy individuals. Furthermore, after operation, the survivin level of patients dropped to the control level while the recurrence patients still showed a higher survivin expression. We proposed that survivin can be an indicator for recurrences and the higher survivin expression level may due to the presence of sensitized cell.

4.4.2 Characteristic of transformed HUC-PC

In our studies, a wide range of functional assays was applied to determine the phenotypic characteristics of the pre- and post- transformed HUC-PC. By comparing the differences between HUC-PC and its DMSO control after 24-hrs ABP exposure and 6-week incubation, it was found that the transformed HUC-PC displayed a higher tumor-like aggressiveness in which its invasive ability and proliferative power was enhanced. After 6 weeks of incubation, HUC-PC showed a higher proliferative power compared with its control. This uncontrolled cell growth is one of the key characteristics of tumor and maybe the major cause of recurrence.

In order to assess the tumorigenicity of the cells after ABP-induced transformation, bladder cancer markers telomerase and survivin were gauged. Induction of telomerase activity permits unlimited growth of the cell, which confers one of the most critical properties of cancer cell. As is shown, telomerase activity in the transformed HUC-PC was elevated, that may also contribute to the induced cell proliferation. Our data suggested that carcinogen ABP induces telomerase activity which then stimulates the cell proliferation. Also, bladder tumors with high telomerase activity were accompanied with high grade and advanced stage (82) and thus the level of telomerase activity may reflect the malignant potential of the tumor.

As an inhibitor of apoptosis, survivin has been suggested to be a prognostic marker of bladder cancer. We demonstrated a higher survivin mRNA expression level in pre-cancerous HUC-PC than HUC-1. However, its expression in transformed HUC-PC was similar to its DMSO control. These findings suggest that anti-apoptosis

ability is already acquired in the pre-cancerous state but this property may favor the further accumulation of mutations during the transformation.

4.5 Functional role of CD44 in cancer development

4.5.1 CD44 participates in tumorigenesis

CD44 is a transmembrane glycoprotein that acts as a receptor for the ligands hyaluronic acid, osteopontin, collagens, and matrix metalloproteinases (MMPs) for controlling the cell properties such as proliferation and migration. In tumorigenesis, CD44 binds to its ligands and triggers a cascade of signals leading to activation of various genes related to inflammation, cell proliferation and migration as well as anti-apoptosis. It is also claimed as a tumor initiating marker in various cancers including bladder cancer (99, 126). Therefore, CD44 was chosen as our starting point for investigating the transformation process.

In the current study, HUC-PC displayed a higher cell surface CD44 expression that may contribute to its higher malignant potential (sensitized). Consistent with this, many studies have already indicated that CD44 participates in tumor initiation and progression. A bladder cancer research conducted by Sugino et al showed that the amount of CD44 are increased in the epithelial cells composing of malignant tumors (149). The higher CD44 expression in the pre-cancerous HUC-PC may be the sign of having the self-renewal property which enhance its survivability after exposure to

carcinogen. A study on colon cancer demonstrated that cells with high CD44 expression exhibited an up-regulation in stem cell-related genes, Oct4, Sox2, Nanog and c-Myc, which are essential for stem cell pluripotency and self-renewal (101). The high level of CD44 expression can be explained by its binding with the insulin-like growth factor II mRNA-binding protein 3 (IMP3), which in turn stabilized the CD44 mRNA (150). Besides, the promoter region of CD44 has an EGR-1-binding motif and suggested that early growth response protein-1 (EGR-1) can up-regulate the CD44 expression in the presence of the proinflammatory cytokine IL-1 (151).

4.5.2 Expression of CD44 depends on cancer developmental stage

Some findings, however, have demonstrated that expression of CD44 reduces in high grade bladder cancer (130-132). Our data also indicated that the induction of CD44 in the first week after ABP exposures was transient, yet this temporary induction is adequate to transform the cell into cancerous. It raises the possibility that CD44 has multiple roles during the cancer development process.

In the initiation stage, high expression of CD44, as a signaling trigger for cell proliferation and differentiation, may permit and prepare the cells to grow and transform. Lots of studies support CD44 can induce cell proliferation responses via different mechanisms (152-156) and one of these is the reduction of the binding between CD44 and its ligand - HA (155, 157). Some contradictory findings, however, suggest negative regulation of cell proliferation by CD44 (158). To further

investigate the possible roles of CD44 during the transformation process, we generated a stable clone of CD44-shRNA transfected HUC-PC. The CD44 knockdown severely hampered the ability of HUC-PC to proliferate *in vitro* and thus making it difficult to generate adequately sized population of cells for experiments. Nevertheless, the observed suppression well proved the relationship between CD44 and cell proliferation. The proliferation ability of HUC-PC was suggested to be reduced after transfection of CD44 shRNA.

In the later stage, loss of CD44, as a cell adhesion molecule, may facilitate the cancer cells to break-free from cell-cell adhesion and metastasize. The cleavage of extracellular domain of CD44 is triggered by activation signal, such as Ca^{2+} influx, PKC activation Rho family of small GTPases and Ras oncoprotein (159, 160). The ectodomain cleavage is mediated by different membrane-associated MMPs (161-163) such as MT1-MMP, ADAM10, and ADAM17 as well as ECM component chondroitin sulfate E (164). Inhibition of the cleavage of CD44 was shown to suppress the cell migration rate (164). These tightly controlled actions then regulate the turnover of cell adhesion and migration process in a CD44-dependent manner. Besides, the ectodomain cleavage will also trigger the intramembrane cleavage of CD44 mediated by presenilin-dependent γ-secretase (165, 166). In fact, several cell surface receptors, including EGF receptor proteins, FGF receptor and insulin receptor are known to migrate to the nucleus and act as transcription factors (167-170). Similarly, the released intracellular domain of CD44 in cytoplasm can act as a signal transduction molecule which translocates to nucleus and activates the

transcription of various genes including *CD44* itself (171). This self-initiating mechanism allow rapid turnover of CD44 and thus promote cell migration (171).

4.6 Contribution of CD44 variants during transformation process

It is now generally recognized that CD44 and, in particular, its splice variants have major contributions in cancer development. Lots of studies have investigated the possibility for using CD44 or its variants as prognostic and diagnostic markers (123, 127, 128, 172). Recently, Yang et al proposed CD44 is a tumor initiating marker (126), and thus, has a high potential to be applied in predicting the risk of tumor recurrence or progression in bladder cancer patient. Our findings also support the contribution of CD44 in cancerous transformation.

It is worthwhile to note that the involvement of CD44 in transformation process is historically controversial, for instance, opposite findings indicated that focal loss of CD44v3 and v6 immuno-staining is correlated with short recurrence-free interval in superficial TCC (173). This enigma is now explained by the differential expression of CD44 variants (125). Theoretically, there are more than 800 CD44 variants that can be generated by alternative splicing the 9 introns in CD44 pre-mRNA. However, only 6 of them were identified and curated in NCBI RefSeq. It is theorized that each of these splice variants has its specific role in cancer development. In breast cancer,

CD44v6 is the most abundant variant (174, 175); for gastric cancer, expression of CD44v9 correlated to the pathological stage of the cancer (137); for bladder cancer, CD44s and CD44v6 are associated with malignant features and cancer prognosis (176, 177). Physically, CD44s is shorter than CD44v6 (isoforms containing exon 11) due to the alternative splicing. The difference in length may affect the binding between CD44 receptor to its ligands which in turn trigger different downstream pathways that controlling the cell behavior. However, until now, the specific function of these 6 common variants remains unknown, and thus is still one of the major areas in CD44 research. In our study, the contributions of different variants including the standard form and v6 were analyzed by real-time PCR. We demonstrated that only a very low amount of CD44v6 was expressed in the sensitized HUC-PC at the initiation state, and the induction of CD44 is mainly due to the CD44s expression. Thus, we envision that the expression of CD44s and CD44v6 is associated with different malignant features. A study supports this view as it shows that strong expression of CD44s was related to unfavorable outcome, while, opposing, strong expression of CD44v6 was related to high survival probability in bladder cancer patients (176). The functional roles of CD44s are of great interest for studying the transformation process.

4.7 Possible pathways involved in ABP-induced transformation

The pathways that CD44 is involved during cancerous transformation are of great interest for uncovering the cancer development. In this study, one of its ligands, HA, was investigated. According to the result of functional assays, transformed HUC-PC showed an induction of proliferation and invasion, which are regulated by the extracellular matrix (ECM) and cell-cell interactions. It is proposed that the induction of CD44 during tumorigenic transformation may be one of the important mediators that facilitate the binding with HA and thus trigger tumor development. On the other hand, recent studies showed that transcript levels of the HA synthases (1, 2, 3) were 4- to 16-fold higher in bladder cancer tissues than that of normal tissues ($P < .0001$) (178). Also, wealth of data support HAS control cell behavior by modulating the synthesis of HA (95, 96). Therefore, in this study, the quantity of all three types of hyaluronan synthase was measured by real-time PCR and the amount of HA was quantified by HPLC. As is shown, CD44 expression was induced at both mRNA and protein levels in the initial state of tumorigenesis. On the other hand, HA expression and the HAS (1 and 2) were reduced at the same time point. It is proposed that induction of CD44 expression is prerequisite to transformation. The closely followed induction of HA released in the medium binds with CD44 and further activates the transformation process. At the end of transformation, there was a 3-fold increase of HA released in the medium of transformed samples, excess amount of free HA in medium results in weakening cell anchorage to the

extracellular matrix and facilitating cell migration and division (179). Unexpectedly, the higher HA level could not be explained by any change in the mRNA expression of HA synthases, which synthesize HA de novo. This interesting finding indicated that the increase of HA in cell culture medium may due to 1) the release from/ reduce binding by CD44, or 2) modulation of its degradation instead of new HA synthesis (180).

Our results demonstrated that induced expression of CD44 in HUC-PC might associate with the elevated levels of HA. This positive correlation between CD44 and HA reinforced the hypothesis that development of cancer is triggered by the binding between CD44 and HA as one of mechanisms. Lots of studies indicated that treatment with HA enhanced the proliferation, invasion and migration of cell but the effect was abrogated by the suppression of CD44 (157, 181). However, the mechanism by which HAS, HA and CD44 affect the transformation is still poorly understood. One of the CD44-HA signaling pathways was described in an *in vitro* study of bladder cancer cell line T-24 (117), which demonstrated that interaction of CD44 and HA fragments lead to activation of Ras, PKCζ IKK complex and finally up-regulate NF-κB expression - a master activator of inflammatory responses. The triggered inflammation can stimulate the tumor cell growth and development (118). Also, CD44-HA interaction favor the phosphorylation of an Na^+/H^+ exchanger which helps ECM degradation and invasion by providing an acidic environment with activation of HYAL2 and cathepsin (182). Pericellular HA may also provide a mechanical scaffold that traps growth factors and preinflammatory mediators to facilitate their interaction with the nearby cell surface receptor and finally enhancing

cell proliferation (179, 183). Taken together, these pathways may help to explain the induction of cell proliferation and invasion after transformation. However, the signaling cascades are cell-, stimulus- and environment- dependent. It would be of interest to test whether the downstream pathways were also involved in the transformation of sensitized cells. For example erbB2 (111, 114), Ras (117) and Rac1 (184) are shown to be the downstream effectors of CD44 signaling. Measurement of the expression of these effectors may help to identify certain pathways that are related to recurrences.

4.8 Clinical significance of CD44

With the establishment of the probably vital roles of CD44 in bladder cancer development and recurrence, we propose CD44 as a candidate surrogate endpoint for both detection and targeted therapy.

Prognosis

In this study, we demonstrated the pre-cancerous HUC-PC expressed higher level of CD44 than its normal control, HUC-1. The expression level was further elevated at the onset of tumorigenesis. These signified abnormal/induced CD44 expression in urothelial cells is tied to tumorigenesis, and thus can be a potential marker for bladder cancer development and recurrence.

Applicability of CD44 as prognostic and monitoring marker is further realized by the fact that urine carries small quantity of exfoliated urothelial cells. Despite the amount of cells collected through urinary discharge is not adequate for pilot research-use, but it is generally sufficient for prognosis based on sensitive detection of specific macromolecules, e.g. (qPCR, flow cytometry, etc). We contemplate detection of CD44 over-expression in urinary samples can be a highly economical, technically undemanding and non-invasive for bladder cancer detection and monitoring.

Treatment

High CD44 expression was found in the pre-cancerous HUC-PC but absent in normal superficial cells in human. Thus, this cell surface receptor can be a sensitized cell-specific marker for drug targeting and internalization. Recent studies have demonstrated that paclitaxel-hyaluronan bio-conjugate exerts its cytotoxic effect through the binding with CD44 on the bladder cancer cells (185, 186). This specific interaction of bio-conjugate with bladder tumors not only facilitates the drug delivery but also reduces toxicity towards the normal epithelium (186). These warrants further testing of CD44 as a viable, specific target for bladder cancer treatment.

Prevention

Suppression of CD44 expression may help to reduce cancer recurrences. Induction of CD44 was found in the initiation state of transformation, and suggested that CD44 may trigger the transformation progress by promoting cell proliferation and triggered signaling cascade that causes long-lasting, if not permanent, modification of the cell behavior. Our stable CD44-knockdown clone also clearly marked the crucial role of CD44 in cell proliferation. Hence, suppressing CD44 mRNA expression or directly blocking the CD44 receptor on cell surface from ligand-binding, i.e. inactivation, may serve as an effective mean to restrain the proliferation of cancer/sensitized cells. However, CD44 may not be the only factor that controls the transformation process, the effectiveness of this treatment needs to be carefully validated.

4.9 Limitations and further study

It should be stressed again that the proposed relationship between CD44 and tumor initiation was established by the use of a cell line, HUC-PC, which may not completely reflect the biological process *in vivo*. However, the result obtain provide us an insight to study the epithelial cell with high CD44 expression from the bladder cancer patient. With the establishment herein, the use of primary cultures derived from bladder cancer patients are sufficiently justified to provide physiologically relevant confirmation of the involvement of CD44 during transformation.

Clinically, non-invasive measurements, such as collection of exfoliated urothelial cells in urine, can be used to monitor probable coincidence of recurrence and alterations of CD44 expression in patients.

In parallel, studies were warranted to illustrate the mechanism for the induction of CD44 for driving the tumorigenic process. Revealing the downstream pathways of CD44 in tumorigenesis might benefit the prognosis and treatment of bladder cancer.

Chapter 5 **Conclusions**

The present study suggests the existence of sensitized cell may be the cause of high recurrence rate in bladder cancer. Microarray data pointed out the tumor neighboring cells were genetically different from the normal population and suggests that tumor neighboring tissue may have acquired certain degree of genetic changes that are not sufficient to confer malignancy, but predispose (sensitized) the cells to transformation.

The tumorigenic transformation process was visited in attempt to determine suitable markers for cancer/recurrence detection and develop effective treatments for patient. A well-established *in vitro* transformation model, HUC-PC, was employed to model how sensitized cell transform into cancerous. The changes of CD44 expression and the levels of its ligand, HA, during transformation were studied in details. CD44 was induced during tumor initiation; while induction of HA soon followed. In spite of the presumed importance of CD44 variants in tumorigenesis, CD44s, rather than CD44v6, was modulated during the tumor initiation process. The interaction between CD44 and HA may activate several proposed pathways that lead to cancer development. With all the establishments made by this pilot study, further investigation of specific roles of CD44 and discovering any associated intermediate pathways/molecules involved in triggering bladder tumor recurrence is strong yearned for.

Appendices

Appendix I: Chemical, materials and reagents

I.1 Cell culture materials and reagents

Cryotubes Nunc™,	Thermo Fisher Scientific
DMEM	Sigma-Aldrich
DMSO (Tissue culture grade)	ditto
FBS, Certified	Gibco®, Invitrogen
PBS (Calcium- and Magnesium-free)	Sigma-Aldrich
0.25% (w/v) Trypsin/EDTA	ditto
0.4% (w/v) Trypan blue solution	ditto

I.2 Molecular biological materials and reagents

Acrylamide	Sigma-Aldrich
Anti-CD44 antibodies (clone J.173)	Beckman Coulter
Bio-Rad Protein Assay	Bio-Rad Laboratories
BluePrint RT reagent kit	TaKaRa
BSA	Sigma-Aldrich
CD44-specific short hairpin RNA constructs	Origene
CellTiter® 96 AQueous One Solution Cell Proliferation Assay	Promega
Chondroitinase ABC	Sigma-Aldrich
DNase	Promega
DNase-/RNase- free distilled water	Gibco
Ethanol	Sigma-Aldrich
FuGENE HD Transfection Reagent	Promega
Hot-star Taq polymerase	ditto
Hyaluronic acid	Sigma-Aldrich

Kanamycin	ditto
LB agar	ditto
LB broth	ditto
Matrigel	BD Biosciences
Opti-MEM I	Invitrogen
Orthophosphoric acid	BDH Chemicals Ltd.
Primers	Invitrogen
Papain enzyme	Merck
Propan-1-ol	Duksan
Protease inhibitor cocktail	Sigma-Aldrich
PureYield TM Plasmid minprep system	Promega
Puromycin	InvivoGen
RNeasy mini kit	QIAGEN
ROX reference dye	Invitrogen
SDS	Sigma-Aldrich
Streptomyces hyalurinidase	ditto
SYBR Green I dye	Applied Biosystems
SYBR® Premix Ex TaqTM ll	TaKaRa
Toluidine Blue	BDH Chemicals Ltd.
Tris (Tris(hydroxymethyl)aminomethane)	USB Corporation
Tween-20	Sigma-Aldrich
β-mercaptoethanol	ditto

I.3 Equipment

ABI PRISM 7500 System	Applied Biosystems
Partisil SAX 5u (250x4.6-mm inner diameter) column	Alltech Associate, Inc.
Beckman Coulter Cytomics™ FC500 Flow Cytometry Systems	Beckman Coulter, Inc.
Benchmark Plus™ Microplate Reader	Bio-Rad Laboratories

GeneAmp PCR System 9700	Applied Biosystems
Leica DMI4000 B phase-contrast microscope	Leica Microsystems
NanoDrop® ND-1000 spectrophotometer	Thermo Fisher Scientific Inc.
DNA Speed Vac (DNA110)	Savant
Waters 2695 HPLC system	Waters

I.4 Recipes of reagent and buffers

For RTQ-TRAP

1 × CHAPS lysis buffer

10 mM Tris-HCl, pH 7.5, 1 mM $MgCl_2$, 1 mM EGTA, pH 8.0, 0.5% (v/v) CHAPS, 10% glycerol, (Add before use 0.1mM PMSF, 5 mM β-mercaptoethanol)

10 × TRAP buffer

200 mM Tris-HCl, pH 8.3, 630 mM KCl, 35 mM $MgCl_2$, 10 mM EGTA, pH 8.0, 1 mg/ml BSA, 0.05% Tween 20

For HPLC

5% cetylpyridinium chloride in acetate buffer (CPC)

5% cetylpyridinium chloride dissolved in 0.025M sodium acetate buffer (pH 5.8)

Papain buffer (2X)

0.2M sodium dihydrogen phosphate, pH6.4, 0.01M disodium EDTA, 0.01M cysteine hydrochloride, 0.3M sodium chloride

Papain suspension

Papain enzyme (10mg/ml) suspended in papain buffer (1X)

Streptomyces hyalurinidase enzyme

Streptomyces hyalurinidase dissolved in 0.02M sodium acetate/ acetic acid buffer at pH 6

Streptomyces hyalurinidase buffer

0.02M sodium acetate/ acetic acid buffer at pH 6, 0.15M sodium chloride

Chondroitinase-ABC enzyme

Chondroitinase-ABC dissolved in distilled water (10 units/ml)

Chondroitinase-ABC buffer

10mM disodium hydrogen phosphate/ sodium dihydrogen phosphate, pH 7

HPLC running buffer

5mM sodium dihydrogen orthophpsphate/orthophosphoric acid (pH 2.55)

50mM sodium dihydrogen orthophosphate/ orthophosphoric acid (pH 2.5)

Appendix II: Primer efficiency of real-time PCR primers

A) The standard curves of RT-qPCR primers

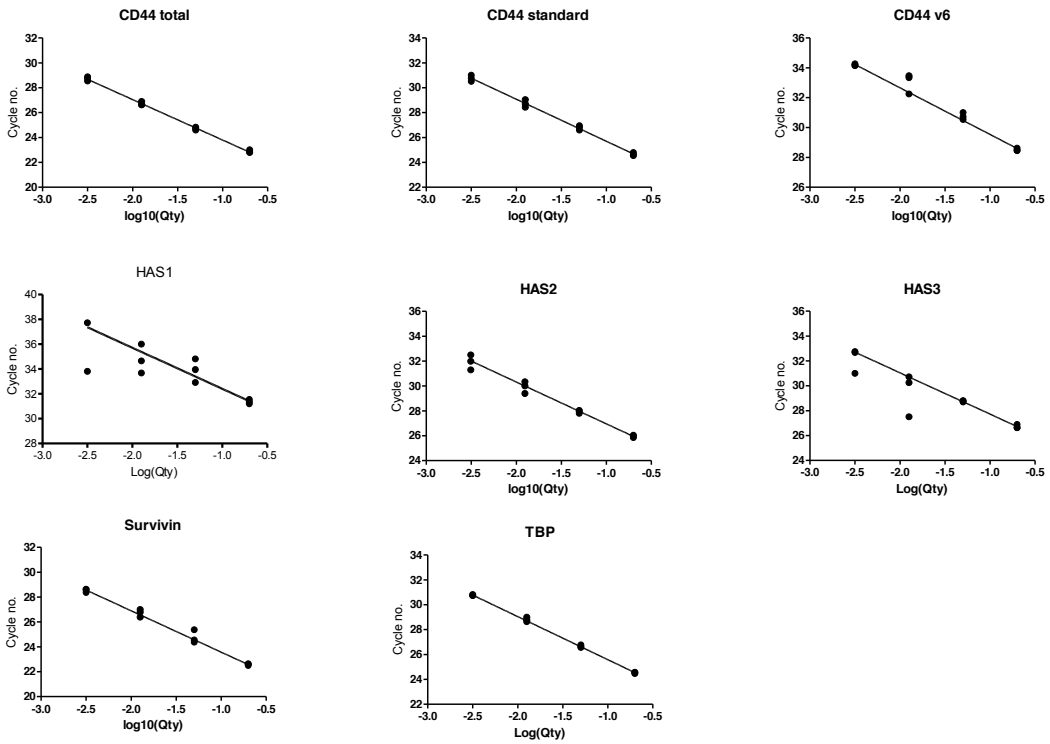

B) Primer efficiency for RT-qPCR

	Slope	Efficiency
CD44 total	-3.257	1.028
CD44 standard	-3.382	0.976
CD44v6	-3.128	1.088
Survivin	-3.329	0.997
HAS1	-3.300	1.009
HAS2	-3.365	0.982
HAS3	-3.319	1.001
TBP	-3.464	0.944

PCR efficiency = ((10^-1/slope)-1)100%

Appendix III: DE gene list report

328 out of 444 genes were labelled by DAVID IDs

ENTREZ_ GENE_ID	Name
79843	family with sequence similarity 124B
57709	solute carrier family 7 (cationic amino acid transporter, y+ system), member 14
10562	olfactomedin 4
50632	calcyon neuron-specific vesicular protein
253559	cell adhesion molecule 2
9863	membrane associated guanylate kinase, WW and PDZ domain containing 2
6622	synuclein, alpha (non A4 component of amyloid precursor)
26289	adenylate kinase 5
1363	carboxypeptidase E
2823	glycoprotein M6A
80975	transmembrane protease, serine 5
79750	zinc finger protein 385D
2583	beta-1,4-N-acetyl-galactosaminyl transferase 1
6368	chemokine (C-C motif) ligand 23
9745	zinc finger protein 536
347	apolipoprotein D
5729	prostaglandin D2 receptor (DP)
2596	growth associated protein 43
9318	COP9 constitutive photomorphogenic homolog subunit 2 (Arabidopsis)
10391	coronin, actin binding protein, 2B
399947	chromosome 11 open reading frame 87
8745	ADAM metallopeptidase domain 23
9378	neurexin 1
23345	spectrin repeat containing, nuclear envelope 1
2769	guanine nucleotide binding protein (G protein), alpha 15 (Gq class)
1496	catenin (cadherin-associated protein), alpha 2
286077	family with sequence similarity 83, member H
5126	proprotein convertase subtilisin/kexin type 2
5101	protocadherin 9
25789	transmembrane protein 59-like
133584	EGF-like, fibronectin type III and laminin G domains
642969	phosphoglycerate mutase 1 pseudogene
645001	similar to heterogeneous nuclear ribonucleoprotein A1

22795	nidogen 2 (osteonidogen)
9079	LIM domain binding 2
4915	neurotrophic tyrosine kinase, receptor, type 2
7857	secretogranin II (chromogranin C)
5649	reelin
10699	corin, serine peptidase
10218	angiopoietin-like 7
30061	solute carrier family 40 (iron-regulated transporter), member 1
56246	melanocortin 2 receptor accessory protein
55228	PNMA-like 1
647436	ribosomal protein L5 pseudogene 34; ribosomal protein L5 pseudogene 1; ribosomal protein L5
4983	oligophrenin 1
55843	Rho GTPase activating protein 15
8321	frizzled homolog 1 (Drosophila)
4223	mesenchyme homeobox 2
5179	proenkephalin
388007	serpin peptidase inhibitor, clade A (alpha-1 antiproteinase, antitrypsin), member 13 (pseudogene)
6900	contactin 2 (axonal)
6616	synaptosomal-associated protein, 25kDa
1776	deoxyribonuclease I-like 3
57509	mitochondrial tumor suppressor 1
23118	mitogen-activated protein kinase kinase kinase 7 interacting protein 2
123041	solute carrier family 24 (sodium/potassium/calcium exchanger), member 4
641654	hepatocyte cell adhesion molecule; HEPACAM opposite strand 1
2560	gamma-aminobutyric acid (GABA) A receptor, beta 1
3897	L1 cell adhesion molecule
644366	hypothetical LOC644366
7356	secretoglobin, family 1A, member 1 (uteroglobin)
116173	CKLF-like MARVEL transmembrane domain containing 5
115827	RAB3C, member RAS oncogene family
6425	secreted frizzled-related protein 5
482	ATPase, Na+/K+ transporting, beta 2 polypeptide
1136	cholinergic receptor, nicotinic, alpha 3
8929	paired-like homeobox 2b
4978	opioid binding protein/cell adhesion molecule-like
730107	similar to Glycine cleavage system H protein, mitochondrial precursor; glycine cleavage system protein H (aminomethyl carrier); similar to Glycine cleavage system H protein, mitochondrial
114815	sortilin-related VPS10 domain containing receptor 1
10752	cell adhesion molecule with homology to L1CAM (close homolog of L1)

55620	signal transducing adaptor family member 2
1446	casein alpha s1
1999	E74-like factor 3 (ets domain transcription factor, epithelial-specific)
1910	endothelin receptor type B
27233	sulfotransferase family, cytosolic, 1C, member 4
1969	EPH receptor A2
54039	poly(rC) binding protein 3
216	aldehyde dehydrogenase 1 family, member A1
3038	hyaluronan synthase 3
286297	hypothetical protein LOC286297
91074	ankyrin repeat domain 30A
645832	SEBOX homeobox
55553	SRY (sex determining region Y)-box 6
286753	tumor suppressor candidate 5
399694	SHC (Src homology 2 domain containing) family, member 4
9211	leucine-rich, glioma inactivated 1
443	aspartoacylase (Canavan disease)
2151	coagulation factor II (thrombin) receptor-like 2
117248	UDP-N-acetyl-alpha-D-galactosamine:polypeptide N-acetylgalactosaminyltransferase-like 2
7482	wingless-type MMTV integration site family, member 2B
163175	leucine-rich repeat LGI family, member 4
2250	fibroblast growth factor 5
23037	PDZ domain containing 2
2785	guanine nucleotide binding protein (G protein), gamma 3
3856	keratin 8 pseudogene 9; similar to keratin 8; keratin 8
83872	hemicentin 1
5010	claudin 11
79614	chromosome 5 open reading frame 23
55102	ATG2 autophagy related 2 homolog B (S. cerevisiae)
4023	lipoprotein lipase
8190	melanoma inhibitory activity
222865	transmembrane protein 130
7096	toll-like receptor 1
51705	endomucin
113612	cytochrome P450, family 2, subfamily U, polypeptide 1
5354	proteolipid protein 1
153642	arylsulfatase family, member K
642938	chromosome 10 open reading frame 141
2810	stratifin
11126	CD160 molecule
5017	ovo-like 1(Drosophila)

3880	keratin 19
78986	dual specificity phosphatase 26 (putative)
57088	phospholipid scramblase 4
1268	cannabinoid receptor 1 (brain)
167465	zinc finger protein 366
51327	erythroid associated factor
2202	EGF-containing fibulin-like extracellular matrix protein 1
59345	guanine nucleotide binding protein (G protein), beta polypeptide 4
29114	transgelin 3
1996	ELAV (embryonic lethal, abnormal vision, Drosophila)-like 4 (Hu antigen D)
10439	olfactomedin 1
387856	chromosome 12 open reading frame 68
4804	nerve growth factor receptor (TNFR superfamily, member 16)
5730	prostaglandin D2 synthase, hematopoietic; prostaglandin D2 synthase 21kDa (brain)
7432	vasoactive intestinal peptide
5806	pentraxin-related gene, rapidly induced by IL-1 beta
80031	sema domain, transmembrane domain (TM), and cytoplasmic domain, (semaphorin) 6D
6286	S100 calcium binding protein P
23683	protein kinase D3
2676	GDNF family receptor alpha 3
284801	hypothetical protein LOC284801; hypothetical LOC649159
114786	XK, Kell blood group complex subunit-related family, member 4
56127	protocadherin beta 10; protocadherin beta 9
5364	plexin B1
9514	galactose-3-O-sulfotransferase 1
26045	leucine rich repeat transmembrane neuronal 2
1745	distal-less homeobox 1
125	alcohol dehydrogenase 1B (class I), beta polypeptide; alcohol dehydrogenase 1A (class I), alpha polypeptide; alcohol dehydrogenase 1C (class I), gamma polypeptide
23284	latrophilin 3
10490	vesicle transport through interaction with t-SNAREs homolog 1B (yeast)
23768	fibronectin leucine rich transmembrane protein 2
1271	ciliary neurotrophic factor receptor
6860	synaptotagmin IV
5348	FXYD domain containing ion transport regulator 1
4504	metallothionein 3
51617	HMP19 protein
5798	protein tyrosine phosphatase, receptor type, N
89795	neuron navigator 3; similar to neuron navigator 3

7430	hypothetical protein LOC100129652; ezrin
9324	high mobility group nucleosomal binding domain 3
54360	cytokine-like 1
283682	hypothetical protein LOC283682
84631	similar to CXorf2 protein; SLIT and NTRK-like family, member 2
28513	cadherin 19, type 2
1435	colony stimulating factor 1 (macrophage)
5577	protein kinase, cAMP-dependent, regulatory, type II, beta
283420	C-type lectin domain family 9, member A
83959	solute carrier family 4, sodium borate transporter, member 11
5803	protein tyrosine phosphatase, receptor-type, Z polypeptide 1
84820	polymerase (RNA) II (DNA directed) polypeptide J4, pseudogene
85444	leucine rich repeat and coiled-coil domain containing 1
10216	proteoglycan 4
57111	RAB25, member RAS oncogene family
10107	tripartite motif-containing 10
26050	SLIT and NTRK-like family, member 5
10402	ST3 beta-galactoside alpha-2,3-sialyltransferase 6
5104	serpin peptidase inhibitor, clade A (alpha-1 antiproteinase, antitrypsin), member 5
80864	EGF-like-domain, multiple 8
1901	sphingosine-1-phosphate receptor 1
641700	endothelial cell-specific chemotaxis regulator
4858	neuro-oncological ventral antigen 2
7373	collagen, type XIV, alpha 1
11075	stathmin-like 2
9506	P antigen family, member 4 (prostate associated)
596	B-cell CLL/lymphoma 2
534	ATPase, H+ transporting, lysosomal 13kDa, V1 subunit G2
5027	purinergic receptor P2X, ligand-gated ion channel, 7
5193	peroxisomal biogenesis factor 12
351	amyloid beta (A4) precursor protein
8522	growth arrest-specific 7
10516	fibulin 5
5346	perilipin
6358	chemokine (C-C motif) ligand 14; chemokine (C-C motif) ligand 15
9452	integral membrane protein 2A
442064	phosphatidylinositol glycan anchor biosynthesis, class Y pseudogene
64641	early B-cell factor 2
6663	SRY (sex determining region Y)-box 10
256130	transmembrane protein 196
50509	collagen, type V, alpha 3

2134	exostoses (multiple)-like 1
11041	UDP-GlcNAc:betaGal beta-1,3-N-acetylglucosaminyltransferase 1; UDP-GlcNAc:betaGal beta-1,3-N-acetylglucosaminyltransferase 2
5627	protein S (alpha)
4359	myelin protein zero
11189	trinucleotide repeat containing 4
54331	guanine nucleotide binding protein (G protein), gamma 2
10888	G protein-coupled receptor 83
116	adenylate cyclase activating polypeptide 1 (pituitary)
643033	similar to Heterogeneous nuclear ribonucleoprotein A1 (Helix-destabilizing protein) (Single-strand binding protein) (hnRNP core protein A1) (HDP-1) (Topoisomerase-inhibitor suppressed)
797	calcitonin-related polypeptide beta
26084	Src homology 3 domain-containing guanine nucleotide exchange factor
56776	formin 2
1267	2',3'-cyclic nucleotide 3' phosphodiesterase
3696	integrin, beta 8
3043	hemoglobin, beta
23302	WSC domain containing 1
1123	chimerin (chimaerin) 1
9353	slit homolog 2 (Drosophila)
6844	vesicle-associated membrane protein 2 (synaptobrevin 2)
3952	leptin
577	brain-specific angiogenesis inhibitor 3
9626	guanylate cyclase activator 1C
4499	metallothionein 1M
6258	retinoid X receptor, gamma
64102	tenomodulin
80149	zinc finger CCCH-type containing 12A
158062	lipocalin 6
151242	protein phosphatase 1, regulatory (inhibitor) subunit 1C
57687	vesicle amine transport protein 1 homolog (T. californica)-like
646981	protein tyrosine phosphatase, non-receptor type-like pseudogene
57863	cell adhesion molecule 3
9244	cytokine receptor-like factor 1
9625	apoptosis-associated tyrosine kinase
222553	solute carrier family 35, member F1
6285	S100 calcium binding protein B
1040	CDP-diacylglycerol synthase (phosphatidate cytidylyltransferase) 1
5420	podocalyxin-like
256435	ST6(alpha-N-acetyl-neuraminyl-2,3-beta-galactosyl-1,3)-N-acetylgalactosaminide alpha-2,6-sialyltransferase 3

7025	nuclear receptor subfamily 2, group F, member 1
80704	solute carrier family 19, member 3
114897	C1q and tumor necrosis factor related protein 1
9890	plasticity related gene 1
5375	peripheral myelin protein 2
255426	RasGEF domain family, member 1C
6855	synaptophysin
3050	hemoglobin, zeta
6252	reticulon 1
3977	leukemia inhibitory factor receptor alpha
4685	neural cell adhesion molecule 2
4747	neurofilament, light polypeptide
50846	desert hedgehog homolog (Drosophila)
63976	PR domain containing 16
80059	leucine rich repeat transmembrane neuronal 4
114800	coiled-coil domain containing 85A
7078	TIMP metallopeptidase inhibitor 3
92293	transmembrane protein 132C
10124	ADP-ribosylation factor-like 4A
8707	UDP-Gal:betaGlcNAc beta 1,3-galactosyltransferase, polypeptide 2
56884	follistatin-like 5
146433	interleukin 34
5950	retinol binding protein 4, plasma
132332	transmembrane protein 155
9618	TNF receptor-associated factor 4
114795	transmembrane protein 132B; hypothetical LOC121296
794	calbindin 2
1995	ELAV (embryonic lethal, abnormal vision, Drosophila)-like 3 (Hu antigen C)
644063	heterogeneous nuclear ribonucleoprotein K; similar to heterogeneous nuclear ribonucleoprotein K
149461	claudin 19
2555	gamma-aminobutyric acid (GABA) A receptor, alpha 2
5063	p21 protein (Cdc42/Rac)-activated kinase 3
167359	serine/threonine-protein kinase NIM1
51143	dynein, cytoplasmic 1, light intermediate chain 1
28954	RAS (RAD and GEM)-like GTP-binding 1
3872	keratin 17; keratin 17 pseudogene 3
183	angiotensinogen (serpin peptidase inhibitor, clade A, member 8)
81847	ring finger protein 146
11096	ADAM metallopeptidase with thrombospondin type 1 motif, 5
30820	Kv channel interacting protein 1

1524	chemokine (C-X3-C motif) receptor 1
84504	NK6 homeobox 2
10382	tubulin, beta 4
7412	vascular cell adhesion molecule 1
57689	leucine rich repeat containing 4C
51560	RAB6B, member RAS oncogene family
201134	coiled-coil domain containing 46
7439	bestrophin 1
2262	glypican 5
8618	Ca++-dependent secretion activator
55026	family with sequence similarity 70, member A
146894	CD300 molecule-like family member g
23017	Fas apoptotic inhibitory molecule 2
56603	cytochrome P450, family 26, subfamily B, polypeptide 1
285533	ring finger protein 175
163782	KN motif and ankyrin repeat domains 4
8325	frizzled homolog 8 (Drosophila)
796	calcitonin-related polypeptide alpha
5122	proprotein convertase subtilisin/kexin type 1
2824	glycoprotein M6B
158763	hypothetical protein FLJ30058
23504	RIMS binding protein 2
55900	zinc finger protein 302
55022	phosphotyrosine interaction domain containing 1
3547	immunoglobulin superfamily, member 1
50863	neurotrimin
55312	riboflavin kinase
50614	UDP-N-acetyl-alpha-D-galactosamine:polypeptide N-acetylgalactosaminyltransferase 9 (GalNAc-T9)
5630	peripherin
81551	stathmin-like 4
114	adenylate cyclase 8 (brain)
54463	family with sequence similarity 134, member B
6327	sodium channel, voltage-gated, type II, beta
54413	neuroligin 3
64581	C-type lectin domain family 7, member A
7010	TEK tyrosine kinase, endothelial
7092	tolloid-like 1
1366	claudin 7
3188	ribosomal protein L36a pseudogene 51; ribosomal protein L36a pseudogene 37; ribosomal protein L36a pseudogene 49; heterogeneous nuclear ribonucleoprotein H2 (H'); ribosomal protein L36a
3898	ladinin 1

27022	forkhead box D3
26052	dynamin 3
2352	folate receptor 3 (gamma)
5167	ectonucleotide pyrophosphatase/phosphodiesterase 1
3426	complement factor I
6857	synaptotagmin I
5373	phosphomannomutase 2
10351	ATP-binding cassette, sub-family A (ABC1), member 8
23644	enhancer of mRNA decapping 4
2986	guanylate cyclase 2F, retinal
25817	family with sequence similarity 19 (chemokine (C-C motif)-like), member A5
3572	interleukin 6 signal transducer (gp130, oncostatin M receptor)
148753	family with sequence similarity 163, member A
170575	GTPase, IMAP family member 1
1113	chromogranin A (parathyroid secretory protein 1)
387755	inscuteable homolog (Drosophila)
9283	G protein-coupled receptor 37 like 1
51313	chromosome 4 open reading frame 18
23671	transmembrane protein with EGF-like and two follistatin-like domains 2

Appendix IV: Biological functions of DE transcripts

Annotation Cluster 1	Enrichment Score: 11.01	Count	P_Value	Benjamini
signal peptide		126	9.6E-22	1.1E-18
signal		126	1.1E-21	3.7E-19
glycoprotein		146	4.8E-20	8.5E-18
glycosylation site:N-linked (GlcNAc...)		137	8.0E-18	4.6E-15
disulfide bond		100	2.6E-13	3.1E-11
disulfide bond		96	1.1E-12	4.3E-10
Secreted		68	1.2E-11	1.1E-9
membrane		162	2.1E-11	1.5E-9
topological domain:Cytoplasmic		103	2.3E-10	6.6E-8
extracellular region		79	8.3E-10	2.1E-7
transmembrane region		128	1.1E-8	2.5E-6
transmembrane		128	1.9E-8	1.1E-6
topological domain:Extracellular		83	2.5E-8	4.8E-6
extracellular region part		47	4.2E-8	3.6E-6
extracellular space		34	4.5E-6	2.3E-4
intrinsic to membrane		141	5.1E-5	1.3E-3
integral to membrane		134	2.4E-4	5.5E-3

Annotation Cluster 2	Enrichment Score: 8.6	Count	P_Value	Benjamini
neuron differentiation		35	2.5E-12	5.2E-9
neuron projection morphogenesis		24	1.6E-11	1.7E-8
neuron development		29	5.9E-11	4.1E-8
axonogenesis		22	1.1E-10	5.7E-8
cell projection morphogenesis		24	2.7E-10	1.1E-7
cell morphogenesis involved in neuron differentiation		22	4.8E-10	1.7E-7
neuron projection development		24	6.5E-10	1.9E-7
cell part morphogenesis		24	6.5E-10	1.9E-7
cell morphogenesis		28	8.9E-10	2.3E-7
cellular component morphogenesis		29	2.0E-9	4.6E-7
cell morphogenesis involved in differentiation		22	8.1E-9	1.2E-6
cell projection organization		26	3.5E-8	4.6E-6
axon guidance		10	2.0E-4	1.3E-2
cell motion		22	3.0E-4	1.6E-2

Annotation Cluster 3	Enrichment Score: 7.04	Count	P_Value	Benjamini
cell adhesion		39	3.3E-9	5.7E-7
biological adhesion		39	3.4E-9	5.5E-7
cell adhesion		25	3.0E-7	1.5E-5
cell-cell adhesion		18	2.1E-5	1.8E-3

157 out of 444DE transcripts between normal and tumor surrounding tissue were annotated into 114 functional clusters and the top 3 clusters were enclosed for reference. The first cluster indicated that the DE genes are cell membrane related. The second and third clusters demonstrated that these genes are commonly classified for cell movement and adhesion. The data was generated by using DAVID bioinformatics database.

Reference

1. Bladder Cancer. 18 July , 2011 [cited 2012 27 April]; Available from: http://www.cancer.net/portal/site/patient
2. van Rhijn BW, Burger M, Lotan Y, et al. Recurrence and progression of disease in non-muscle-invasive bladder cancer: from epidemiology to treatment strategy. Eur Urol 2009; 56: 430-42.
3. Bladder cancer. [cited 2012 27 April]; Available from: http://www.montereybayurology.com/urocond/bladdercancer.htm#typesbladdercancer
4. Siegel R, Ward E, Brawley O, Jemal A. Cancer statistics, 2011: the impact of eliminating socioeconomic and racial disparities on premature cancer deaths. CA Cancer J Clin; 61: 212-36.
5. HKSAR. Bladder cancer. 21 Jan, 2011 [cited 2011 24 June]; Available from: http://www.chp.gov.hk/en/content/9/25/6574.html
6. Negri E, La Vecchia C. Epidemiology and prevention of bladder cancer. Eur J Cancer Prev 2001; 10: 7-14.
7. Golka K, Wiese A, Assennato G, Bolt HM. Occupational exposure and urological cancer. World J Urol 2004; 21: 382-91.
8. Silverman DT, Levin LI, Hoover RN, Hartge P. Occupational risks of bladder cancer in the United States: I. White men. J Natl Cancer Inst 1989; 81: 1472-80.
9. Yu MC, Skipper PL, Tannenbaum SR, Chan KK, Ross RK. Arylamine exposures and bladder cancer risk. Mutat Res 2002; 506-507: 21-8.
10. Smith CJ, Perfetti TA, Garg R, Hansch C. IARC carcinogens reported in cigarette mainstream smoke and their calculated log P values. Food Chem Toxicol 2003; 41: 807-17.
11. Freedman ND, Silverman DT, Hollenbeck AR, Schatzkin A, Abnet CC. Association between smoking and risk of bladder cancer among men and women. JAMA; 306: 737-45.

12. Alberg AJ, Kouzis A, Genkinger JM, et al. A prospective cohort study of bladder cancer risk in relation to active cigarette smoking and household exposure to secondhand cigarette smoke. Am J Epidemiol 2007; 165: 660-6.
13. Castelao JE, Yuan JM, Skipper PL, et al. Gender- and smoking-related bladder cancer risk. J Natl Cancer Inst 2001; 93: 538-45.
14. Morrison AS, Buring JE, Verhoek WG, et al. An international study of smoking and bladder cancer. J Urol 1984; 131: 650-4.
15. SEER Cancer Statistics. [cited 2012 27 April]; Available from: http://seer.cancer.gov/
16. Feng Z, Hu W, Rom WN, Beland FA, Tang MS. 4-aminobiphenyl is a major etiological agent of human bladder cancer: evidence from its DNA binding spectrum in human p53 gene. Carcinogenesis 2002; 23: 1721-7.
17. Talaska G, al-Juburi AZ, Kadlubar FF. Smoking related carcinogen-DNA adducts in biopsy samples of human urinary bladder: identification of N-(deoxyguanosin-8-yl)-4-aminobiphenyl as a major adduct. Proc Natl Acad Sci U S A 1991; 88: 5350-4.
18. Airoldi L, Orsi F, Magagnotti C, et al. Determinants of 4-aminobiphenyl-DNA adducts in bladder cancer biopsies. Carcinogenesis 2002; 23: 861-6.
19. Turesky RJ, Lang NP, Butler MA, Teitel CH, Kadlubar FF. Metabolic activation of carcinogenic heterocyclic aromatic amines by human liver and colon. Carcinogenesis 1991; 12: 1839-45.
20. Butler MA, Guengerich FP, Kadlubar FF. Metabolic oxidation of the carcinogens 4-aminobiphenyl and 4,4'-methylene-bis(2-chloroaniline) by human hepatic microsomes and by purified rat hepatic cytochrome P-450 monooxygenases. Cancer Res 1989; 49: 25-31.
21. Wise RW, Zenser TV, Kadlubar FF, Davis BB. Metabolic activation of carcinogenic aromatic amines by dog bladder and kidney prostaglandin H synthase. Cancer Res 1984; 44: 1893-7.
22. Beland FA, Kadlubar FF. Formation and persistence of arylamine DNA adducts in vivo. Environ Health Perspect 1985; 62: 19-30.

23. Saletta F, Matullo G, Manuguerra M, Arena S, Bardelli A, Vineis P. Exposure to the tobacco smoke constituent 4-aminobiphenyl induces chromosomal instability in human cancer cells. Cancer Res 2007; 67: 7088-94.
24. Takahashi T, Habuchi T, Kakehi Y, et al. Clonal and chronological genetic analysis of multifocal cancers of the bladder and upper urinary tract. Cancer Res 1998; 58: 5835-41.
25. Mitra AP, Datar RH, Cote RJ. Molecular pathways in invasive bladder cancer: new insights into mechanisms, progression, and target identification. J Clin Oncol 2006; 24: 5552-64.
26. Lerner S.P. SMP, Sternberg C.N. , editor. Textbook of bladder cancer. UK: Taylor & Francis; 2006.
27. Bakkar AA, Wallerand H, Radvanyi F, et al. FGFR3 and TP53 gene mutations define two distinct pathways in urothelial cell carcinoma of the bladder. Cancer Res 2003; 63: 8108-12.
28. Maeng YH, Eun SY, Huh JS. Expression of fibroblast growth factor receptor 3 in the recurrence of non-muscle-invasive urothelial carcinoma of the bladder. Korean J Urol; 51: 94-100.
29. van Oers JM, Wild PJ, Burger M, et al. FGFR3 mutations and a normal CK20 staining pattern define low-grade noninvasive urothelial bladder tumours. Eur Urol 2007; 52: 760-8.
30. Schena M, Shalon D, Davis RW, Brown PO. Quantitative monitoring of gene expression patterns with a complementary DNA microarray. Science 1995; 270: 467-70.
31. Thykjaer T, Workman C, Kruhoffer M, et al. Identification of gene expression patterns in superficial and invasive human bladder cancer. Cancer Res 2001; 61: 2492-9.
32. Dyrskjot L, Thykjaer T, Kruhoffer M, et al. Identifying distinct classes of bladder carcinoma using microarrays. Nat Genet 2003; 33: 90-6.
33. Zaravinos A, Lambrou GI, Boulalas I, Delakas D, Spandidos DA. Identification of common differentially expressed genes in urinary bladder cancer. PLoS One 2011; 6: e18135.

34. Modlich O, Prisack HB, Pitschke G, et al. Identifying superficial, muscle-invasive, and metastasizing transitional cell carcinoma of the bladder: use of cDNA array analysis of gene expression profiles. Clin Cancer Res 2004; 10: 3410-21.
35. Sanchez-Carbayo M, Socci ND, Lozano JJ, et al. Gene discovery in bladder cancer progression using cDNA microarrays. Am J Pathol 2003; 163: 505-16.
36. Schultz IJ, Wester K, Straatman H, et al. Prediction of recurrence in Ta urothelial cell carcinoma by real-time quantitative PCR analysis: a microarray validation study. Int J Cancer 2006; 119: 1915-9.
37. Dyrskjot L, Zieger K, Real FX, et al. Gene expression signatures predict outcome in non-muscle-invasive bladder carcinoma: a multicenter validation study. Clin Cancer Res 2007; 13: 3545-51.
38. Kim WJ, Kim SK, Jeong P, et al. A four-gene signature predicts disease progression in muscle invasive bladder cancer. Mol Med 2011; 17: 478-85.
39. Prout GR, Wesley MN, Yancik R, Ries LAG, Havlik RJ, Edwards BK. Age and Comorbidity impact surgical therapy in older bladder carcinoma patients - A population-based study. Cancer 2005; 104: 1638-47.
40. Zhang Y, Mahendran R, Yap LL, Esuvaranathan K, Khoo HE. The signalling pathway for BCG-induced interleukin-6 production in human bladder cancer cells. Biochem Pharmacol 2002; 63: 273-82.
41. Bohle A, Brandau S. Immune mechanisms in bacillus Calmette-Guerin immunotherapy for superficial bladder cancer. J Urol 2003; 170: 964-9.
42. Luo Y, Yamada H, Evanoff DP, Chen X. Role of Th1-stimulating cytokines in bacillus Calmette-Guerin (BCG)-induced macrophage cytotoxicity against mouse bladder cancer MBT-2 cells. Clin Exp Immunol 2006; 146: 181-8.
43. Ludwig AT, Moore JM, Luo Y, et al. Tumor necrosis factor-related apoptosis-inducing ligand: a novel mechanism for Bacillus Calmette-Guerin-induced antitumor activity. Cancer Res 2004; 64: 3386-90.
44. Jansson OT, Morcos E, Brundin L, et al. The role of nitric oxide in bacillus Calmette-Guerin mediated anti-tumour effects in human bladder cancer. Br J Cancer 1998; 78: 588-92.

45. Lamm D, Colombel M, Persad R, et al. Clinical Practice Recommendations for the Management of Non–Muscle Invasive Bladder cancer. European Urology Supplements 2008; 7: 651-66.
46. Sylvester RJ, van der Meijden AP, Oosterlinck W, et al. Predicting recurrence and progression in individual patients with stage Ta T1 bladder cancer using EORTC risk tables: a combined analysis of 2596 patients from seven EORTC trials. Eur Urol 2006; 49: 466-5; discussion 75-7.
47. Brausi M, Collette L, Kurth K, et al. Variability in the recurrence rate at first follow-up cystoscopy after TUR in stage Ta T1 transitional cell carcinoma of the bladder: a combined analysis of seven EORTC studies. Eur Urol 2002; 41: 523-31.
48. Hoglund M. Bladder cancer, a two phased disease? Semin Cancer Biol 2007; 17: 225-32.
49. Botteman MF, Pashos CL, Redaelli A, Laskin B, Hauser R. The health economics of bladder cancer: a comprehensive review of the published literature. Pharmacoeconomics 2003; 21: 1315-30.
50. Avritscher EB, Cooksley CD, Grossman HB, et al. Clinical model of lifetime cost of treating bladder cancer and associated complications. Urology 2006; 68: 549-53.
51. Kondas J, Kiss L, Hatar A, et al. The effect of intravesical mitomycin C on the recurrence of superficial (Ta-T1) bladder cancer. A Hungarian Multicenter Study. Int Urol Nephrol 1999; 31: 451-6.
52. Bryan RT, Collins SI, Daykin MC, et al. Mechanisms of recurrence of Ta/T1 bladder cancer. Ann R Coll Surg Engl; 92: 519-24.
53. Holmang S, Hedelin H, Anderstrom C, Holmberg E, Busch C, Johansson SL. Recurrence and progression in low grade papillary urothelial tumors. J Urol 1999; 162: 702-7.
54. Leppert JT, Shvarts O, Kawaoka K, Lieberman R, Belldegrun AS, Pantuck AJ. Prevention of bladder cancer: a review. Eur Urol 2006; 49: 226-34.

55. Grimm MO, Steinhoff C, Simon X, Spiegelhalder P, Ackermann R, Vogeli TA. Effect of routine repeat transurethral resection for superficial bladder cancer: a long-term observational study. J Urol 2003; 170: 433-7.
56. Muto S, Horie S, Takahashi S, Tomita K, Kitamura T. Genetic and epigenetic alterations in normal bladder epithelium in patients with metachronous bladder cancer. Cancer Res 2000; 60: 4021-5.
57. Slaughter DP, Southwick HW, Smejkal W. Field cancerization in oral stratified squamous epithelium; clinical implications of multicentric origin. Cancer 1953; 6: 963-8.
58. Campisi J. Cancer, aging and cellular senescence. In Vivo 2000; 14: 183-8.
59. Coleman WB, Tsongalis GJ. Multiple mechanisms account for genomic instability and molecular mutation in neoplastic transformation. Clin Chem 1995; 41: 644-57.
60. Rao JY, Hemstreet GP, 3rd, Hurst RE, et al. Alterations in phenotypic biochemical markers in bladder epithelium during tumorigenesis. Proc Natl Acad Sci U S A 1993; 90: 8287-91.
61. Sturgeon CM, Duffy MJ, Hofmann BR, et al. National Academy of Clinical Biochemistry Laboratory Medicine Practice Guidelines for use of tumor markers in liver, bladder, cervical, and gastric cancers. Clin Chem 2010; 56: e1-48.
62. Sarosdy MF, Hudson MA, Ellis WJ, et al. Improved detection of recurrent bladder cancer using the Bard BTA stat Test. Urology 1997; 50: 349-53.
63. Huber S, Schwentner C, Taeger D, et al. Nuclear matrix protein-22: a prospective evaluation in a population at risk for bladder cancer. Results from the UroScreen study. BJU Int 2011.
64. Fradet Y, Lockhard C. Performance characteristics of a new monoclonal antibody test for bladder cancer: ImmunoCyt trade mark. Can J Urol 1997; 4: 400-5.
65. Vriesema JL, Atsma F, Kiemeney LA, Peelen WP, Witjes JA, Schalken JA. Diagnostic efficacy of the ImmunoCyt test to detect superficial bladder cancer recurrence. Urology 2001; 58: 367-71.

66. Cordon-Cardo C, Wartinger DD, Melamed MR, Fair W, Fradet Y. Immunopathologic analysis of human urinary bladder cancer. Characterization of two new antigens associated with low-grade superficial bladder tumors. Am J Pathol 1992; 140: 375-85.
67. Mian C, Pycha A, Wiener H, Haitel A, Lodde M, Marberger M. Immunocyt: a new tool for detecting transitional cell cancer of the urinary tract. J Urol 1999; 161: 1486-9.
68. Hautmann S, Toma M, Lorenzo Gomez MF, et al. Immunocyt and the HA-HAase urine tests for the detection of bladder cancer: a side-by-side comparison. Eur Urol 2004; 46: 466-71.
69. Halling KC, King W, Sokolova IA, et al. A comparison of cytology and fluorescence in situ hybridization for the detection of urothelial carcinoma. J Urol 2000; 164: 1768-75.
70. Maffezzini M, Capponi G, Casazza S, Campodonico F, Bandelloni R, Puntoni M. The UroVysion F.I.S.H. test compared to standard cytology for surveillance of non-muscle invasive bladder cancer. Arch Ital Urol Androl 2008; 80: 127-31.
71. Skacel M, Fahmy M, Brainard JA, et al. Multitarget fluorescence in situ hybridization assay detects transitional cell carcinoma in the majority of patients with bladder cancer and atypical or negative urine cytology. J Urol 2003; 169: 2101-5.
72. Hajdinjak T. UroVysion FISH test for detecting urothelial cancers: meta-analysis of diagnostic accuracy and comparison with urinary cytology testing. Urol Oncol 2008; 26: 646-51.
73. Moyzis RK, Buckingham JM, Cram LS, et al. A highly conserved repetitive DNA sequence, (TTAGGG)n, present at the telomeres of human chromosomes. Proc Natl Acad Sci U S A 1988; 85: 6622-6.
74. Allsopp RC, Vaziri H, Patterson C, et al. Telomere length predicts replicative capacity of human fibroblasts. Proc Natl Acad Sci U S A 1992; 89: 10114-8.
75. Hayflick L. The Limited in Vitro Lifetime of Human Diploid Cell Strains. Exp Cell Res 1965; 37: 614-36.

76. Blackburn EH. Switching and signaling at the telomere. Cell 2001; 106: 661-73.
77. Hanahan D, Weinberg RA. The hallmarks of cancer. Cell 2000; 100: 57-70.
78. Kim NW, Piatyszek MA, Prowse KR, et al. Specific association of human telomerase activity with immortal cells and cancer. Science 1994; 266: 2011-5.
79. Kageyama Y, Kamata S, Yonese J, Oshima H. Telomere length and telomerase activity in bladder and prostate cancer cell lines. Int J Urol 1997; 4: 407-10.
80. Yoshida K, Sugino T, Tahara H, et al. Telomerase activity in bladder carcinoma and its implication for noninvasive diagnosis by detection of exfoliated cancer cells in urine. Cancer 1997; 79: 362-9.
81. Muller M, Heine B, Heicappell R, et al. Telomerase activity in bladder cancer, bladder washings and in urine. Int J Oncol 1996; 9: 1169-73.
82. Lin Y, Miyamoto H, Fujinami K, et al. Telomerase activity in human bladder cancer. Clin Cancer Res 1996; 2: 929-32.
83. Shaker OG, Hammam OA, El Leithy TR, El Ganzoury H, Wishahi MM, Mikhailidis DP. Molecular markers and bladder carcinoma: Schistosomal and non-schistosomal. Clin Biochem; 44: 237-44.
84. Bennett A. Telomerase and other novel approaches to bladder cancer detection. Clin Lab Sci 2008; 21: 185-90; quiz 91-2, following 92.
85. Abd El Gawad IA, Moussa HS, Nasr MI, et al. Comparative study of NMP-22, telomerase, and BTA in the detection of bladder cancer. J Egypt Natl Canc Inst 2005; 17: 193-202.
86. Ambrosini G, Adida C, Altieri DC. A novel anti-apoptosis gene, survivin, expressed in cancer and lymphoma. Nat Med 1997; 3: 917-21.
87. Li F, Ambrosini G, Chu EY, et al. Control of apoptosis and mitotic spindle checkpoint by survivin. Nature 1998; 396: 580-4.
88. Ku JH, Kwak C, Lee HS, Park HK, Lee E, Lee SE. Expression of survivin, a novel inhibitor of apoptosis, in superficial transitional cell carcinoma of the bladder. J Urol 2004; 171: 631-5.

89. Shariat SF, Karakiewicz PI, Godoy G, et al. Survivin as a prognostic marker for urothelial carcinoma of the bladder: a multicenter external validation study. Clin Cancer Res 2009; 15: 7012-9.
90. Schultz IJ, Kiemeney LA, Karthaus HF, et al. Survivin mRNA copy number in bladder washings predicts tumor recurrence in patients with superficial urothelial cell carcinomas. Clin Chem 2004; 50: 1425-8.
91. Xia Y, Liu YL, Yang KH, Chen W. The diagnostic value of urine-based survivin mRNA test using reverse transcription-polymerase chain reaction for bladder cancer: a systematic review. Chin J Cancer 2010; 29: 441-6.
92. Spicer AP, Olson JS, McDonald JA. Molecular cloning and characterization of a cDNA encoding the third putative mammalian hyaluronan synthase. J Biol Chem 1997; 272: 8957-61.
93. Aruffo A, Stamenkovic I, Melnick M, Underhill CB, Seed B. CD44 is the principal cell surface receptor for hyaluronate. Cell 1990; 61: 1303-13.
94. Miyake H, Hara I, Okamoto I, et al. Interaction between CD44 and hyaluronic acid regulates human prostate cancer development. J Urol 1998; 160: 1562-6.
95. Golshani R, Lopez L, Estrella V, Kramer M, Iida N, Lokeshwar VB. Hyaluronic acid synthase-1 expression regulates bladder cancer growth, invasion, and angiogenesis through CD44. Cancer Res 2008; 68: 483-91.
96. Li Y, Li L, Brown TJ, Heldin P. Silencing of hyaluronan synthase 2 suppresses the malignant phenotype of invasive breast cancer cells. Int J Cancer 2007; 120: 2557-67.
97. Udabage L, Brownlee GR, Waltham M, et al. Antisense-mediated suppression of hyaluronan synthase 2 inhibits the tumorigenesis and progression of breast cancer. Cancer Res 2005; 65: 6139-50.
98. Liu N, Gao F, Han Z, Xu X, Underhill CB, Zhang L. Hyaluronan synthase 3 overexpression promotes the growth of TSU prostate cancer cells. Cancer Res 2001; 61: 5207-14.
99. Chan KS, Espinosa I, Chao M, et al. Identification, molecular characterization, clinical prognosis, and therapeutic targeting of human bladder tumor-initiating cells. Proc Natl Acad Sci U S A 2009; 106: 14016-21.

100. Al-Hajj M, Wicha MS, Benito-Hernandez A, Morrison SJ, Clarke MF. Prospective identification of tumorigenic breast cancer cells. Proc Natl Acad Sci U S A 2003; 100: 3983-8.
101. Botchkina GI, Zuniga ES, Das M, et al. New-generation taxoid SB-T-1214 inhibits stem cell-related gene expression in 3D cancer spheroids induced by purified colon tumor-initiating cells. Mol Cancer 2010; 9: 192.
102. Du L, Wang H, He L, et al. CD44 is of functional importance for colorectal cancer stem cells. Clin Cancer Res 2008; 14: 6751-60.
103. Takaishi S, Okumura T, Tu S, et al. Identification of gastric cancer stem cells using the cell surface marker CD44. Stem Cells 2009; 27: 1006-20.
104. Collins AT, Berry PA, Hyde C, Stower MJ, Maitland NJ. Prospective identification of tumorigenic prostate cancer stem cells. Cancer Res 2005; 65: 10946-51.
105. Patrawala L, Calhoun T, Schneider-Broussard R, et al. Highly purified CD44+ prostate cancer cells from xenograft human tumors are enriched in tumorigenic and metastatic progenitor cells. Oncogene 2006; 25: 1696-708.
106. Misra S, Heldin P, Hascall VC, et al. Hyaluronan-CD44 interactions as potential targets for cancer therapy. FEBS J 2011; 278: 1429-43.
107. Sneath RJ, Mangham DC. The normal structure and function of CD44 and its role in neoplasia. Mol Pathol 1998; 51: 191-200.
108. Naor D, Nedvetzki S, Golan I, Melnik L, Faitelson Y. CD44 in cancer. Crit Rev Clin Lab Sci 2002; 39: 527-79.
109. Bartolazzi A, Peach R, Aruffo A, Stamenkovic I. Interaction between CD44 and hyaluronate is directly implicated in the regulation of tumor development. J Exp Med 1994; 180: 53-66.
110. Bartolazzi A, Jackson D, Bennett K, et al. Regulation of growth and dissemination of a human lymphoma by CD44 splice variants. J Cell Sci 1995; 108 (Pt 4): 1723-33.
111. Ghatak S, Misra S, Toole BP. Hyaluronan constitutively regulates ErbB2 phosphorylation and signaling complex formation in carcinoma cells. J Biol Chem 2005; 280: 8875-83.

112. Bajorath J, Greenfield B, Munro SB, Day AJ, Aruffo A. Identification of CD44 residues important for hyaluronan binding and delineation of the binding site. J Biol Chem 1998; 273: 338-43.
113. Hayen W, Goebeler M, Kumar S, Riessen R, Nehls V. Hyaluronan stimulates tumor cell migration by modulating the fibrin fiber architecture. J Cell Sci 1999; 112 (Pt 13): 2241-51.
114. Bourguignon LY, Peyrollier K, Gilad E, Brightman A. Hyaluronan-CD44 interaction with neural Wiskott-Aldrich syndrome protein (N-WASP) promotes actin polymerization and ErbB2 activation leading to beta-catenin nuclear translocation, transcriptional up-regulation, and cell migration in ovarian tumor cells. J Biol Chem 2007; 282: 1265-80.
115. Bourguignon LY, Wong G, Earle C, Krueger K, Spevak CC. Hyaluronan-CD44 interaction promotes c-Src-mediated twist signaling, microRNA-10b expression, and RhoA/RhoC up-regulation, leading to Rho-kinase-associated cytoskeleton activation and breast tumor cell invasion. J Biol Chem 2010; 285: 36721-35.
116. Wang SJ, Bourguignon LY. Hyaluronan and the interaction between CD44 and epidermal growth factor receptor in oncogenic signaling and chemotherapy resistance in head and neck cancer. Arch Otolaryngol Head Neck Surg 2006; 132: 771-8.
117. Fitzgerald KA, Bowie AG, Skeffington BS, O'Neill LA. Ras, protein kinase C zeta, and I kappa B kinases 1 and 2 are downstream effectors of CD44 during the activation of NF-kappa B by hyaluronic acid fragments in T-24 carcinoma cells. J Immunol 2000; 164: 2053-63.
118. Coussens LM, Werb Z. Inflammation and cancer. Nature 2002; 420: 860-7.
119. Lin YH, Yang-Yen HF. The osteopontin-CD44 survival signal involves activation of the phosphatidylinositol 3-kinase/Akt signaling pathway. J Biol Chem 2001; 276: 46024-30.
120. Wobus M, Rangwala R, Sheyn I, et al. CD44 associates with EGFR and erbB2 in metastasizing mammary carcinoma cells. Appl Immunohistochem Mol Morphol 2002; 10: 34-9.

121. Southgate J, Trejdosiewicz LK, Smith B, Selby PJ. Patterns of splice variant CD44 expression by normal human urothelium in situ and in vitro and by bladder-carcinoma cell lines. Int J Cancer 1995; 62: 449-56.
122. Kuncova J, Urban M, Mandys V. Expression of CD44s and CD44v6 in transitional cell carcinomas of the urinary bladder: comparison with tumour grade, proliferative activity and p53 immunoreactivity of tumour cells. APMIS 2007; 115: 1194-205.
123. Sugiyama M, Woodman A, Sugino T, et al. Non-invasive detection of bladder cancer by identification of abnormal CD44 proteins in exfoliated cancer cells in urine. Clin Mol Pathol 1995; 48: M142-7.
124. Ross JS, del Rosario AD, Bui HX, Kallakury BV, Okby NT, Figge J. Expression of the CD44 cell adhesion molecule in urinary bladder transitional cell carcinoma. Mod Pathol 1996; 9: 854-60.
125. Chuang CK, Liao SK. Differential expression of CD44 variant isoforms by cell lines and tissue specimens of transitional cell carcinomas. Anticancer Res 2003; 23: 4635-9.
126. Yang YM, Chang JW. Bladder cancer initiating cells (BCICs) are among EMA-CD44v6+ subset: novel methods for isolating undetermined cancer stem (initiating) cells. Cancer Invest 2008; 26: 725-33.
127. Matsumura Y, Hanbury D, Smith J, Tarin D. Non-invasive detection of malignancy by identification of unusual CD44 gene activity in exfoliated cancer cells. BMJ 1994; 308: 619-24.
128. Takada S, Namiki M, Matsumiya K, et al. Expression of CD44 splice variants in human transitional cell carcinoma. Eur Urol 1996; 29: 370-3.
129. Miyake H, Hara I, Gohji K, Yamanaka K, Arakawa S, Kamidono S. Urinary cytology and competitive reverse transcriptase-polymerase chain reaction analysis of a specific CD44 variant to detect and monitor bladder cancer. J Urol 1998; 160: 2004-8.
130. Kan M, Furukawa A, Aki M, Kanayama H, Kagawa S. Expression of CD44 splice variants in bladder cancer. Int J Urol 1995; 2: 295-301.

131. Wu Z, Zhang Y, Liu D. [Diagnostic value of CD44 splice variants in urine exfoliated cells of bladder cancer]. Zhonghua Wai Ke Za Zhi 1997; 35: 533-5.
132. Omran OM, Ata HS. CD44s and CD44v6 in diagnosis and prognosis of human bladder cancer. Ultrastruct Pathol 2012; 36: 145-52.
133. Reznikoff CA, Kao C, Messing EM, Newton M, Swaminathan S. A molecular genetic model of human bladder carcinogenesis. Semin Cancer Biol 1993; 4: 143-52.
134. Meisner LF, Wu SQ, Christian BJ, Reznikoff CA. Cytogenetic instability with balanced chromosome changes in an SV40 transformed human uroepithelial cell line. Cancer Res 1988; 48: 3215-20.
135. Lu QY, Jin YS, Pantuck A, et al. Green tea extract modulates actin remodeling via Rho activity in an in vitro multistep carcinogenic model. Clin Cancer Res 2005; 11: 1675-83.
136. Jin Y, Iwata KK, Belldegrun A, et al. Effect of an epidermal growth factor receptor tyrosine kinase inhibitor on actin remodeling in an in vitro bladder cancer carcinogenesis model. Mol Cancer Ther 2006; 5: 1754-63.
137. Rao JY, Bonner RB, Hurst RE, Liang YY, Reznikoff CA, Hemstreet GP, 3rd. Quantitative changes in cytoskeletal and nuclear actins during cellular transformation. Int J Cancer 1997; 70: 423-9.
138. Savage RE, Jr., DeBord DG, Swaminathan S, et al. Occupational applications of a human cancer research model. J Occup Environ Med 1998; 40: 125-35.
139. Bookland EA, Swaminathan S, Oyasu R, Gilchrist KW, Lindstrom M, Reznikoff CA. Tumorigenic transformation and neoplastic progression of human uroepithelial cells after exposure in vitro to 4-aminobiphenyl or its metabolites. Cancer Res 1992; 52: 1606-14.
140. Herbert BS, Hochreiter AE, Wright WE, Shay JW. Nonradioactive detection of telomerase activity using the telomeric repeat amplification protocol. Nat Protoc 2006; 1: 1583-90.
141. Au DW, Mok HO, Elmore LW, Holt SE. Japanese medaka: a new vertebrate model for studying telomere and telomerase biology. Comp Biochem Physiol C Toxicol Pharmacol 2009; 149: 161-7.

142. Horstmann M, Bontrup H, Hennenlotter J, et al. Clinical experience with survivin as a biomarker for urothelial bladder cancer. World J Urol 2010; 28: 399-404.
143. Pina-Cabral L, Santos L, Mesquita B, Amaro T, Magalhaes S, Criado B. Detection of survivin mRNA in urine of patients with superficial urothelial cell carcinomas. Clin Transl Oncol 2007; 9: 731-6.
144. Sun J, Hou JQ, He J, He XF, Wen DG. [Expression of survivin mRNA in urine exfoliated cells of patients with bladder transitional cell carcinoma detected by real-time PCR]. Ai Zheng 2009; 28: 1100-2.
145. Ohl F, Jung M, Radonic A, Sachs M, Loening SA, Jung K. Identification and validation of suitable endogenous reference genes for gene expression studies of human bladder cancer. J Urol 2006; 175: 1915-20.
146. Phull JS, Jefferies ER, Bates TS, et al. Modern transurethral resection in the management of superficial bladder tumours. British Journal of Medical and Surgical Urology. 2011; 4: 91-100.
147. Gulzar ZG, McKenney JK, Brooks JD. Increased expression of NuSAP in recurrent prostate cancer is mediated by E2F1. Oncogene 2012.
148. Sarela AI, Macadam RC, Farmery SM, Markham AF, Guillou PJ. Expression of the antiapoptosis gene, survivin, predicts death from recurrent colorectal carcinoma. Gut 2000; 46: 645-50.
149. Sugino T, Gorham H, Yoshida K, et al. Progressive loss of CD44 gene expression in invasive bladder cancer. Am J Pathol 1996; 149: 873-82.
150. Vikesaa J, Hansen TV, Jonson L, et al. RNA-binding IMPs promote cell adhesion and invadopodia formation. EMBO J 2006; 25: 1456-68.
151. Fitzgerald KA, O'Neill LA. Characterization of CD44 induction by IL-1: a critical role for Egr-1. J Immunol 1999; 162: 4920-7.
152. Singleton PA, Bourguignon LY. CD44 interaction with ankyrin and IP3 receptor in lipid rafts promotes hyaluronan-mediated Ca2+ signaling leading to nitric oxide production and endothelial cell adhesion and proliferation. Exp Cell Res 2004; 295: 102-18.

153. Marhaba R, Bourouba M, Zoller M. CD44v6 promotes proliferation by persisting activation of MAP kinases. Cell Signal 2005; 17: 961-73.
154. Luo X, Ruhland MK, Pazolli E, Lind AC, Stewart SA. Osteopontin stimulates preneoplastic cellular proliferation through activation of the MAPK pathway. Mol Cancer Res 2011; 9: 1018-29.
155. Wang YZ, Cao ML, Liu YW, He YQ, Yang CX, Gao F. CD44 mediates oligosaccharides of hyaluronan-induced proliferation, tube formation and signal transduction in endothelial cells. Exp Biol Med (Maywood) 2011; 236: 84-90.
156. Brown RL, Reinke LM, Damerow MS, et al. CD44 splice isoform switching in human and mouse epithelium is essential for epithelial-mesenchymal transition and breast cancer progression. J Clin Invest 2011; 121: 1064-74.
157. Hanagiri T, Shinohara S, Takenaka M, et al. Effects of hyaluronic acid and CD44 interaction on the proliferation and invasiveness of malignant pleural mesothelioma. Tumour Biol 2012.
158. Zhang LS, Ma HW, Greyner HJ, Zuo W, Mummert ME. Inhibition of cell proliferation by CD44: Akt is inactivated and EGR-1 is down-regulated. Cell Prolif; 43: 385-95.
159. Okamoto I, Kawano Y, Matsumoto M, et al. Regulated CD44 cleavage under the control of protein kinase C, calcium influx, and the Rho family of small G proteins. J Biol Chem 1999; 274: 25525-34.
160. Kawano Y, Okamoto I, Murakami D, et al. Ras oncoprotein induces CD44 cleavage through phosphoinositide 3-OH kinase and the rho family of small G proteins. J Biol Chem 2000; 275: 29628-35.
161. Okamoto I, Kawano Y, Tsuiki H, et al. CD44 cleavage induced by a membrane-associated metalloprotease plays a critical role in tumor cell migration. Oncogene 1999; 18: 1435-46.
162. Nagano O, Murakami D, Hartmann D, et al. Cell-matrix interaction via CD44 is independently regulated by different metalloproteinases activated in response to extracellular Ca(2+) influx and PKC activation. J Cell Biol 2004; 165: 893-902.

163. Nakamura H, Suenaga N, Taniwaki K, et al. Constitutive and induced CD44 shedding by ADAM-like proteases and membrane-type 1 matrix metalloproteinase. Cancer Res 2004; 64: 876-82.
164. Sugahara KN, Hirata T, Tanaka T, et al. Chondroitin sulfate E fragments enhance CD44 cleavage and CD44-dependent motility in tumor cells. Cancer Res 2008; 68: 7191-9.
165. Lammich S, Okochi M, Takeda M, et al. Presenilin-dependent intramembrane proteolysis of CD44 leads to the liberation of its intracellular domain and the secretion of an Abeta-like peptide. J Biol Chem 2002; 277: 44754-9.
166. Murakami D, Okamoto I, Nagano O, et al. Presenilin-dependent gamma-secretase activity mediates the intramembranous cleavage of CD44. Oncogene 2003; 22: 1511-6.
167. Lin SY, Makino K, Xia W, et al. Nuclear localization of EGF receptor and its potential new role as a transcription factor. Nat Cell Biol 2001; 3: 802-8.
168. Ni CY, Murphy MP, Golde TE, Carpenter G. gamma -Secretase cleavage and nuclear localization of ErbB-4 receptor tyrosine kinase. Science 2001; 294: 2179-81.
169. Stachowiak MK, Maher PA, Joy A, Mordechai E, Stachowiak EK. Nuclear localization of functional FGF receptor 1 in human astrocytes suggests a novel mechanism for growth factor action. Brain Res Mol Brain Res 1996; 38: 161-5.
170. Gletsu N, Dixon W, Clandinin MT. Insulin receptor at the mouse hepatocyte nucleus after a glucose meal induces dephosphorylation of a 30-kDa transcription factor and a concomitant increase in malic enzyme gene expression. J Nutr 1999; 129: 2154-61.
171. Okamoto I, Kawano Y, Murakami D, et al. Proteolytic release of CD44 intracellular domain and its role in the CD44 signaling pathway. J Cell Biol 2001; 155: 755-62.
172. Yang GH, Fan J, Xu Y, et al. Osteopontin combined with CD44, a novel prognostic biomarker for patients with hepatocellular carcinoma undergoing curative resection. Oncologist 2008; 13: 1155-65.

173. Toma V, Hauri D, Schmid U, et al. Focal loss of CD44 variant protein expression is related to recurrence in superficial bladder carcinoma. Am J Pathol 1999; 155: 1427-32.
174. Khan SA, Cook AC, Kappil M, et al. Enhanced cell surface CD44 variant (v6, v9) expression by osteopontin in breast cancer epithelial cells facilitates tumor cell migration: novel post-transcriptional, post-translational regulation. Clin Exp Metastasis 2005; 22: 663-73.
175. Afify A, Purnell P, Nguyen L. Role of CD44s and CD44v6 on human breast cancer cell adhesion, migration, and invasion. Exp Mol Pathol 2009; 86: 95-100.
176. Lipponen P, Aaltoma S, Kosma VM, Ala-Opas M, Eskelinen M. Expression of CD44 standard and variant-v6 proteins in transitional cell bladder tumours and their relation to prognosis during a long-term follow-up. J Pathol 1998; 186: 157-64.
177. Stavropoulos NE, Filliadis I, Ioachim E, et al. CD44 standard form expression as a predictor of progression in high risk superficial bladder tumors. Int Urol Nephrol 2001; 33: 479-83.
178. Kramer MW, Escudero DO, Lokeshwar SD, et al. Association of hyaluronic acid family members (HAS1, HAS2, and HYAL-1) with bladder cancer diagnosis and prognosis. Cancer 2011; 117: 1197-209.
179. Solis MA, Chen YH, Wong TY, Bittencourt VZ, Lin YC, Huang LL. Hyaluronan regulates cell behavior: a potential niche matrix for stem cells. Biochem Res Int 2012; 2012: 346972.
180. Nykopp TK, Rilla K, Sironen R, et al. Expression of hyaluronan synthases (HAS1-3) and hyaluronidases (HYAL1-2) in serous ovarian carcinomas: inverse correlation between HYAL1 and hyaluronan content. BMC Cancer 2009; 9: 143.
181. Sugahara KN, Hirata T, Hayasaka H, Stern R, Murai T, Miyasaka M. Tumor cells enhance their own CD44 cleavage and motility by generating hyaluronan fragments. J Biol Chem 2006; 281: 5861-8.

182. Bourguignon LY, Singleton PA, Diedrich F, Stern R, Gilad E. CD44 interaction with Na+-H+ exchanger (NHE1) creates acidic microenvironments leading to hyaluronidase-2 and cathepsin B activation and breast tumor cell invasion. J Biol Chem 2004; 279: 26991-7007.
183. Sironen RK, Tammi M, Tammi R, Auvinen PK, Anttila M, Kosma VM. Hyaluronan in human malignancies. Exp Cell Res 2011; 317: 383-91.
184. Oliferenko S, Kaverina I, Small JV, Huber LA. Hyaluronic acid (HA) binding to CD44 activates Rac1 and induces lamellipodia outgrowth. J Cell Biol 2000; 148: 1159-64.
185. Montagner IM, Banzato A, Zuccolotto G, et al. Paclitaxel-hyaluronan hydrosoluble bioconjugate: Mechanism of action in human bladder cancer cell lines. Urol Oncol 2012.
186. Bassi PF, Volpe A, D'Agostino D, et al. Paclitaxel-hyaluronic acid for intravesical therapy of bacillus Calmette-Guerin refractory carcinoma in situ of the bladder: results of a phase I study. J Urol 2011; 185: 445-9.